Optimization Problems of Electricity Market Under Modern Power Grid

by

Ming Lei
B.Eng., Hebei Normal University of Science and Technology, 2008
M.Eng., South China University of Technology, 2011

A Dissertation Submitted in Partial Fulfillment of the
Requirements for the Degree of

DOCTOR OF PHILOSOPHY

in the Department of Electrical and Computer Engineering

Optimization Problems of Electricity Market Under Modern Power Grid

by

Ming Lei
B.Eng., Hebei Normal University of Science and Technology, 2008
M.Eng., South China University of Technology, 2011

Supervisory Committee

Prof. Xiaodai Dong, Supervisor
(Department of Electrical and Computer Engineering)

Prof. Hongchuan Yang, Departmental Member
(Department of Electrical and Computer Engineering)

Prof. Jane J. Ye, Outside Member
(Department of Mathematics and Statistics)

Supervisory Committee

Prof. Xiaodai Dong, Supervisor
(Department of Electrical and Computer Engineering)

Prof. Hongchuan Yang, Departmental Member
(Department of Electrical and Computer Engineering)

Prof. Jane J. Ye, Outside Member
(Department of Mathematics and Statistics)

ABSTRACT

Nowadays, electricity markets are becoming more deregulated, especially development of smart grid and introduction of renewable energy promote regulations of energy markets. On the other hand, the uncertainties of new energy sources and market participants' bidding bring more challenges to power system operation and transmission system planning. These problems motivate us to study spot price (also called locational marginal pricing) of electricity markets, the strategic bidding of wind power producer as an independent power producer into power market, transmission expansion planning considering wind power investment, and analysis of the maximum loadability of a power grid.

The work on probabilistic spot pricing for a utility grid includes renewable wind power generation in a deregulated environment, taking into account both the uncertainty of load forecasting and the randomness of wind speed. Based on the forecasted normal-distributed load and Weibull-distributed wind speed, probabilistic optimal power flow is formulated by including spinning reserve cost associated with wind power plants and emission cost in addition to conventional thermal power plant cost model. Simulations show that the integration of wind power can effectively decrease spot price, also increase the risk of over-voltage.

Based on the concept of loacational marginal pricing which is determined by a market-clearing algorithm, further research is conducted on optimal offering strategies for wind power

producers participating in a day-ahead market employing a stochastic market-clearing algorithm. The proposed procedure to drive strategic offers relies on a stochastic bilevel model: the upper level problem represents the profit maximization of the strategic wind power producer, while the lower level one represents the marketing clearing and the corresponding price formulation aiming to co-optimize both energy and reserve.

Thirdly, to improve wind power integration, we propose a bilevel problem incorporating two-stage stochastic programming for transmission expansion planning to accommodate large-scale wind power investments in electricity markets. The model integrates co-optimizations of energy and reserve to deal with uncertainties of wind power production. In the upper level problem, the objective of independent system operator (ISO) modelling transmission investments under uncertain environments is to minimize the transmission and wind power investment cost, and the expected load shedding cost. The lower level problem is composed of a two stage stochastic programming problem for energy schedule and reserve dispatch simultaneously. Case studies are carried out for illustrating the effectiveness of the proposed model.

The above market-clearing or power system operation is based on direct current optimal power flow (DC-OPF) model which is a linear problem without reactive power constraints. Power system maximum loadability is a crucial index to determine voltage stability. The fourth work in this thesis proposes a Lagrange semi-definite programming (SDP) method to solve the non-linear and non-convex optimization alternating current (AC) problem of the maximum loadability of security constrained power system. Simulation results from the IEEE three-bus system and IEEE 24-bus Reliability Test System (RTS) show that the proposed method is able to obtain the global optimal solution for the maximum loadability problem.

Lastly, we summarize the conclusions from studies on the above mentioned optimization problems of electric power market under modern grid, as well as the influence of wind power integration on power system reliability, and transmission expansion planning, as well as the operations of electricity markets. Meanwhile, we also present some open questions on the related research, such as non-convex constraints in the lower-level problem of a bilevel problem, and integrating N-1 security criterion of transmission planning.

Contents

List of Tables

List of Figures

ACKNOWLEDGEMENTS

First of all, let me express my most sincere thanks to my supervisor, Prof. Xiaodai Dong for her endless support and encouragement through my whole Ph.D research, for her patient and heuristic guidance in the academic research, and for her kind love and care in my life. To be honest, without my supervisor's always help, I could not finish this thesis.

I am also grateful for my committee members, Prof. Jane J. Ye and Prof. Hong-chuan Yang for their suggestions in the my research proposal, as well as valuable comments on my research papers. In addition, I very much appreciate Prof. Gang Liu and his wife Xuemei Wang's thoughtful and considerate care to me since I started to live in Canada.

I would like to thank my friends from our research group, Dr. Yi Shi, Dr. Tong Xue, Youjun Fan, Dr. Binyan Zhao, Zheng Xu, Biao Yu, Leyuan Pan, Yongyu Dai, Ping Chen, Guang Zeng, Wanbo Li, Le Liang, Yuejiao Hui, Weizheng Li, Jun Zhou, Tianyang Li and Lan Xu. I also need to thank my friend Jin Zhang's help in research. Thank for all my friends' help, and I will always remember their support in my research and life.

Lastly I want to give my special thanks and love to my girlfriend Xiao Xie who always stays with me to go through rain and wind of life, to overcome all kinds of difficulties, to explore future. Just because of my girlfriend's love, I am motivated to keep moving forward, and her standing by me gives me the strength to pursue my dream. I certainly really want to say thanks to my parents for their amazing love, and to my brothers and sisters for shouldering life burden for me to maintain our warm and happy big family.

Everyone prefers happiness, success, wealth, sunshine, rather than sadness, failure, poverty, rain. But sometimes I could not have a choice to choose some positive things, as I really do not know what is happening tomorrow. And negative things always visit our life, as they are some parts of life. I want to say so-called enjoying life is not only to enjoy the warm sunshine, but also to feel the rainy season, and experiencing all kinds of aspects will enrich life.

Ming Lei, University of Victoria

DEDICATION

To my family,

My girlfriend,

And all the people who love me and whom I love.

Standing on solid ground, Looking up at the star-filled sky

Chapter 1

Introduction

Optimization problems of electric power markets are always hot topics to study, as non-linearity and non-convexity of power systems make these problems hard to solve. Especially, recently with the introduction of renewable energy and the development of smart grid, power market becomes more and more complicated. Many advanced algorithms and optimization methods have been proposed for modern power market problems. Our research is focused on several important market problems, such as the wind power producers' bidding, transmission planning considering wind power introduction and integration, and semidefinite programming for the security-constrained maximum loadablity. We firstly conduct the research on spot pricing of electricity markets, which is also the basics of the following work. Based on the electricity market background, we propose the bilevel programming to solve the e-quilibria between the wind power problems' bidding and electricity market clearing. Then a bilevel problem with two-stage stochastic programming will be formulated for the transmission planning problem with wind power investment. Finally, to deal with the non-linear and non-convex characteristics of the security-constrained maximum loadability problem, we develop the method of semidefinite programming to solve the non-linear and non-convex maximum loadability problem.

1.1 Electricity Market

Nowadays, to guarantee the fairness and competitiveness of electricity markets, traditional power systems are deregulated into independent companies and organizations. Taking Alberta as an example, the electricity power market is composed of Transmission Facilities Owners (TFOs), Distribution Facilities Owners (DFOs), Generations Facilities Owners(GFOs), and

Alberta Electricity System Operator (AESO). AESO is responsible for the safe, reliable and economic planning and operation of the Alberta Interconnected Electric System (AIES) as an Independent System Operator (ISO). AESO facilitates Alberta's competitive wholesale electricity market, and it is focused on ensuring a fair, open and efficient market for the exchange of electric energy in Alberta and effective relationships with neighbouring jurisdictions. Specifically, the AESO has some responsibilities to plan and develop the transmission system, also to provide customer access to the transmission system, and these customers can be called market participants including loads, generations, and even renewable energy sources.

ISOs provide market participants with the option to join a forward market which consists of day-ahead market and real-time market (balancing market). In the real-time market ancillary service will be achieved. The ancillary service has two functions: one is regulation which is the ability to automatically control the output of generators, and the other is about reserve ability to supply energy upon request due to the loss of supply. The day-ahead market is to develop day-ahead schedule using minimum-cost security constrained unit commitment and economic dispatch programs that simultaneously optimize energy and reserves. Day-ahead prices are hourly locational marginal prices (LMPs) which are calculated by market-clearing algorithm based on generation offers, demand bids, and bilateral transaction schedules. In the real-time market, real-time prices is calculated every 5-minutes according to actual operating conditions.

1.2 Locational Marginal Pricing

According to the definition, the locational marginal price (LMP) of an electricity market at a locational (bus) is equal to the minimum cost for the next increment of loads demand at a bus while satisfying all power system operating constraints. LMP is also called a spot price or a nodal price [1]. The LMPs are determined by the bids and offers submitted by market participants based on an AC-OPF or DC-OPF model. LMP is critical to guarantee a power market's smooth and secure operation [2]. LMP is a mechanism using market-based price to manage power system effectively, because the signal of LMPs can encourage new generators to find a location which has a high price and help large new users to locate a bus which a lower price, also promote new transmission line investment to relieve the congestion of power networks. In the following chapters, we will specifically introduce how the pricing signal of LMP improve wind power integration, and transmission facility investment.

1.3 Research Issues

1.3.1 Probabilistic Spot Pricing Considering Uncertainties

Spot price is a very important index for operation of electricity market, which is also called LMP. The uncertainties of renewable energy are challenging the current market-clearing algorithm. This thesis presents a solution of probabilistic spot pricing for a utility grid integrating renewable wind power generation, taking into account both the uncertainty of load forecasting and the randomness of wind speed. Based on the forecasted normal-distributed load and Weibull-distributed wind speed, probabilistic optimal power flow is formulated by including spinning reserve cost associated with wind power plants and emission cost in addition to conventional thermal power plant cost model. Probabilistic spot pricing is then obtained by differentiating the augmented Lagrange objective function with respect to the increment of the bus power injection. The effectiveness of the proposed method is validated through an exemplary three-machine nine-bus system.

1.3.2 Wind Power Producers' Bidding

Due to the unpredictable nature of wind power, it is important to modify the production and consumption scheduled in an electricity market during the actual operation of the power system [3]. The required adjustments can be materialized physically by the service traded in the market under the reserve. [4] proposes a market clearing model that corresponds to a single-period network-constrained auction, similar to those used by ISO-New England [5] and PJM [6]. This market clearing model is cast as a two-stage stochastic program in which a day-ahead schedule is determined in the first-stage, while the deployed reserve to cope with uncertain wind variations is determined at the second stage. Large scale wind power introduction is making wind power producers (WPPs) into pricer-makers from pricer-takers in the power pool. In this thesis we propose a new stochastic bilevel model where the upper level problem is similar to the one proposed in [7] and the lower level problem adopts the market clearing model proposed in [4]. Within the above framework, the contributions of this thesis are fourfold:
1) To provide a new stochastic bilevel model for a strategic WPP with two-stage stochastic market clearing. The model that we propose integrates the day-ahead market stage and the balancing market stage to co-optimize energy and reserve. The balancing market is stochastically cleared with all plausible realizations of the wind power production, resulting in the

balancing price introduced into the objective function of the strategic WPP as a variable. Since the balancing price is chosen to maximize the strategic WPPs profit, in the proposed market settlement which co-optimizes day-ahead and real-time dispatches in a single shot, the strategic WPP can exercise more market power so as to gain steady income.
2) To reformulate the stochastic bilevel program into a stochastic MPEC and solve it numerically using a relaxation scheme.
3) To take two illustrative examples as case studies, where optimal bidding strategies are discussed in details. The comparison between strategic and non-strategic WPPs and the comparison between reserve and non-reserve are presented.

1.3.3 Transmission Planning with Wind power Investment

Transmission planning problems are always hot topics for power field, especially considering future uncertain renewable energy introduction. Now new policy has been issued to encourage clean energy integration, however, good wind sources are usually located far away from demand areas. Therefore, transmission planning is critical for wind power introduction. Until now no papers study on transmission expansion planning problems consider strategic wind power investment, together with wind power bidding, and pool-clearing outcomes. This motivates us to propose the two-stage stochastic programs with a bilevel problems to model transmission expansion planning problem integrating wind power investment, bids and market-clearing.

1.3.4 Semidefinite Programing for Maximum Loadability

The impotance of voltage stability has been regarded by system operators as major force fastening development of modern electricity markets. Power system maximum loadability is a crucial index to determine voltage stability. This thesis proposes a Lagrange semi-definite programming (SDP) method to solve the non-linear and non-convex optimization problem of maximum loadability of security constrained power systems. We derive the Lagrange function of the primal maximum loadability, further get the dual problem of the primal maximum loadability problem through equivalent transformations, which is a convex SDP optimization. We also prove zero duality gap between primal maximum loadability and the dual problem satisfying necessary and sufficient condition, which can guarantee the global optimal solution. Simulation results from the IEEE three-bus system and IEEE 24-bus reliability test system (RTS) show that the proposed method in this dissertation is effective to handle the complicated non-liner and non-convex maximum loadability problem.

1.4 Dissertation Organization

Chapter 2 presents a probabilistic spot price model for power systems with integrated wind power and uncertain loads forecast. Also, the concept of the probabilistic spot price (Locational Marginal Price) also provides foundation to the following Chapters, such as wind power producers'bidding, transmission expansion planning. In Chapter 3, a proposed procedure to drive strategic offers relies on a stochastic bilevel model: the upper level problem represents the profit maximization of the strategic wind power producer, while the lower level one represents the marketing clearing and the corresponding price formulation aiming to co-optimize both energy and reserve. Chapter 4 studies the transmission expansion planning considering the strategic wind power investment, and the proposed model is composed of a bilevel problem for the coordination of transmission expansion planning and wind power investment, and two-stage stochastic programming for co-optimization of energy and reserve. In Chapter 5, the global optimal solution for the non-linear maximum loadability problem is presented. Finally, the related conclusions and open questions of the research topics are given in Chapter 6.

Chapter 2

Probabilistic Spot Pricing Considering Wind Power Integration and Loads Forecasting Uncertainty

This chapter presents a solution of probabilistic spot pricing for a utility grid integrating renewable wind power generation, taking into account both the uncertainty of load forecasting and the randomness of wind speed. Based on the forecasted normal-distributed load and Weibull-distributed wind speed, probabilistic optimal power flow is formulated by including spinning reserve cost associated with wind power plants and emission cost in addition to conventional thermal power plant cost model. The effectiveness of the proposed method is validated through an exemplary three-machine nine-bus system.

2.1 Introduction

One of the biggest challenges that face human society is the declining availability of non-renewable resources (e.g., fossil fuels) and the continuing environmental deterioration due to pollution [8, 9]. As such, increasing attention has been paid to explore the applicability of renewable resources, such as photovoltaic power, wind power, tidal power and so on, in replace of the dwindling conventional thermal power plants. Wind power, in particular, is deemed as an essential technology in developing modern electrical generation [10, 11]. However, when massive wind turbines are connected to the smart grid, their intermittent nature could aggravate the uncertainty and instability of system operations [8–15].

Spot price, also known as nodal price or local marginal price, represents the cost to serve the power load at a specific location, using all available generation while observing all transmission limits. Spot pricing comprises three components including marginal generation cost, marginal congestion cost, and marginal loss cost [16]. The hourly spot price based energy marketplace involves a variety of utility-customer transactions, such as customers selling to, as well as buying from, the utility. With the deregulation of power industry, spot pricing forecasting plays a key role in advancing active demand side management and achieving peak shaving, which promotes the development of smart grid. One of the decisive factors that influences spot pricing is load forecasting. Apparently, short-term forecasted load unavoidably carries certain degree of inaccuracy, which leads to the uncertainty of spot pricing. To investigate the impact of load uncertainty on spot pricing, the authors in [16] derived the expected load value as well as the upper and lower bound of load sensitivity, given a normal-distributed load model. In [17], probabilistic spot pricing is formulated with consideration of uncertainties in generation, load, and topology. A point estimation method is adopted to obtain statistical moments of LMP. Besides, load and generation cost uncertainties are considered in [18], where the authors obtained accurate membership functions through multi-parametric programming techniques.

As renewable energy sources gradually enter into the power grid paradigm, they have created non-negligible effects on the wholesale electricity price, making accurate electricity price calculation a very challenging problem [19, 20]. In particular, their intermittent nature further increases uncertainties of power output and thus spot pricing forecasting. The information on the probability distribution of prices is of particular useful in managing risk and improving the decision-making, also very important in managing transmission congestion. To investigate the impact of wind power uncertainty on spot pricing, the authors in [21] proposed a margin-cost-based optimal power flow (OPF) method assisted by interior point algorithms. In order to cope with uncertain factors such as loads, generators outage, system networks, as well as various weather conditions, stochastic analysis tools were applied and the probability distribution of the spot price was obtained. In [22], an efficient sampling-based method was proposed to address uncertainty in wind power generation, through which the mean and variance of spot prices were obtained. The authors in [23] assumed Weibull-distributed wind speed and empirically obtained spot price statistics based on historical data records. Another data-based study was carried out in [24], where the impact of wind generation on spot price was studied based on historical data collected in Texas. Very recently, a two-step forecasting method was proposed in [25], where a nonparametric regression model and a ARMA time-series model were applied to account for residual autocorrelation and seasonal dynamics in wind power uncertainties.

Most of the above-mentioned works either focus on the sole impact of load forecasting uncertainty or that of the wind power on spot pricing, thereby overlooking the combined effects of the two important system parameters. In this work, Monte Carlo simulation methods are employed to investigate the forecasting uncertainties of both load and wind power in spot pricing. To be specific, we first generate normal-distributed power load sequences [16] and Weibull-distributed wind speed sequences [23], which are then used as inputs of the optimization problem to calculate the corresponding state variables, such as power flow and voltage, based on which the probability density functions of system cost and spot price are finally derived. As the reference mentioned, inter-temporal variation of wind power has negative impact on security of system [10, 14], so we have also discussed the impact of wind power on the power grid reliability, which intends to illustrate, besides the positive effect of energy saving, the potential negative effects of energy instability and over power injection on power system. These findings are substantiated through a exemplary case study of a 3-machine, 9-bus system, where it is shown that although integration of wind power can effectively lower spot prices, large penetrations may raise over-voltage risk and an increase in reliability cost.

The rest of this chapter is organized as follows. Section 2.2 describes the characteristics of the random variables including the forecasted loads, the wind farm output power as well as the wind speed. Then, several cost models including power generation cost, spinning reserve cost, and emission cost are introduced in Section 2.3, followed by an optimal power flow model. Section 2.4 introduces the probabilistic optimal power flow (P-OPF) model with Weibull-distributed wind power and normal-distributed loads. The problem is then solved using Monte Carlo simulations, through which the probabilistic spot price is obtained. An exemplary case study of a 3-machine, 9-bus system is provided in Section 2.5. Finally, conclusions are drawn in Section 2.6.

2.2 Probabilistic Distributions and Cost Models

2.3 Notation

The main notation used throughout this chapter is stated below, while other symbols are defined when needed.

$\alpha_{(.)}, \beta_{(.)}, \gamma_{(.)}, \rho_{(.)}, \kappa_{(.)}$	Emission cost coefficients of a unit
$\delta_{(.)(.)}$	Voltage angle difference between two buses
$\delta^{\max}_{(.)(.)},\ \delta^{\min}_{(.)(.)}$	Upper and lower voltage angle difference
δ_w	Wind power penetration coefficient limits between two buses
$\boldsymbol{\lambda}, \boldsymbol{\nu}, \boldsymbol{\eta}$	Lagrange multipliers
μ, σ	Mean and standard deviation of a bus load
π_i^P, π_i^Q	Active and reactive spot prices
$a_{(.)}, b_{(.)}, c_{(.)}$	Generation cost coefficients of a unit
c_e	Unit emission cost
$f_v(.)$	PDF of wind speed
$f_w(.)$	PDF of wind power
$k,\ c$	Shape and scale factors of Weibull distribution
$m_{(.)}, n_{(.)}, l_{(.)}$	Spinning reserve cost coefficients of a bus
$\mathbf{u}, \mathbf{l}$	Slack variables
v_{in}	Cut-in wind speed
v_{out}	Cut-out wind speed
v_r	The rated wind speed
v	Wind speed
$\mathcal{A}_{(.)}$	Set of nodes adjacent to a unit
$B_{(.)(.)}$	Transfer susceptance between two buses
$C^P(.),\ C^Q(.)$	Active and reactive output generation power
$C^{\mathrm{PG}}(.)$	Power generation cost function
$C^{\mathrm{SR}}(.)$	Spinning reserve cost function
$C^{\mathrm{EM}}(.)$	Emission cost function
$F_v(.)$	CDF of wind speed
G_e	Total amount of emissions
$G_{(.)(.)}$	Transfer Conductance between two buses
$\boldsymbol{\mathcal{L}}$	Lagrange function
M	Number of buses
N	Number of generators
$P_{(.)},\ Q_{(.)}$	Active and reactive injection power of a bus
P_l	Total load power

P_w	Output power of wind turbine
P_{wr}	Rated power of wind turbine
$P^g_{(.)}$, $Q^g_{(.)}$	Generated active and reactive power of a bus
$P^w_{(.)}$, $Q^w_{(.)}$	Active and reactive wind power introductions to a bus
$P^l_{(.)}$, $Q^l_{(.)}$	Active and reactive load power of a bus cost functions
$P_{(.)(.)}, P^{\max}_{(.)(.)}$	Flowing power and maximum allowable power between two buses
$P^{g,\max}_{(.)}$, $P^{g,\min}_{(.)}$	Upper and lower active power generation limits
$Q^{g,\max}_{(.)}$, $Q^{g,\min}_{(.)}$	Upper and lower reactive power generation limits
$R_{(.)}$	Spinning reserves of a bus
$R^{\max}_{(.)}$, $R^{\min}_{(.)}$	Upper and lower spinning reserve limits
$\mathcal{U}$	Set of generators with spinning reserve
$V_{(.)}$	Voltage of a bus
$V^{\max}_{(.)}$, $V^{\min}_{(.)}$	Upper and lower bus voltage limits

2.3.1 Wind Farm Distribution

According to the significant amount of data collected from wind farms, the relationship between the output power of wind turbine generators and the wind speed is commonly expressed as

$$P_w = \begin{cases} 0 & v > v_{out} \quad \text{or} \quad v < v_{in} \\ P_{wr}\dfrac{v - v_{in}}{v_r - v_{in}} & v_{in} \le v \le v_r \\ P_{wr} & v_r \le v \le v_{out}. \end{cases} \tag{2.1}$$

The probability density function (PDF) of the wind speed can be described accurately by a Weibull distribution (see [23] and references therein)

$$f_v(v) = \begin{cases} 0 & v < 0 \\ \dfrac{k}{c}\left(\dfrac{v}{c}\right)^{k-1} \exp\left[-\left(\dfrac{v}{c}\right)^k\right] & v \ge 0. \end{cases} \tag{2.2}$$

From (2.1) and (2.2), the wind power PDF can be obtained as

$$f_w(x) = \begin{cases} [F_v(v_{in}) + 1 - F_v(v_{out})]\delta(x) & x = 0 \\ f_v\left(v_{in} + \dfrac{x(v_r - v_{in})}{P_{wr}}\right)\dfrac{v_r - v_{in}}{P_{wr}} & 0 < x < P_{wr} \\ [F_v(v_{out}) - F_v(v_r)]\delta(x - P_{wr}) & x = P_{wr}. \end{cases} \tag{2.3}$$

Due to the intermittent nature of wind, the power output of wind turbines also subjects to severe instabilities. In order to limit the impact of wind power on the power grid, we introduce a wind power penetration coefficient δ_w such that

$$P_w \leq \delta_w P_l. \tag{2.4}$$

2.3.2 Bus Forecasted Load PDFs

Load forecasting is a challenging task that requires the detailed modeling of the effects of a number of factors. In the modeling framework of stochastic programming, many researchers utilize the expected value and the corresponding standard deviation to model the predicted value and the associated prediction error. Generally, forecasted loads satisfy a normal distribution (see [16] and references therein)

$$f(x) = \frac{1}{\sqrt{2\pi}\sigma} \exp\left[-\frac{(x-\mu)^2}{2\sigma^2}\right]. \tag{2.5}$$

2.3.3 Power Generation Cost

In order to meet load requirement, the power generation cost is mainly from the thermal power plant. Mathematically, the cost can be modeled as

$$C^{\mathrm{PG}}(P_i^g, Q_i^g) = \sum_{i=1}^{N}[(C_i^P(P_i^g) + C_i^Q(Q_i^g)]. \tag{2.6}$$

The active output power cost function $f_i(P_i^g)$ admits a quadratic approximation as follows [26]

$$C_i^a(P_i^g) = a_i + b_i P_i^g + c_i\left(P_i^g\right)^2. \tag{2.7}$$

2.3.4 Spinning Reserve Cost

Due to the inherent intermittent nature of wind power, spinning reserve serves as a back-up power source that output power when wind power is unavailable. The corresponding constraints are as follows.

$$\max(R_i^{\min}, P_i^{g,\min} - P_i^g) \leq R_i \leq \min(R_i^{\max}, P_i^{g,\max} - P_i^g). \tag{2.8}$$

If the marginal cost of reserve from unit i is c_i, the total reserve cost can be expressed as

$$C^{\text{SR}}(R_i) = \sum_{i \in \mathcal{U}} m_i R_i^2 + n_i R_i + l_i. \tag{2.9}$$

2.3.5 Emission Cost

One of the main purposes of renewable energy is to reduce pollutant emissions from fossil fuels, thereby improving environmental benefits of the electric power. The atmospheric pollutants include SO_2, CO_2, and NO_x coming from the generators units. To simplify the model, the total emissions of these pollutes are expressed as [27]

$$G_e(P_i^g) = \sum_{i=1}^{N} 10^{-2}(\alpha_i + \beta_i P_i^g + \gamma_i \, (P_i^g)^2) + \rho_i \exp(\kappa_i P_i^g). \tag{2.10}$$

Further, the emission pollutants from thermal units translate into environmental cost as the following

$$C^{\text{EM}}(P_i^g) = G_e(P_i^g) c_e. \tag{2.11}$$

2.4 Probabilistic Optimal Power Flow Model

2.4.1 Problem Formulation

The integration of wind power to the main grid can effectively reduce atmosphere pollutants from thermal generators. Nevertheless, it necessitates large numbers of reserves in order to cope with the inherent variability and unpredictability of the wind generation source. As such, we introduce in this subsection an extended OPF model, which incorporates additional optional spinning reserve and environmental cost into the standard formulation. The problem can be formulated as, for $i = 1, \cdots, M$ and $j \in \mathcal{A}_i$

$$\min \; C^{\text{PG}} + C^{\text{SR}} + C^{\text{EM}} \tag{2.12a}$$

$$\text{s.t.} \; P_i = P_i^g + P_i^w - P_i^l = V_i \sum_{j \in \mathcal{A}_i} V_j (G_{ij} \cos \delta_{ij} + B_{ij} \sin \delta_{ij}) \tag{2.12b}$$

$$Q_i = Q_i^g + Q_i^w - Q_i^l = V_i \sum_{j \in \mathcal{A}_i} V_j (G_{ij} \sin \delta_{ij} - B_{ij} \cos \delta_{ij}) \tag{2.12c}$$

$$V_i^{\min} \leq V_i \leq V_i^{\max} \tag{2.12d}$$

$$\delta_{ij}^{\min} \leq \delta_{ij} \leq \delta_{ij}^{\max} \tag{2.12e}$$

$$P_i^{g,\min} \leq P_i^g + R_i \leq P_i^{g,\max} \tag{2.12f}$$

$$Q_i^{g,\min} \leq Q_i^g \leq Q_i^{g,\max} \tag{2.12g}$$

$$|P_{ij}| = \left| V_i^2 G_{ij} - V_i V_j (G_{ij} \cos \delta_{ij} + B_{ij} \sin \delta_{ij}) \right| \leq P_{ij}^{\max}, \tag{2.12h}$$

where (2.12b) and (2.12c) are the injection power balance constraints, (2.12d) and (2.12e) the security voltage constraints angle stability constraints of the overhead lines, (2.12f) and (2.12g) the generator output constraints, and (2.12h) the branch thermal constraint.

2.4.2 Standard Problem Transformation

The aforementioned probabilistic OPF problem can be written into the following standard form

$$\min \; f(\mathbf{x}) \tag{2.13a}$$

$$\text{s.t.} \; g_i(\mathbf{x}_i, \boldsymbol{\xi}_i) = 0 \quad i = 1, \cdots, M \tag{2.13b}$$

$$h_i^{\min}(\mathbf{x}_i) \leq h_i(\mathbf{x}_i) \leq h_i^{\max}(\mathbf{x}_i) \;\; i = 1, \cdots, M, \tag{2.13c}$$

where $\mathbf{x} = [\mathbf{x}_1^T, ..., \mathbf{x}_M^T]^T$ and $\boldsymbol{\xi} = [\boldsymbol{\xi}_1^T, ..., \boldsymbol{\xi}_M^T]^T$. The column vector $\mathbf{x}_i = [P_i^g, Q_i^g, V_i, \delta_i]$ consists of the system output variables and control variables, while the column vector $\boldsymbol{\xi}_i = [P_i^w, P_i^l]$ consists of the random input variables.

With the Lagrange multipliers $\boldsymbol{\lambda}$, $\boldsymbol{\nu}$, $\boldsymbol{\eta}$, the Lagrange function can be written as

$$\mathcal{L}(\mathbf{x}, \boldsymbol{\xi}, \boldsymbol{\lambda}, \boldsymbol{\nu}, \boldsymbol{\eta}) = f(\mathbf{x}) - \boldsymbol{\lambda}^T \mathbf{g}(\mathbf{x}, \boldsymbol{\xi}) + \boldsymbol{\nu}^T (\mathbf{h}(\mathbf{x}) - \mathbf{h}^{\min}(\mathbf{x})) - \boldsymbol{\eta}^T (\mathbf{h}(\mathbf{x}) - \mathbf{h}^{\max}(\mathbf{x})) \tag{2.14}$$

where $\mathbf{g}(\mathbf{x}, \boldsymbol{\xi}) = [g_1(\mathbf{x}_1, \boldsymbol{\xi}_1), ..., g_M(\mathbf{x}_M, \boldsymbol{\xi}_M)]$ and $\mathbf{h}(\mathbf{x}) = [h_1(\mathbf{x}_1), ..., h_M(\mathbf{x}_M)]$. Note that the Lagrangian multipliers are kept positive.

According to the short-term marginal cost theory, the spot prices of the active and reactive power π_i^P and π_i^Q of bus i are defined as the marginal system costs as a result of the active and reactive power variations. By definition, the spot prices are just the optimal Lagrangian multipliers that correspond to the active and reactive power balance constraints (2.12b) and (2.12c), respectively. Mathematically, the spot prices can be expressed [21, 28]

$$\pi_i^P = \left.\frac{\partial \mathcal{L}}{\partial P_i}\right|_* = \lambda_{pi}, \tag{2.15}$$

$$\pi_i^Q = \left.\frac{\partial \mathcal{L}}{\partial Q_i}\right|_* = \lambda_{qi}, \tag{2.16}$$

where the notation $|_*$ denotes the optimal OPF solution that satisfies the Karush-Kuhn-Tucker (KKT) conditions.

Probabilistic Spot Price Calculation

We use Monte Carlo simulation to generate random sequences for the normal distributed forecasted load and Weibull distributed forecasted wind speed. In order to produce a non-uniform probability distribution sequence, we first generate uniform distribution sequence, then use mathematical tools to transform it into the distribution sequence. Steps of solving probabilistic spot price are given as follows.

1. Construct probability model for the wind speed according to (2.1) and (2.2), as well as probability model for load according to (2.5).

2. Generate random sequences using the constructed models in step 1, which are then used as inputs for the P-OPF model proposed in Section 2.4.

3. Solve the P-OPF model using MATPOWER and obtain the optimal Lagrangian multipliers.

4. Calculate the spot prices by substituting the obtained Lagrangian multiplier into (2.15) and (2.16).

5. Perform statistical analysis to obtain the statistical property of the spot price, such as PDF and mean value.

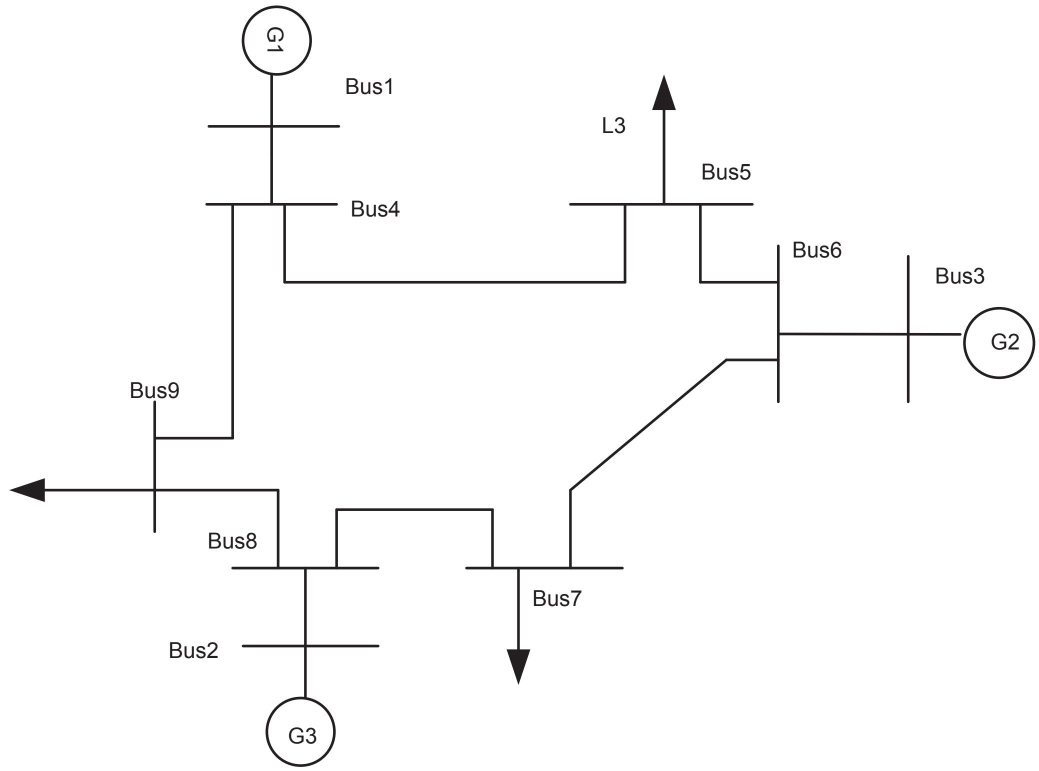

Figure 2.1: IEEE 9 buses system topology.

2.5 Case Study

An IEEE three-machine and nine-bus system is considered, which is shown in Fig. 2.1. Two wind farms are assumed to have been built at both the nodes 5 and 7. The same Weibull distribution, with shape and scale parameters equal to 2 and 6.7703, respectively, is used to model wind speed at both sites. The mean value of the normal-distributed load model equals the mean of the load profile given by the IEEE nine-bus system, while the variance is set as 0.05.

Using the proposed P-OPF model, the probabilistic spot price is obtained through Monte Carlo simulations with 10000 samples. In particular, the impact of the wind farm size on various aspects of the main power system has been investigated, in terms of the probability density function of spot price and distribution of bus voltage.

As can be observed from Fig. 2.2, given the normal-distributed forecasted load inputs, the obtained spot price follows normal distribution as well, with a mean value of about 20 MWh. With the integration of wind power, the mean spot price decreases from 20 MWh to approximately 17.5 MWh as shown in Fig. 2.3. Nevertheless, it should be noted that the

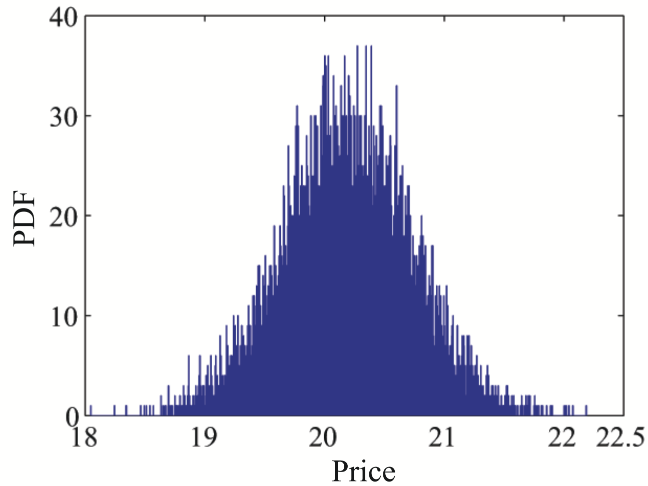

Figure 2.2: Spot price without wind power of the 7 th bus node

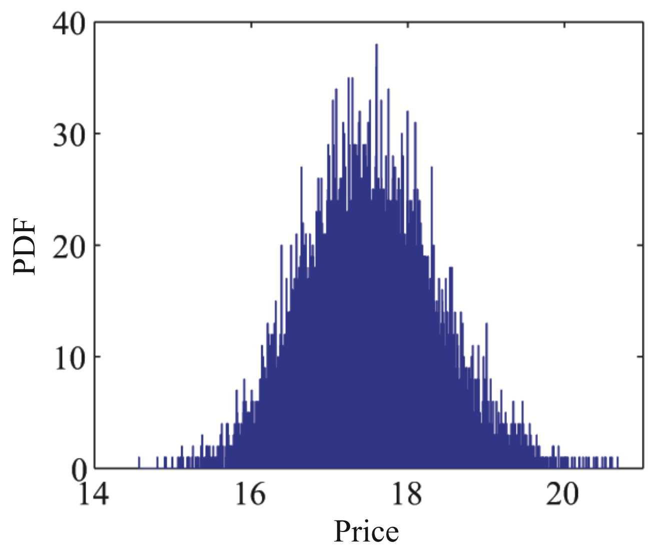

Figure 2.3: Spot price of the 7 th integrating mean 20 MW wind power

decline of the mean spot price is accompanied by an increase of the standard deviation, which implies that the intermittent nature of the wind power exacerbates the stability of real-time price and creates difficulty in predicting electricity price as well. Note that the results in Fig. 2.3 have neglected the maintenance and construction costs of the wind turbines and therefore are optimistic predictions. Finally, when the emission cost comes into the picture, the spot price profile rockets to a mean value of 32 MWh as is shown in Fig. 2.4.

Fig. 2.5-Fig. 2.7 illustrate the impact of wind power integration on the reliability of the main grid with a focus on the voltage stability, when the wind power rises from 20 MW to 60 MW. By focusing again on the 7 th bus, we observe that as the wind power rises, the risk of

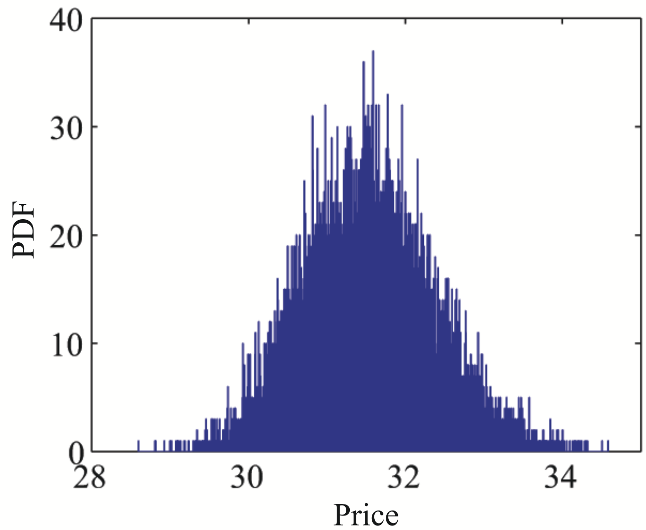

Figure 2.4: Spot price of the 7 th bus with wind power and emission cost

overvoltage on the 7 th bus increases simultaneously. For example, as can be observed from Fig. 2.5, the frequency of voltage magnitude (pu) keeping under 1.097 pu is approximately 6000 per 10000 samples, and the rate of 1.098 pu voltage is around 3000. As the mean wind energy integration increase from 20 MW to 35 MW, Fig. 2.6 exhibits an apparent probabilistic risk increase. For example, the frequencies of 1.098 pu and 1.099 pu voltage reach 6000 and 2000, respectively, while the rate of lower voltages occurrence becomes smaller. Further increasing the wind output power to 60 MW, the frequency of 1.1 pu voltage arises to 3000, while at the same time, the rate of 1.099 pu voltage reaches 4000, which implies that the voltage of the 7 th bus has exceeded its power limits. In other words, although increasing integration of the renewable energy into the main grid decreases system operation cost, the reliability cost surfaces and becomes a non-negligible factor that drives the escalation of the spot prices.

2.6 Conclusion

A probabilistic optimal power flow model considering load uncertainty and wind speed randomness has been proposed in this work. The extended objective function has included emission cost to take into account environmental benefits and spinning reserve fee to address the reserve cost owing to the introduction of wind power. The spot price is then obtained from the P-OPF result. Simulation results for the IEEE 3-machine and 9-bus test system show renewable wind energy is beneficial for cost reduction. However, once over penetration,

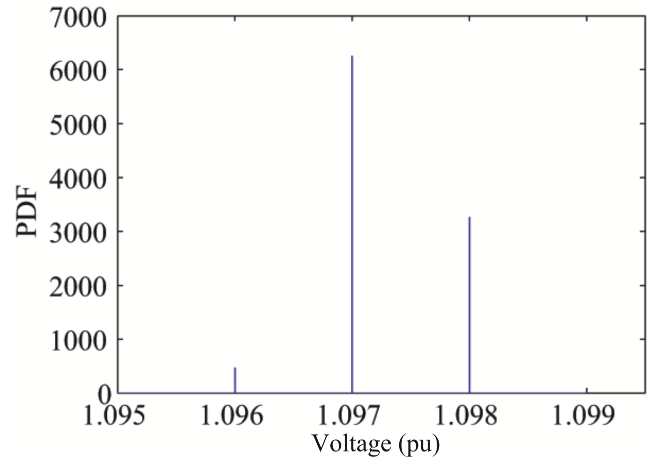

Figure 2.5: Voltage of the 7 th bus with mean 20 MW wind power

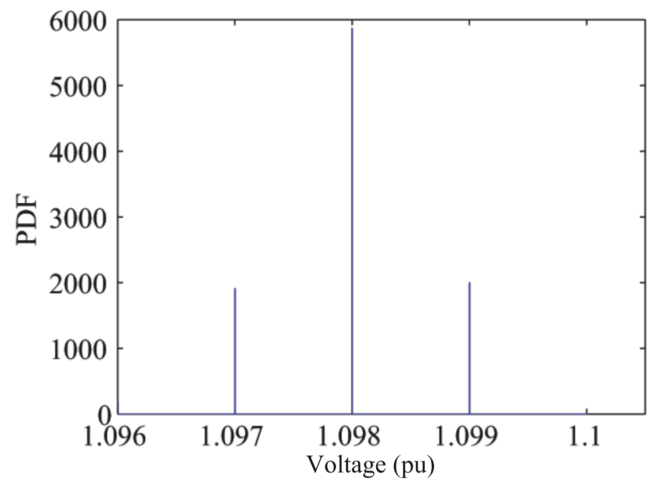

Figure 2.6: Voltage of the 7 th bus with mean 35 MW wind power

intermittent wind power may bring serious reliability problem and cause cost climbing. The separate effect of the wind and load randomness can also be studied using the approach in this Chapter.

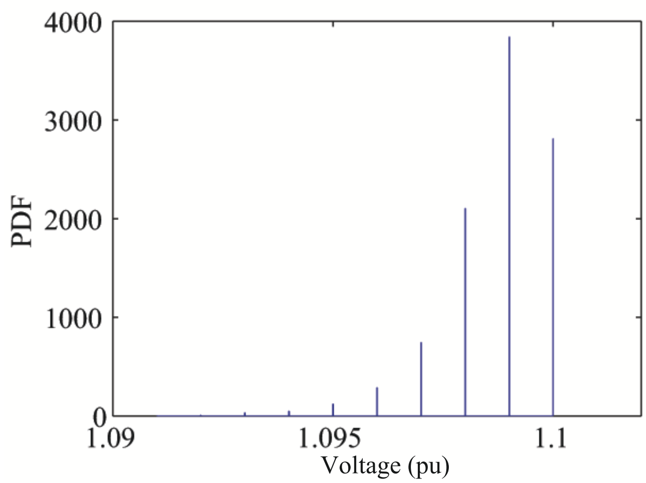

Figure 2.7: Voltage of the 7 th bus with mean 60 MW wind power

Chapter 3

Modeling The Bids of Wind Power Producers in The Day-ahead Market with Stochastic Security-constrained Market Clearing

In Chapter 2, we studied the probabilistic spot price, which is calculated by the market-clearing agorithm. In this chapter, we further study the wind power producers' bidding considering the stochastic market-clearing algorithm based on the general equilibrium theory. Specifically, a bilevel problem models the strategic bids of a strategic wind power producer as the upper-level problem and the stochastic market-clearing as the low-level problem. The proposed model effectively solves the interaction between the offers of wind power producers and the clearing prices of electric markets, and helps wind power producers participate in the markets like other traditional independent power producers.

3.1 Introduction

3.1.1 Motivation

In the mordern world, wind power has become an essential technology in the developing modern electrical generation [29, 30]. In some countries such as Denmark and Germany, wind power producers (WPPs) have taken dominant positions in the electricity pools. U.S. Department of Energy also set the goal of 20% of electricity energy consumed by wind power generation by 2030. Wind power will have increasing influence on the marginal cost in market clearing, where energy is scheduled [31]. In Denmark and Spain, such high wind power prompted Independent System Operators (ISOs)/Market Operators to allow wind power producers to bid in the day-ahead market as other traditional sources. Similarly, in ISOs/Transmission System Operator markets of North America that have high penetration of wind power, WPPs are increasingly authorized to bid in the day-ahead market [32]. Like PJM, ERCOT and MISO, these ISOs/Region System Operators with high wind power installed require that wind power producers must bid in the day-ahead market.

Integrating wind power into a short term electricity market brings many challenges for the current electricity market operations, because the high penetration and inherent uncertainty of wind power significantly impact the security of system operation. A variety of relevant research have gained in popularity in recent years [33]. To participate in the deregulated markets, WPPs bid the price and quantity of wind power in the day-ahead market, which operates once a day, one day ahead, and on an hourly basis. However, the high risk of financial penalties from realized wind power production's deviation from day-ahead schedule in the real-time market is hindering WPPs' participation in markets like other independent power producers. To mitigate the financial risk of failing to meet day-ahead schedule due to variable wind power production, the Federal Energy Regulatory Commission is discussing and working on changing the market rules of day-ahead and capacity [34]. Generally the transaction in the day-ahead market and the balancing market is settled based on pool prices or locational marginal prices (LMPs) depending on the particular market rules. For ISOs in the east coast of U.S., the hourly LMPs in the day-ahead market are derived through a security-constrained unit comment and economic dispatch market clearing algorithm which simultaneously optimizes energy and reserve, in contrast to European markets' sequential schedule of energy and reserve. All current market clearing practices are based on deterministic methods where scheduling reserve is based on a worst-case scenario. However, current deterministic market clearing cannot fully integrate the uncertainty of wind power [35]. In regard to market redesign for distributed energy, [36] discussed the necessity of stochastic procedures to guarantee efficient and fair market clearing. Additionally, [37] and [4] proposed a two-stage stochastic programming with network-constrained market clearing model to deal with the uncertainty of wind power. [35] formulates a short-term stochastic market clearing model for operation planning and demonstrates economical benefit of the stochastic method comparing with a deterministic worst-case scenario method. Reference [38] which models the effect of a WPP as a price-maker based on deterministic market clearing recommends further work of the effect of stochastic optimization to be done. Therefore, it is necessary and urgent to study the effect of stochastic procure in market clearing on bidding of renewable energy. In this chapter, our main purpose is to study the strategic behavior of a WPP who participates in the day-ahead market with stochastic security-constrained market clearing as a price-marker and analyze the effect of simultaneous scheduling energy and reserve on WPPs' bidding.

3.1.2 Literature

There has been many approaches proposed to solve wind power trading problems [39–42]. [39] models optimal wind power bids for a short-term market to minimize the imbalance cost considering uncertain imbalance prices and wind power predictions. In [40], a two-stage stochastic programming method is used to obtain the optimal offering strategy of WPPs. The paper [41] formulates a general methodology for deriving optimal bidding strategies based on probabilistic wind power forecasting and the sensitivity of a WPP to regulation costs. [42] derives the optimal contract offerings in a perfectly competitive two-settlement market. Recently, the bilevel model has become attractive in modelling wind power markets [7,43,44], as bilevel programming works well in modelling the strategic bidding problems. [7] proposes an optimal offering strategy for a strategic WPP that participates in the day-ahead market as a price maker and in the balancing market as a deviator. [43] studies the equilibria of wind power producers in an oligopolistic market. [44] considers the problem of a wind power producer that is a price-taker in the day-ahead market, but a price-maker in the balancing market. A bilevel program can be reformulated as a mathematical program with equilibrium constraints (MPEC) under suitable convexity conditions and constraint qualifications in the lower level problem. MPECs are known to be a highly difficult class of NP hard problems, due to the fact that usual constraint qualifications are violated at any feasible point (see [45, Proposition 1.1]). Hence, the classical Karush-Kuhn-Tucker (KKT) condition is not always a necessary optimality condition for an MPEC. Most literature on this topic, including [7,43,44], transform the complementarity constraints into mixed integer linear constraints by using Fortuny-Amat transformations [46] and solve the resulting mixed integer linear program. Alternatively, [47] approximates an MPEC using a relaxed family of better-behaved nonlinear programs (NLPs), solves the sequence of the NLPs and drives the relaxation parameter to zero. In all related literatures, generators' true quadratic cost functions are linearised. Although the linearization simplifies the computation and make the problem tractable, it introduces many more new constraints and variables [48]. Moreover the linearisation sections are hard to choose [48].

To the best of our knowledge, there are no papers or references which focus on strategic bidding behavior of a WPP in the *stochastic security-constrained market clearing*. This paper proposes a new stochastic bilevel model where the upper level problem represents the decision of variable wind sources and the lower level problem adopts the two-stage stochastic security-constrained market clearing model. The proposed bilevel problem is casted as a stochastic MPEC problem which is solved by a relaxation method.

3.1.3 Contribution

Within the above framework, the contributions of this chapter are fourfold:
1) To provide a new stochastic bilevel model for a strategic WPP with two-stage stochastic market clearing. The model that we propose integrates the day-ahead market stage and the balancing market stage to co-optimize energy and reserve. The balancing market is "s-tochastically" cleared with all plausible realizations of the wind power production, resulting in the "balancing price" introduced into the objective function of the WPP as a variable. Since the balancing price is chosen to maximize the strategic WPPs profit, in the proposed market settlement which co-optimizes day-ahead and real-time dispatches in a single shot, the strategic WPP can exercise more market power so as to gain steady income.
2) To reformulate the stochastic bilevel program into a stochastic MPEC and solve it numerically using a relaxation scheme.
3) To take two illustrative examples as case studies, where optimal bidding strategies are discussed in details. The comparison between strategic and non-strategic WPPs and the comparison between reserve and non-reserve are presented.

This paper is organized as follows. Section II gives a detailed problem description. Section III presents the mathematical formulation of the bi-level model, derives the stochastic MPEC reformulation of the bilevel program and proposes the relaxation scheme for solving the stochastic MPEC. Two case studies based on a three-bus system and the IEEE 30-bus Test System (TS) are given in Section IV. Finally, Section V concludes the paper.

3.2 Problem Description

3.2.1 Stochastic Market-clearing Model

The day-ahead market clearing is a two-stage procedure in most markets, which is composed of security-constrained unit commitment and security-constrained economic dispatch. In the day-ahead market energy and reserve clearing methods differ from different market rules of regions. European markets like Iberian Peninsula market sequentially clear energy and reserve, while most ISOs in the east coast of U.S., such as PJM, New-York ISO and New-England ISO, simultaneously co-optimize reserve and energy. Detailed advantages of the simultaneous method are described in [49]. In PJM, LMPs of the day-ahead market are calculated according to generation offer and demand bidding of each hour with network constrains. In this paper unit commitment constraints (e.g. ramping rates, startup costs/times, minimum down-times) are not considered. However, the the proposed single period market clearing model can be extended to multi-period.

As stated in [31], integrating wind power forecasting information into the day-ahead market clearing is necessary. Considering integrating uncertainty of wind power in the day-ahead market clearing, the above mentioned references [4, 37] are proposing a two-stage stochastic programming as the day-ahead market clearing. Recently much research is in favour of stochastic market clearing over current deterministic worst-case methods used in the real world because of the potential economic benefit. To study the behavior of a WPP in stochastic market clearing, this paper proposes a single-period stochastic security-market clearing with co-optimization of energy and reserve as the lower level problem of the WPP bidding bilevel problem.

3.2.2 Model Assumptions

The main model assumptions are listed below:
1) Loads are charged by the LMP of a bus, at which point the demand is connected and the WPP is paid by the LMP of the bus at which wind power is introduced into power network. Also we assume that loads are inelastic without load shedding [7].
2) Wind power introduced into the power system is treated as a negative load, and the penalty for wind power that deviates from the scheduled power production is charged at a price which is a dual variable of the balancing equations in the real-time market.
3) Each displaceable unit whose upward/downward reserve capacity is deployed in the real-

time market is in accordance with the supply cost functions submitted to the day-ahead market by the generation units.
4) We are using a direct current optimal power flow (DC-OPF) model without power system losses to clear the market, obtaining LMPs in the day-ahead market and real-time market [7].
5) The strategic WPP makes bidding decisions in the day-ahead market anticipating the equilibrium of the market. Anticipating the market equilibrium is necessary [50].
6) Wind power uncertainty can be efficiently modeled through a finite set of scenarios. This assumption makes the proposed stochastic bilevel model computationally solvable.
7) Only wind generation uncertainty is considered. However, some other uncertainties such as equipments failure, demand uncertainty and competing offers from other producers can be easily integrated into the market-clearing model through scenarios.
8) To simplify the proposed model, ramping rates, startup costs/times, minimum down-times noncovex constraints such as ramp limits are not included in the market-clearing algorithm; this problem will be discussed in our next paper on unit commitment problem.
9) Wind power is produced by a private renewable energy company under private ownership, and the private WPP can independently bid wind power offer and offer price.
10) Operating reserve this paper considers is mainly spinning reserves, as spinning reserves can send the response fast to the power imbalance while supplemental reserves serve a longer disturbance [49]. Therefore, we just take spinning reserves into account for the uncertainties of wind power.

3.3 Mathematical Formulation

3.3.1 Notation

The main notation used throughout this paper is stated below, while other symbols are defined when needed.

Indices and Sets

Ψ_n^D Set of indices of the demands located at bus n.

Ψ_n^G Set of indices of the generation units located at bus n.

Θ_n Set of the buses connected to the bus n.

Ψ_n^W Set of indices of the wind power units located at bus n.

Ω^D Set of indices of demands.

Ω^G	Set of indices of generation units other than wind power units.
Ω^N	Set of indices of buses.
Ω^W	Set of indices of wind power units.
Ω^ω	Set of indices of scenarios.
Ω_d^D	Set of indices of the blocks of the dth demand.
$r_i^D(\omega)$	Reserve down deployed by the ith generation unit under scenario ω.
$r_i^U(\omega)$	Reserve up deployed by the ith generation unit under scenario ω.
$P_l^{\mathrm{W,Sp}}(\omega)$	Wind power generation spillage of the lth wind power unit under scenario ω.
P_{dj}^D	Power scheduled to be consumed by the jth block of the dth demand.
	Variables
P_i^G	Power scheduled to be produced by the ith generation unit.
P_l^W	Wind power cleared in the day-ahead market for the lth wind power unit.
$P_l^{\mathrm{W,Of}}$	Wind power offered to the day-ahead market by the lth wind power unit.
α_l^W	Offer price of the lth wind power unit.
δ_n^0	Voltage angle at bus n at the day-ahead market stage.
$\delta_n(\omega)$	Voltage angle at bus n under scenario ω.
λ_n	Day-ahead price at bus n.
$\mu_n(\omega)$	Balancing market price at bus n under scenario ω.
	Constants and Constraints:
$\bar{P}_l^{W,P}(\omega)$	Wind power produced by the lth wind power unit under scenario ω.
λ_{dj}^D	Marginal utility of the jth block of the dth demand.
$\lambda_i^{(\cdot)G}$	Coefficients of the quadratic cost functions of the ith generation unit.
λ_l^W	Marginal cost of the lth wind power unit.
$\gamma(\omega)$	Weights of scenario ω.
$\overline{P}_{dj}^D$	Upper limit of the bth block of the jth demand.
$\overline{P}_i^G$	Upper limit of the ith generation unit.
$r_i^{D,max}$	Maximum reserve down deployed by the ith generation unit.
$r_i^{U,max}$	Maximum reserve up deployed by the ith generation unit.
$\overline{P}_l^W$	Wind power capacity of the lth wind power unit.
T_{nm}^{max}	Transmission line capacity for line $n-m$.
B_{nm}	Absolute value of the susceptance of line $n-m$.

3.3.2 Bidding Model

In PJM market, wind power who is a capacity resource must bid and set market price in the day-ahead market and pay for balancing reserve due to deviations in real time from day-ahead schedules, which is represented in the upper level problem in our proposed model. To mitigate independent power producers' market power, we also set a cap price for the bidding price given by (3.1c). Wind power spillage is also integrated in the upper level problem as the reference [7]. The lower level problem represents a security-constrained market clearing in the day-ahead market, which jointly optimize energy and reserve. The problem of finding the optimal offering strategy for a strategic WPP can be formulated as the following bilevel model:

$$
\begin{aligned}
&\text{Maximize}_{\Delta^{UL}\bigcup\Delta^{LL}} \\
&\sum_{\omega\in\Omega^{\omega}}\gamma(\omega)\sum_{l\in\Omega^{W}}\Big[\lambda_{n(l)}P_l^{W}-\lambda_l^{W}(\bar{P}_l^{W,P}(\omega)-P_l^{W,Sp}(\omega)) \\
&-\mu_{n(l)}(\omega)(P_l^{W}-(\bar{P}_l^{W,P}(\omega)-P_l^{W,Sp}(\omega)))\Big]
\end{aligned}
\tag{3.1a}
$$

subject to

$$0\leq P_l^{W,Of}\leq\overline{P}_l^{W},\forall l \tag{3.1b}$$

$$\alpha_l^{W}\leq P^{Cap},\forall l \tag{3.1c}$$

$$0\leq P_l^{W,Sp}(\omega)\leq\bar{P}_l^{W,P}(\omega),\forall l,\forall\omega \tag{3.1d}$$

where P_l^W solves the following lower-level problem, $\lambda_{n(l)}=\lambda_n, \mu_{n(l)}(\omega)=\mu_n(\omega)$ for all $l\in\Psi_n^W$ and $\lambda_n, \mu_n(\omega)$ are dual variables for the constraints (4.2b) and (3.2b) respectively.

The lower problem represent the stochastic security-constrained market clearing in the day-ahead market, which jointly optimize energy and reserve. ISOs located at the east coast of US, like PJM, New York ISO and New England ISO, all adopt co-optimization of energy and reserve. The mathematical formulation of the low level problem is given by

$$\text{Minimize}_{\Delta^{LL}}$$
$$\sum_{\omega\in\Omega^{\omega}} r(\omega)\Big[\sum_{i\in\Omega^{G}}(\lambda_i^{(2)G}(P_i^G + r_i^U(\omega) - r_i^D(\omega))^2 + \lambda_i^{(1)G}(P_i^G \tag{3.2a}$$
$$+ r_i^U(\omega) - r_i^D(\omega)) + \lambda_i^{(0)G})\Big] + \sum_{l\in\Omega^W}\alpha_l^W P_l^W - \sum_{d\in\Omega^D}\sum_{j\in\Omega_d^D}\lambda_{dj}^D P_{dj}^D$$

subject to:

$$\sum_{i\in\Psi_n^G}(r_i^U(\omega) - r_i^D(\omega)) + \sum_{l\in\Psi_n^W}(\overline{P}_l^{W,P}(\omega) - P_l^{W,Sp}(\omega) - P_l^W)$$
$$-\sum_{m\in\Theta_n} B_{nm}(\delta_n(\omega) - \delta_m(\omega) - \delta_n^0 + \delta_m^0) = 0 : \mu_n(\omega), \forall\omega, \forall n \tag{3.2b}$$
$$\sum_{i\in\Psi_n^G} P_i^G + \sum_{l\in\Psi_n^W} P_l^W - \sum_{d\in\Psi_n^D}\sum_{j\in\Omega_d^D} P_{dj}^D = \sum_{m\in\Theta_n} B_{nm}(\delta_n^0 - \delta_m^0) : \lambda_n, \forall n \tag{3.2c}$$
$$0 \le P_{dj}^D \le \overline{P}_{dj}^D : \phi_{dj}^{min}\phi_{dj}^{max}, \forall k, \forall j \tag{3.2d}$$
$$0 \le P_i^G \le \overline{P}_i^G : \varphi_i^{min}, \varphi_i^{max}, \forall i \tag{3.2e}$$
$$0 \le P_l^W \le P_l^{W,Of} : \varsigma_l^{min}, \varsigma_l^{max}, \forall l \tag{3.2f}$$
$$0 \le r_i^U(\omega) \le r_i^{U,max} : \sigma_i^{min}(\omega), \sigma_i^{max}(\omega), \forall i, \forall\omega \tag{3.2g}$$
$$0 \le P_i^G + r_i^U(\omega) - r_i^D(\omega) \le \overline{P}_i^G : \pi_i^{min}(\omega), \pi_i^{max}(\omega), \forall i, \forall\omega \tag{3.2h}$$
$$0 \le r_i^D(\omega) \le r_i^{D,max} : \beta_i^{min}(\omega), \beta_i^{max}(\omega), \forall i, \forall\omega \tag{3.2i}$$
$$-T_{nm}^{max} \le B_{nm}(\delta_n^0 - \delta_m^0) \le T_{nm}^{max} : \psi_{nm}^{min}, \psi_{nm}^{max}, \forall n, \forall m \in \Theta_n \tag{3.2j}$$
$$-T_{nm}^{max} \le B_{nm}(\delta_n(\omega) - \delta_m(\omega)) \le T_{nm}^{max}$$
$$: \eta_{nm}^{min}(\omega), \eta_{nm}^{max}(\omega), \forall n, \forall m \in \Theta_n, \forall\omega \tag{3.2k}$$
$$-\pi \le \delta_n^0 \le \pi : \xi_n^{min}, \xi_n^{max}, \forall n \setminus 1, \forall\omega \tag{3.2l}$$
$$-\pi \le \delta_n(\omega) \le \pi : \varpi_n^{min}(\omega), \varpi_n^{max}(\omega), \forall n \setminus 1, \forall\omega \tag{3.2m}$$
$$\delta_1(\omega) = 0 : \vartheta_1(\omega), \forall\omega \tag{3.2n}$$
$$\delta_1^0 = 0 : \kappa_1^0. \tag{3.2o}$$

$\Delta^{LL} := \{P_i^G, r_i^U(\omega), r_i^D(\omega), \forall i; \omega; P_{dj}^D, \forall d, j; P_l^W, \forall l; \delta_n^0, \forall n; \delta_n(\omega), \forall n, \omega\}$ and $\Delta^{UL} := \{\alpha_l^W, P_l^{W,Of}, \forall l; P_l^{W,Sp}(\omega), \forall l, \omega\}$ are the lower and upper level decision variables respectively, while the set who denotes the dual variables of the constraints of the lower level problem is shown as follow:

$$\Delta^{LL}_{Dual} := \{\lambda_n, \forall n; \mu_n(\omega), \forall n, \omega; \varsigma_n, \forall n; \rho^{min}_{dj}(\omega), \rho^{min}_{dj}(\omega), \forall d, j, \omega; \phi^{min}_{dj}, \phi^{max}_{dj}, \\ \forall d, j; \varphi^{min}_{i}, \varphi^{max}_{i}, \forall i; \varsigma^{min}_{l}, \varsigma^{max}_{l}, \forall l; \sigma^{min}_{i}(\omega), \sigma^{max}_{i}(\omega), \forall i, \omega; \beta^{min}_{i}(\omega), \beta^{max}_{i}(\omega), \\ \forall i, \omega; \pi^{min}_{i}(\omega), \pi^{max}_{i}(\omega), \forall i, \omega; \psi^{min}_{nm}, \psi^{max}_{nm}(\omega), \forall n, m, \omega; \eta^{min}_{nm}(\omega), \eta^{max}_{nm}(\omega), \\ \forall n, m, \omega; \xi^{min}_{n}, \xi^{max}_{n}, \forall n, \omega; \vartheta_1(\omega), \forall \omega; \kappa^0_1\}$$

The upper level problem (3.1a)-(3.1c) represents the profit maximization problem of the strategic WPP, while the lower level problem (3.2a)-(3.2o) represents the market clearing that aims to minimize the social cost. As a decision maker in the upper level problem, the strategic WPP determines the offering price α^W_l, the offer quantity $P^{\mathrm{W,Of}}_l$ and the wind power generation spillage $P^{\mathrm{W,spill}}_l(\omega)$ to maximize the expected profit (3.1a) subject to constraints (3.1b)-(3.1c) as well as the additional constraints that P^W_l are solutions of the lower level problem and $\lambda_n, \mu_n(\omega)$ are dual variables of the power balancing equations for the day-ahead market and the balancing market (4.2b) and (3.2b) respectively. The profit comprises three terms:

1) Each term $\lambda_{n(l)} P^W_l$ represents the revenue obtained from selling wind power in the day-ahead market, which is computed as the wind power cleared in this market times the LMP of the bus at which such wind power is produced. LMPs are computed as the dual variables associated with the balancing constraints (3.2a).

2) Each term $\lambda^W_l(\bar{P}^{W,P}_l(\omega) - P^{W,Sp}_l(\omega))$ represents the cost of wind power production in scenario ω.

3) Each term $\mu_{n(l)}(\omega)(P^W_l - (\bar{P}^{W,P}_l(\omega) - P^{W,Sp}_l(\omega)))$ is the cost/profit of purchasing/selling energy in the balancing market due to the wind power uncertainty. It is computed as the difference of the wind power cleared in the day-ahead market and the power generated in scenario ω, times the LMP of the bus at which the wind power is produced. In contrast to the bilevel model in [7], the balancing price $\mu_n(\omega)$ computed as the dual variables associated with the power balancing equations in the balancing market (3.2b) are variables not constants. Since the reserves have been considered in the marketing clearing algorithm in all scenarios, including the balancing price as a variable can reduce the risk of the strategic WPP.

The constraints (3.1b) impose the nonnegativity of wind power offered to the day ahead market, simultaneously confining wind power offer within the maximum capacity of the wind turbine, and the constraints (3.1d) bound the wind power spillage to be smaller than or equal to the actual wind power production.

After the WPP bids its offering price and quantity, the ISO computes the wind power to be cleared in the day-ahead market (P_i^G, P_{dj}^D, P_l^W) and the reserve up and down $(r_i^U(\omega), r_i^D(\omega))$ so as to maximize the expected social welfare (3.2a) subject to the constraints (4.2b)-(3.2o). Note that the offering price and quantity $\alpha_l^W, P_l^{\mathrm{W,Of}}$ are considered to be constants in the lower level problem. In contrast to the bilevel model in [7], the lower level problem is also a stochastic problem combining the day-ahead market and the real-time market. The social welfare in scenario ω comprises three terms:

1) Each term $\alpha_l^W P_l^W$ represents the revenue obtained from the WPP biding.
2) Each term $\lambda_i^{(2)G}(P_i^G + r_i^U(\omega) - r_i^D(\omega))^2 + \lambda_i^{(1)G}(P_i^G + r_i^U(\omega) - r_i^D(\omega)) + \lambda_i^{(0)G}$ represents the cost of the ith generation unit in scenario ω.
3) Each term $\lambda_{dj}^D P_{dj}^D$ is the utility of the jth block of the dth demand.

Constraints (4.2b) and (3.2b) are power balancing equations of the day-ahead and the balancing market respectively. The dual variables for constraints (4.2b) and (3.2b) are the day-ahead prices λ_n and real-time prices $\mu_n(\omega)$ respectively. When the ISO finds the wind power to be cleared in the day-ahead market and the reserve up and down, they can determine the the day-ahead prices λ_n and real-time prices $\mu_n(\omega)$ as well. The constraints (3.2d) guarantee the lower and upper bounds for the quantities of schedule load demands, and constraints (3.2e) and (3.2h) impose schedule generation power production together with reserve above zero and below capacity of each generation. Constraints (3.2j) and (3.2k) limit the transmission flow. Constraints (3.2f) bind the cleared wind power below the wind power offer. The other constraints (3.2g) and (3.2i) enforce the lower and upper bounds on the upward and downward reserves deployed from each displaceable unit. The constraints (3.2l) and (3.2m) enhance the limits for voltage angle at each bus, and the constraints (3.2n) and (3.2o) fix zero as the voltage angle of the reference bus.

3.3.3 Reformulation

Since the upper decision variables are considered to be constants, the lower level problem is a convex quadratic programming problem. In particular, the composition of convexity and linearity preserves convexity of the lower level problem [51]. Hence the bilevel problem (1)-(2) can be cast as a MPEC by replacing the lower level problem by its KKT condition equivalently:

$$max_{\Delta^{UL}\bigcup\Delta^{LL}\bigcup\Delta^{LL}_{Dual}}$$

(3.1a) (3.3a)

subject to

Constraints (3.1b)-(3.1c) and (4.2b)-(3.2h) (3.3b)

Complementarity constraints:

$$0 \leq \phi_{dj}^{min} \perp P_{dj}^{D} \geq 0, \forall d, \forall j \tag{3.3c}$$

$$0 \leq \phi_{dj}^{max} \perp \overline{P}_{dj}^{D} - P_{dj}^{D} \geq 0, \forall d, \forall j \tag{3.3d}$$

$$0 \leq \varphi_{i}^{min} \perp P_{i}^{G} \geq 0, \forall i \tag{3.3e}$$

$$0 \leq \varphi_{i}^{max} \perp \overline{P}_{i}^{G} - P_{i}^{G} \geq 0, \forall i \tag{3.3f}$$

$$0 \leq \varsigma_{l}^{min} \perp P_{l}^{W} \geq 0, \forall l \tag{3.3g}$$

$$0 \leq \varsigma_{l}^{max} \perp P_{l}^{W,Of} - P_{l}^{W} \geq 0, \forall l \tag{3.3h}$$

$$0 \leq \sigma_{i}^{min}(\omega) \perp r_{i}^{U}(\omega) \geq 0, \forall i, \forall \omega \tag{3.3i}$$

$$0 \leq \sigma_{i}^{max}(\omega) \perp r_{i}^{U,max} - r_{i}^{U}(\omega) \geq 0, \forall i, \forall \omega \tag{3.3j}$$

$$0 \leq \beta_{i}^{min}(\omega) \perp r_{i}^{D}(\omega) \geq 0, \forall i, \forall \omega \tag{3.3k}$$

$$0 \leq \beta_{i}^{max}(\omega) \perp r_{i}^{D,max} - r_{i}^{D}(\omega) \geq 0, \forall i, \forall \omega \tag{3.3l}$$

$$0 \leq \pi_{i}^{min}(\omega) \perp P_{i}^{G} + r_{i}^{U}(\omega) - r_{i}^{D}(\omega) \geq 0, \forall i, \forall \omega \tag{3.3m}$$

$$0 \leq \pi_{i}^{max}(\omega) \perp \overline{P}_{i}^{G} - (P_{i}^{G} + r_{i}^{U}(\omega) - r_{i}^{D}(\omega)) \geq 0, \forall i, \forall \omega \tag{3.3n}$$

$$0 \leq \psi_{nm}^{min} \perp B_{nm}(\delta_{n}^{0} - \delta_{m}^{0}) + T_{nm}^{max} \geq 0, \forall n, \forall m \in \Theta_{n} \tag{3.3o}$$

$$0 \leq \psi_{nm}^{max} \perp -B_{nm}(\delta_{n}^{0} - \delta_{m}^{0}) + T_{nm}^{max} \geq 0, \forall n, \forall m \in \Theta_{n} \tag{3.3p}$$

$$0 \leq \eta_{nm}^{min}(\omega) \perp B_{nm}(\delta_{n}(\omega) - \delta_{m}^{0}(\omega)) + T_{nm}^{max} \geq 0, \forall n, \forall m \in \Theta_{n}, \forall \omega \tag{3.3q}$$

$$0 \leq \eta_{nm}^{max}(\omega) \perp -B_{nm}(\delta_{n}(\omega) - \delta_{m}^{0}(\omega)) + T_{nm}^{max} \geq 0, \forall n, \forall m \in \Theta_{n}, \forall \omega \tag{3.3r}$$

$$0 \leq \xi_{n}^{min} \perp \delta_{n}^{0} + \pi \geq 0, \forall n \backslash 1 \tag{3.3s}$$

$$0 \leq \xi_{n}^{max} \perp -\delta_{n}^{0} + \pi \geq 0, \forall n \backslash 1 \tag{3.3t}$$

$$0 \leq \varpi_{n}^{min}(\omega) \perp \delta_{n}(\omega) + \pi \geq 0, \forall n \backslash 1, \forall \omega \tag{3.3u}$$

$$0 \leq \varpi_{n}^{max}(\omega) \perp -\delta_{n}(\omega) + \pi \geq 0, \forall n \backslash 1, \forall \omega. \tag{3.3v}$$

KKT conditions constraints:

$$\sum_{\omega \in \Omega^{\omega}} \gamma(\omega)[\pi_i^{max}(\omega) - \pi_i^{min}(\omega) + 2\lambda_i^{(2)G} r(\omega)(P_i^G + r_i^U(\omega) - r_i^D(\omega)] + \lambda_i^{(1)G} + \lambda_{n(i)}$$
$$+ \varphi_i^{max} - \varphi_i^{min} = 0, \forall i \tag{3.4a}$$
$$\alpha_l^W + \lambda_{n(l)} - \sum_{\omega \in \Omega^{\omega}} \gamma(\omega)\mu_{n(l)}(\omega) + \varsigma_l^{max} - \varsigma_l^{min} = 0, \forall l \tag{3.4b}$$
$$2\lambda_i^{(2)G}(P_i^G + r_i^U(\omega) - r_i^D(\omega)) + \lambda_i^{(1)G} + \pi_i^{max}(\omega) - \pi_i^{min}(\omega)$$
$$+ \mu_{n(i)}(\omega) + \sigma_i^{max}(\omega) - \sigma_i^{min}(\omega) = 0, \forall i, \forall n, \forall \omega \tag{3.4c}$$
$$2\lambda_i^{(2)G}(r_i^D(\omega) - P_i^G - r_i^U(\omega)) - \lambda_i^{(1)G} - \pi_i^{max}(\omega) + \pi_i^{min}(\omega)$$
$$- \mu_{n(i)}(\omega) + \beta_i^{max}(\omega) - \beta_i^{min}(\omega) = 0, \forall i, \forall n, \forall \omega \tag{3.4d}$$
$$\sum_{m \in \Theta_n} B_{nm}(\lambda_n - \lambda_m) + \sum_{m \in \Theta_n} B_{nm}(\psi_{nm}^{max} + \psi_{mn}^{min} - \psi_{mn}^{max} - \psi_{nm}^{min})$$
$$+ \xi_n^{max} - \xi_n^{min} - (\kappa_1^0)_{n=1} = 0, \forall n \tag{3.4e}$$
$$\sum_{m \in \Theta_n} B_{nm}(\mu_n(\omega) - \mu_m(\omega)) + \sum_{m \in \Theta_n} B_{nm}(\eta_{nm}^{max}(\omega) - \eta_{nm}^{min}(\omega)$$
$$- \eta_{mn}^{max}(\omega) + \eta_{mn}^{min}(\omega)) + \varpi_n^{max}(\omega) - \varpi_n^{min}(\omega) - \kappa_1(\omega)_{n=1} = 0, \forall \omega, \forall n \tag{3.4f}$$
$$- \lambda_{dj}^D + \lambda_{n(d)} + \phi_{dj}^{max} - \phi_{dj}^{min} = 0, \forall d, \forall j \tag{3.4g}$$

3.3.4 Relaxation Scheme

Due to the existence of the complementarity constraints, it is difficult to solve the MPEC (3.3a)-(3.3v) via standard NLP algorithms. Several more specialized algorithms for solving MPECs that take into account the particular structure of the additional complementarity constraints are known in the literature. These algorithms include smoothing, penalizing, lifting, relaxation (or regularization), and suitable modifications of standard NLP solvers. Among these MPEC-tailored solution schemes, the relaxation schemes are one of the most prominent classes of solution methods. Several different relaxation schemes are available, but the basic idea of all these relaxation methods is the same: approximate (usually enlarge) the feasible set of the MPEC in a suitable way to get a nonlinear program NLP(t) depending on a certain parameter t such that the relaxed programs NLP(t) converge to the original MPEC when t approaches zero. In this paper, we employ the first and most popular relaxation scheme, the global relaxation method by Scholtes [52, 53]. Algorithmically, we consider a sequence $t_s \to 0$ and for each s, relax each of the complementarity constraints in a way that is controllable by the choice of t_s. In our preceding MPEC problem, for instance, the complementarity condition (3.3c) can be approximated by the relaxation:

$$\phi_{dj}^{min} \geq 0, P_{dj}^{D} \geq 0, \phi_{dj}^{min} P_{dj}^{D} \leq t_s, \forall d, \forall j.$$

At each iteration s and the corresponding value of $t = t_s$, we then compute a sequence of KKT points of the relaxed nonlinear programs NLP(t_s), figure out the limiting point to which the sequence converges. The limiting point is then, under suitable conditions, a stationary point of the underlying MPEC.

In all existing works, the non-linear terms in the objective function of the reformulated problem are linearized using the strong duality theorem and the linearity in the objective function of the lower level problem as explained in [7]. Moreover the nonlinearity in the complementarity constraints are further linearised by using binary variables and some sufficiently large constants, resulting in solving a mixed integer linear program. The linearisation technique for the objective function, however, is only applicable for the case where the lower level problem is a linear program. Although one can still linearise the nonlinearity in the complementarity constraints, it would result in a mixed nonlinear integer program which is a nontractable NP hard problem. To the contrary, by the relaxation scheme, each relaxed problem is a standard well-behaved nonlinear program that can be easily solved by any commercial optimization toolbox. Although theoretically one needs to take a sequence of relaxation parameter $t_s \to 0$, in practice only a couple of these nonlinear programs are needed to be solved when the parameters t_s are chosen sufficiently small.

3.4 Case Study

The proposed model is illustrated by using the IEEE three-bus system shown in Fig. 3.1 and the IEEE 30-bus TS.

In our case studies, we compare the results for the strategic WPP and non-strategic WPP in the reserved and non-reserved markets. The reserved case requires solving the proposed model (3.3)-(4), while in the non-reserved case one needs to solve model (3.3)-(4) with all reserve variables and reserve constraints eliminated. Notice that the balancing prices $\mu_n(\omega)$ in the reserved case becomes a constant to be specified in the non-reserved case since it can no longer be derived as dual variables. We also compare the results for the strategic and non-strategic cases. In the strategic WPP case, we solve the model (3.3)-(4), whereas in the non-strategic WPP case we solve a modified model (3.3)-(4) in which we assume that the WPP's offer price α_l^W is zero, and the offered power $P_l^{W,Of}$ equals to its expected production.

3.4.1 Wind Speed Data

Although the market we modelled is not the European one, since it is easier to access the wind speed data from Copenhagen, we have used the historical wind speed data of the 14 representative days in June 2013 collected from Copenhagen in the following two case studies. To further represent the uncertain wind power, each original scenario is then multiplied by 0.8 and 1.2 respectively, resulting in a total of 42 scenarios for each hour and the 42 scenarios change throughout the 24 hour planning horizon. The wind speed of each hour is transformed into wind power production using the wind-speed/wind-power production curve of a Nordex N80/2500 turbine. The wind power production are used as input scenarios of the two case studies. All scenarios are assumed to have the same weight.

3.4.2 IEEE three-bus System

Table 3.1: DATA FOR THE GENERATING UNITS OF THE IEEE THREE-BUS SYSTEM

Generator(i)	Gen1	Gen2	Gen3
$\bar{P}_i^G$[MWh]	150	200	250
$\lambda_i^{(2)G}$	0.02	0.0175	0.065
$\lambda_i^{(1)G}$	20	20	20
$\lambda_i^{(0)G}$	0	0	0
$r_i^{U,max}$[MW]	23	16	37
$r_i^{D,max}$[MW]	23	16	37

The three-bus system contains one conventional generation unit per bus (G1 through G3) and one wind power plant (WP). All lines have the same susceptance of 2.5 p.u. Detailed data for the conventional generators on the three-bus system is shown in Table 3.1.

There are three load demands in this system (L1-L3). Table 3.2 shows demand bids including energy and price as observed through a 24 hour planning horizon. We assume that offers from the conventional generators are constants and that bids from the load demands

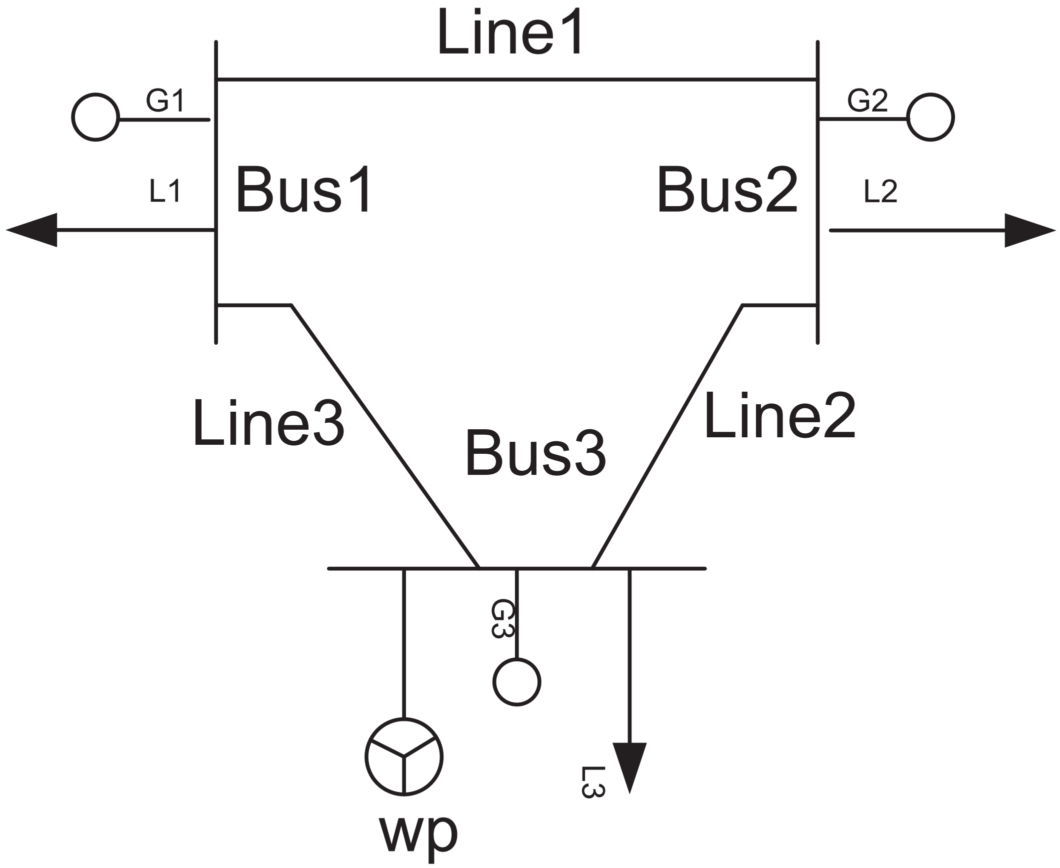

Figure 3.1: IEE three-bus system

are those in the first two rows multiplied by the hourly demand factors as shown in Fig. 3.2. The wind plant with an installed capacity of 150 MW is physically located on bus 3.

Table 3.2: DATA FOR THE DEMANDS OF THE IEEE THREE-BUS SYSTEM

Demand(d)	Demand1	Demand2	Demand3
$\bar{P}^D_{d1}$[MW]	30	40	40
$\bar{P}^D_{d2}$[MW]	40	60	10
λ^D_{d1}[$/MWh]	41.7	45.6	53.5
λ^D_{d2}[$/MWh]	38.3	74.4	46.5

We set all the transmission line capacity limits sufficiently large in order to eliminate congestions. Consequently we obtain identical day-ahead price of $118.80/MWh for each bus at hour 21. The wind power offer is 130.200 MWh, with the corresponding bidding price

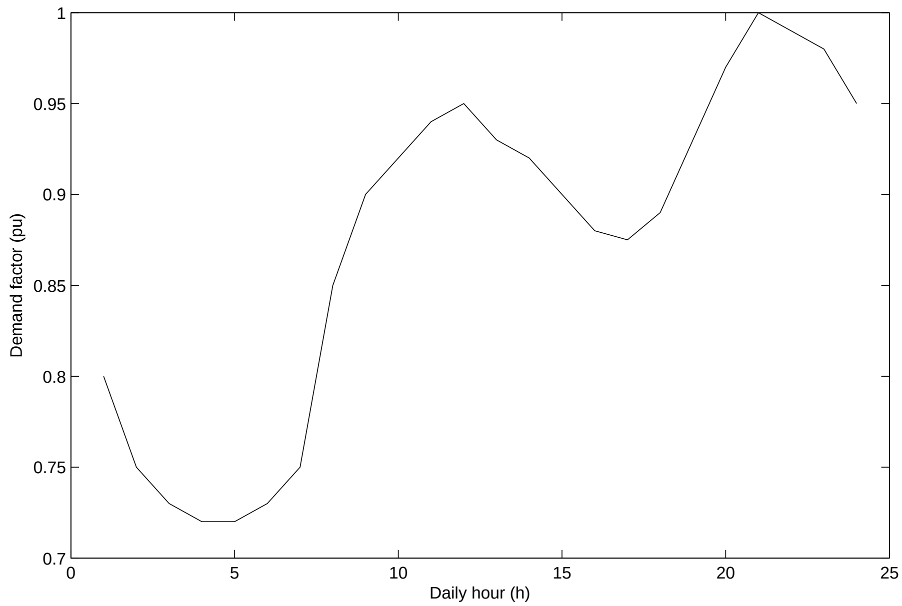

Figure 3.2: Hourly demand factors

of \$139.504/MWh. In our work, the wind power offer price is different from the day-ahead price of the bus that contains the wind power plant, whereas in the reference [7], the wind power offer price is equal to the day-ahead price. The reason of the difference between offer price and the day-ahead price can be explained by the K.K.T constraint (3.4a) which not only considers the day-ahead prices λ, but also integrates the influence of balancing prices $\mu(\omega)$. Similar simulation results are further shown in Fig. 3.3. When we set the balancing price as given data instead of a variable, we can obtain the same conclusion as [7], in which the lower level problem includes just the day-ahead price, while the balancing price is obtained from the historical data. No transmission congestion occurs when we fix all lines with identical transmission capacity at 130 MW, as shown in Table 3.3. From this table, we observe different prices for different scenarios on the same bus but same balancing price for different buses under the same scenario. This shows the effects of no transmission congestion.

We now investigate the bidding strategy for the strategic WPP throughout the 24 hours planning horizon. We fix all line capacity at 130 MW. Working with the above data, we calculate the offer prices (the upper plot of Fig. 3.3) and the wind power offered (Fig. 3.4) of the strategic WPP. The lower plot of Fig. 3.3 depicts the LMP on bus 3. The offer price (shown in Fig. 3.3) changes with the variation in demands throughout the day. We observe that the offer price and the demand have a similar profile. Fig. 3.3 also confirms that by

Table 3.3: DAY-AHEAD AND BALANCING PRICE WITH 130 MW TRANSMISSION LINE CAPACITY OF THE THREE-BUS SYSTEM AT HOUR 21 [$/Mwh]

Buses	Bus 1	Bus 2	Bus 3
λ_n	118.800	118.800	118.800
$\mu_n(1)/scenerio1$	-20.132	-20.132	-20.132
$\mu_n(4)/scenerio4$	-24.719	-24.719	-24.719
$\mu_n(9)/scenerio9$	19.709	19.709	19.709
$\mu_n(12)/scenerio12$	20.000	20.000	20.000

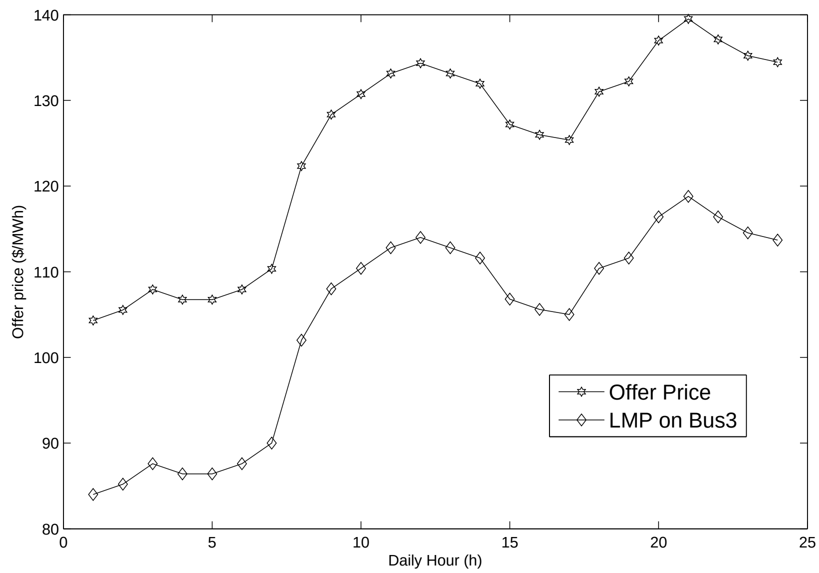

Figure 3.3: Strategic wind power producer's offer prices and resulting LMP on Bus3

exercising its market power, the strategic WPP is able to bid offering prices higher than the resulting LMPs, and the reason is stated in the last paragraph.

Concerning the wind power offered as shown in Fig. 3.4, the strategic WPP offers a more stable power level to the day-ahead market throughout the whole day, compared to the non-reserve case in [7, upper plot of Fig. 2]. This is mainly due to the reserve operation in the real-time market. In the proposed market environment, even though the strategic WPP is aware of the potential risks posed by a lower/higher scheduled wind power production than its actual production, the strategic WPP believes that the reserve operation in real-time market can effectively compensate the production deviation, thus can trustingly offer a

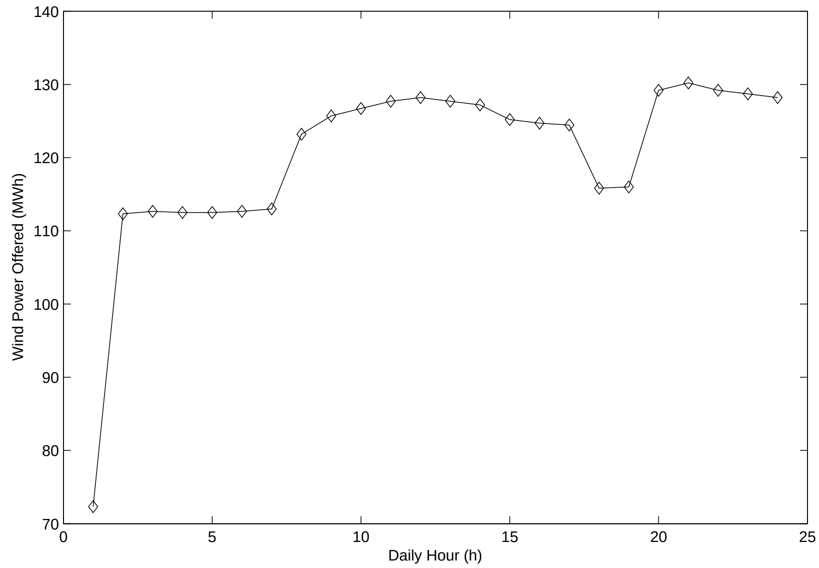

Figure 3.4: Strategic wind power producer's wind power offered

more stable production level to the day-ahead market basically only in terms of the demand changes.

Since the power offered to the day-ahead market by the strategic WPP, which equals to the cleared wind power in our case, is fairly stable, it results in a steady expected gain obtained by the strategic WPP in each hour, which can be seen in Fig. 3.5.

Another issue is that, since in this paper we highlight the offering strategy, it is very important to make a comparison of the profits obtained by strategic WPPs and non-strategic WPPs. By adopting a strategic behavior, the WPP increases its expected profit by 17.33%, precisely from $238910.70 to $280321.13.

Transmission line capacity is critical to the wind power introduction. To study the transmission line capacity's influence on the strategic WPP's strategy, we impose the transmission capacity limit of all lines as 100 MW. In this case, transmission congestion occurs in some hours and scenarios, which causes different LMPs at different buses. Concerning the expected profit, the WPP has a 23.65% profit reduction from $280321.13 down to $214077.17, as a result of the transmission congestion and difference in LMPs.

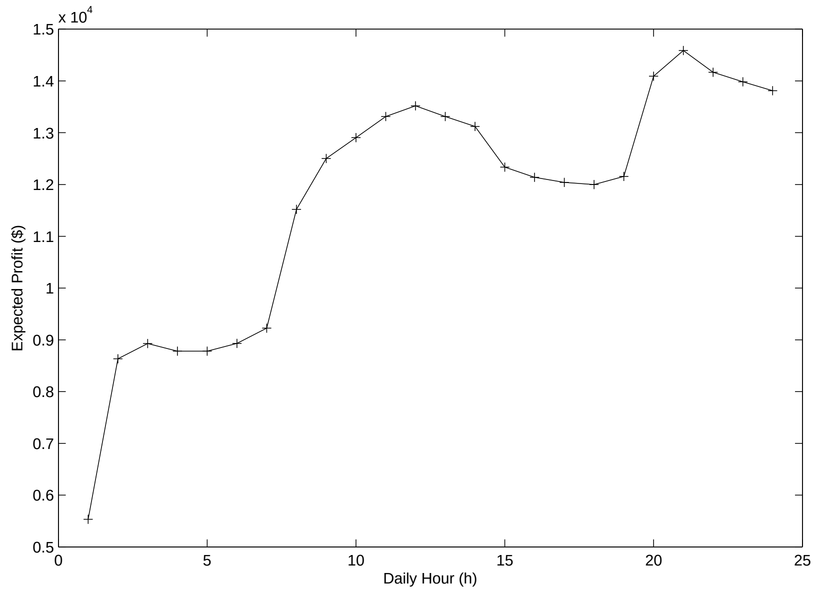

Figure 3.5: Daily expected profit of the strategic WPP

3.4.3 IEEE 30-bus TS

In this section, additional simulations are carried out on the IEEE 30-bus TS with data obtained from the reference. Prices offered by demand are within the range $100-140 per MWh. First we compare the expected profit for the reserved and the non-reserved case. Assume the strategic WPP owns a wind farm at bus 3. We observe from the simulation that the expected profit of the strategic WPP increases from $2123.63 to $3107.07 with a growth rate of 46% at hour 16, compared to the non-reserved case.

Table 3.4: STRATEGIC AND NON-STRATEGIC WPPs LOCATED AT BUS 16 AT HOUR 16 [$/Mwh]

Cases	Expected profit	Social welfare	Generation cost
Strategic WPP	3329.68	45970.00	61916.24
Non-strategic WPP	2904.76	74410.00	92585.54
Increment	14.66%	-38.22%	-33.13%

Table 3.4 shows the difference of expected profit, social welfare and generation cost between strategic WPP and non-strategic WPP. From this table we observe that, the WPP adopting strategic offering has 14.66% higher expected profit than the non-strategic WP-

P. Besides, strategic offering effectively reduces the generation cost by 33.13% in this case. Meanwhile, the social welfare also declines from $74410 to $45970 as a result of the strategic behavior of the WPPs.

Table 3.5: EXPECTED PROFITS FOR STRATEGIC AND NON-STRATEGIC WPPs AT HOUR 16 [$/Mwh]

Buses	Bus 3	Bus 12	Bus 15
Strategic WPP	3107.37	3932.94	5529.63
Non-strategic WPP	2973.53	2775.97	4470.47
Increment	4.5%	41.68%	23.69%

To show the influence of locations of wind farms on the expected profit between strategic and non-strategic bidding, we assume that the WPP owns a wind farm located at bus 3, bus 12 and bus 15, respectively. In Table 3.5 we report the expected profits of the strategic and the non-strategic WPPs at hour 16. We observe that the profit of the strategic WPPs increases by 4.5%, 41.68% and 23.69% at bus 3, bus 10, and bus 15 respectively, comparing with the non-strategic WPP. The analysis indicates that the expected profit depends on the location of wind farms in the power system network.

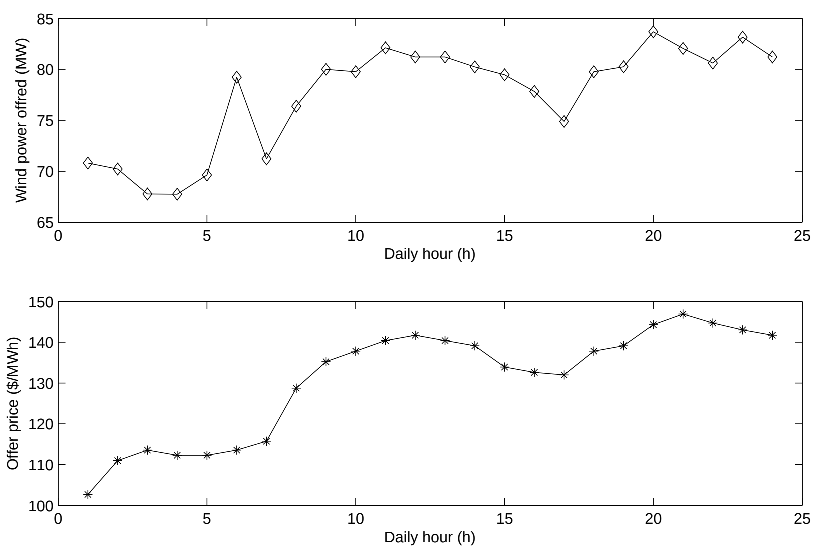

Figure 3.6: Wind power offered and offer prices at bus-10

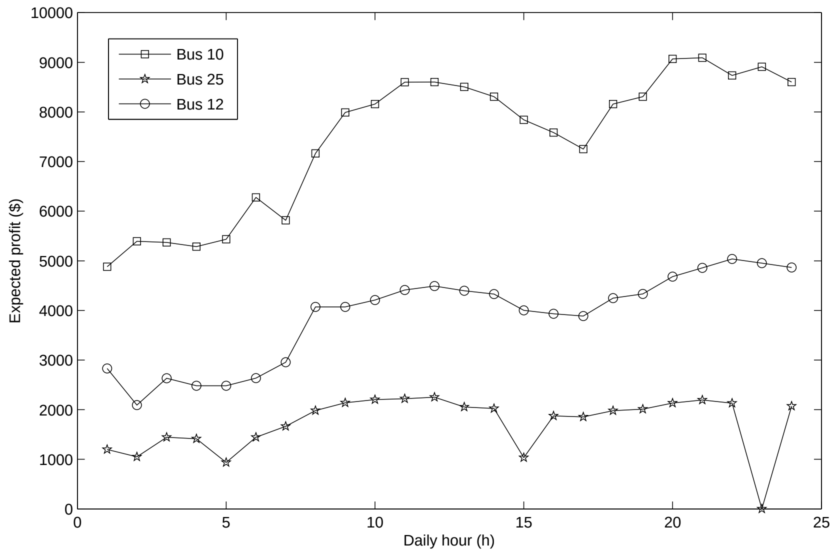

Figure 3.7: Expected profit at different buses

In Fig. 3.6 we show the wind power offered to the day-ahead market and the offer prices over the whole day (24 hours), which are depicted at the upper and the lower plots, respectively. It is interesting to see that the profiles of the wind power offered and offer prices are similar to the demand factors, but not exactly the same. This is reasonable since the strategic offer is not only influenced by the demands, but also depends on the uncertainty of wind power productions. Similar to the three-bus test case, the wind power offered is rather steady over the 24 hours due to the presence of reserve.

To study the dependence of expected profits on location, first we investigate the influence of transmission network configuration on WPP's profits. We set a farm at bus 10, 25 and 12 successively, with the installed capacity of 1500 MW. Initially, the transmission capacity of each branch connected to bus 10, bus 12 and bus 25 is 65 MW, 32 MW, and 16 MW respectively. The expected profits are shown in Fig. 3.7. According to this figure, it is obvious that the trends of the expected profits at the different buses are very similar, but the values are different significantly. This can be explained as follows. High wind power production at bus 25 leads to the higher probability of network congestion than the other two due to the lower transmission capacity connected. The consequent LMP difference between bus 25 and the rest of the system explains the profit difference in Fig. 3.7. If we increase the transmission line capacity connected to bus 25 to 32 MW, the profit of WPP will rise from \$1309 to \$1335 at Hour 16.

Further we consider the influence of demand variation on WPP's profits. To this end we increase the load on bus 25 from 20 MW to 40 MW, 50 MW, and it results in the growth of expected profit from $2205 to $2563.04, $2955 respectively at Hour 16. The strategic WPP expects to make more profits in the area where there is high demand.

To conclude, for better profit the WPP should choose a location with high demand and well-connected to the system to build the wind farms.

3.4.4 Computational Performance

Results for the three case studies are obtained under GAMS [54] on a Windows-based desktop PC with AMD Athlon II X2 B26 processor clocking at 3.20 GHz and 12 GB installed memory. The computation time required to obtain the optimal solution for the three-bus system and the IEEE 30-bus RTS are 6.52 and 35.2 s, respectively.

3.5 Conclusion

A new stochastic bilevel model for a strategic WPP taking into account wind power production uncertainty has been proposed in this work. This strategic WPP participates as a price-maker in the day-ahead market, and a deviator in the balancing market to compensate for production deviations due to wind power uncertainty. The lower level problem co-optimizes energy and reserve and determines the day-ahead prices and the balancing prices. The proposed stochastic bilevel model is reformulated as a solvable stochastic MPEC and solved using a relaxation method. The following conclusions can be obtained from the three-bus and IEEE 30-bus test systems case studies:

1) The proposed model in this paper has an advantage in that the strategic WPP can make more informed decisions. In particular, they can derive the day-ahead clearing price and predict the balancing price to help making the day-ahead offer.

2) The proposed stochastic bilevel model with quadratic generators cost functions is solved via a relaxation scheme which can reduce errors in piecewise linear approximation and avoid introducing new constraints and variables.

3) The strategic offering can increase the expected profit, reduce the conventional generators cost and decrease the social welfare, compared with the non-strategic WPP.

4) The increment of the strategic WPP's profit over non-strategic WPPs depends on the strategic behavior. The amount of increment is different when the wind farm is connected to different buses.

5) The strategic WPP makes more steady expected profit in a reserved market than in a non-reserved market. In other words, considering the operation of the reserve market can reduce the risk of the day-ahead offer.
6) In the clearing algorithm, if other constraints such as voltage constraints and reactive power output constraints are considered, the lower level program will not be a convex problem. In future work, we will set AC-OPF as the lower level problem and consider solving the corresponding bilevel problem.

Chapter 4

Coordinating Transmission Expansion Planning and Wind Power Investment with Co-optimization of Energy and Reserve

Chapter 3 solves the problems of wind power producers' participation in the electric markets like other traditional power producers. Actually most suitable wind power sources are usually far away from the loads areas, and therefore transmission planning is critical for wind power investment. Hence, this chapter proposes a new model which coordinators transmission expansion planning and wind power investment, as well as takes into account of operations of energy and research in transmission planning. The proposed new model of transmission planning can effectively improve wind power investment, also provide reserve assessment for the uncertainty of wind power production.

4.1 Introduction

4.1.1 Motivation and Aim

Recently, wind power is rapidly introduced into power systems because of the improved wind turbine technology, higher fossil fuel prices, government subsidies, and other policy incentives [55]. In 2002 U.S.A. passed legislation (SB1078) that created the California Renewable Portfolio Standard (RPS). California Independent System Operator (CAISO) is currently developing transmission planning to increase renewable energy generation from the current 20% to 33% by 2020 in accordance with RPS. This law requires the investor-owned utilities (IOUs) to increase their procurement of renewable energy to 20%, based on the total energy they deliver to customers by 2017 [56]. However, [57] shows only a large amount of investment on transmission investment can satisfy the requirement of future loads growth and RPS. A big concern on introducing wind power into electricity power system is the lack of transmission capacity due to that most suitable wind energy is located far away from the load centers [58, 59], and aggregating renewable energy will require significant expansion in transmission infrastructure. Therefore, wind power integration heavily depends on transmission capacity planning. To break the impasse between transmission and wind generation development, Texas passed Bill 20 to build Completive Renewable Energy Zones (CREZ) [60].

Based on the policy like RPS, for Independent System Operators (ISOs), the decision-maker on transmission expansion investment should not only consider meeting future loads requirement, but also take into account wind power investment. [61] applied a mathematical program with equilibrium constraints (MPEC) method to solve the joint model of transmission and wind power investment. However, high penetration of wind power is bringing significant challenges to power system operation and transmission planning. To serve load reliably and keep the grid stable, operating reserve is secured by power system operators to compensate for uncertainties due to wind power [62]. The reserve assessment is very needy for transmission planning. Reference [63] discussed the necessity of integrating the operation into transmission planning due to advanced unit commitment and reserve scheduling to deal with the uncertainties of wind power and loads forecast.

As reserve is necessary to deal with uncertain wind power in the operation and planning of power system, this paper integrates operating reserve into the problem of transmission expansion planning and wind power investment, and calculates the reserve requirement for transmission system capacity expansion. In this paper we set the objective function of transmission expansion planning to minimize the social cost including transmission investment cost, wind power investment and load shedding cost. The bilevel method is applied to handle the interaction between system planning and operation. While, realizations of uncertain wind power happen after the period of energy and reserve scheduled in the day-ahead market. Therefore, we employ two-stage stochastic programming to address the economic dispatch problem of energy and reserve in the lower level problem.

4.1.2 Literature Review and Contributions

Electricity market is composed of independent power producers, transmission facilities owners, large consumers and ISOs [64]. ISOs as non-profit organizations are responsible for clearing the market, monitoring the grid, ensuring reliable and economic operation, conducting the transmission planning and operating with the ultimate goal of facilitating the trading of electric energy. In the literature, many optimization approaches have been presented for transmission expansion planning. Transmission expansion planning is a nonlinear mixed integer constrained programming, and a large number of research work have been carried out [65–70]. Paper [65] studies the coordination of conventional generation and transmission expansion planning, investigating interaction between generation and transmission sections regarding optimal development of the system. Recently integrating renewable energy is becoming a big concern for transmission expansion planning. For example, most wind power resources are remote from load centers or existing transmission corridors. To integrate wind energy into transmission planning, some planners propose planning transmission lines to promote wind power investment [61]. In the literature, [66] develops a chance constrained transmission network expansion planning model considering wind power and loads, which sets the non-overloaded probability of transmission power flow less than a specific value in the constraints of the proposed optimization model. Reference [67] uses two-stage stochastic programming to solve the problem of transmission expansion planning with uncertain wind power and loads, where transmission investment decision is determined in the first stage, and the second stage is related to an operation problem traversing all different uncertainty scenarios. [68] also proposes a stochastic two-stage optimization model to model transmission planning, where the transmission planners make transmission investment in two time periods, and each time period is followed by a market response in the seconde stage. The paper [69] develops probabilistic transmission expansion planning considering uncertain load and wind power, and the probability of load curtailment exceeding a specified limit is included in the problem formulation. And [70] adopts the line capacity expansion and transmission switching method to integrate large scale wind power, which can deal with remote wind power sources.

Lately, mathematical optimization with equilibrium has been popular in solving more complicated electricity market problems. The paper [71] considers a mixed integer bilevel programming model in which the leader makes capacity expansion decisions in the fuel transportation, generation, and transmission infrastructure of the electricity supply network to maximize social welfare less investment cost. The leader-followers game method has been adopted by [72] to solve the problem of transmission expansion planning in an environment where there is imperfect competition in electricity industry. Paper [73] develops a three-level equilibrium model for expansion of an electric network, where the upper-level representing transmission investment takes into account Nash equilibrium in generation, and considers pool-based market equilibrium in the lower-level model. Transmission expansion planning in [74] is modeled as a four-level optimization problem, where transmission expansion planner makes investment decisions based on GenCon's decisions, bids and market outcomes.

No papers in the literature studying transmission expansion planning problems has considered wind power investment, together with operating energy and reserve economic dispatch. This paper proposes a bilevel problem with stochastic two-stage programming to model the transmission expansion planning problem integrating wind power investment, and the economic dispatch of energy and reserve. Details of the proposed model will be introduced in next section. The contributions of this chapter are summarized as follows.
1)Combine a bilevel problem with two-stage stochastic programming to formulate the problem of transmission expansion planning considering wind power investment, together with co-optimization of energy and reserve;
2) Calculate the reserve requirement for the expansion of transmission planning and wind power integration;
3) Reformulate the primal mixed-integer bilevel problem into into MINLP problem by the global relaxation;
4) Applied our proposed model on the illustrative case studies.

4.2 Mathematical Formulation

The overall hierarchical structure is a bilevel problem with a two-stage stochastic programming as the lower-level problem of the bilevel problem. The two-stage stochastic programming represents energy schedule and reserve dispatch in the first stage and the second stage separatively, where the second stage works for the specific wind power realization under different scenarios. The bilevel problem shows the strategy of both transmission planing and wind power investment considering the operation of power system.

The main model assumptions are listed below:
1) A direct current optimal power flow (DC-OPF) model without losses is used to represent the constrained network for transmission expansion planning, and wind power investment and power system operation.

2) To simplify the proposed model, we do not consider n-1 contingency constraints.
3) Wind power uncertainty can be represented by a finite set of scenarios. This assumption makes the proposed the bilevel problem with two stage stochastic programming model computationally solvable.
4) Only wind power uncertainty is considered. However, some other uncertainties such as equipments failure, demand uncertainty can be easily integrated into the proposed model through scenarios.
5) To simplify the main model, nonconvex constraints, such as ramping rates, startup costs and time, minimum down-time, are not included in the operation model of the lower level problem. These constrains can be further discussed in future work.
6) Operating reserve considered in this paper considers is focused on spinning reserves, because spinning reserve can response sufficiently fast to the power imbalance due to wind power uncertainties [49]. Therefore, we just take spinning reserve into account for the uncertainties of wind power.

4.2.1 Notation

Symbol	***Indices and Sets***:
n,m	Index for buses.
i	Index of candidate generating units.
d	Index of demands.
ξ	Index for uncertain scenarios.
Ω^N	Set of indices of buses.
Ω^D	Set of indices of demands.
Ω^T	Set of indices of periods.
Ω^ξ	Set of indices of scenarios.
Ω^G	Set of generation units.
θ_n	Set of the buses connected to the bus n.
Ω_n^D	Set of indices of demands located on the nth bus.
Ψ_n^G	Set of generation units located by the nth bus.
Δ^{UL}	Set of the optimization variables of the upper level problem.
$\Delta^{LL,f}$	Set of the optimization variables of the fist stage of the lower level problem.
$\Delta^{LL,s}$	Set of the optimization variables of the second stage of the lower level problem.
λ_i^G	Marginal cost by the ith generation unit.
λ_i^{UP}	The offer cost of spinning reserve up supplied by the ith generation unit.

λ_i^{DO}	The offer cost of spinning reserve down supplied by the ith generation unit.
C_L^B	Maximum transmission investment budget by the ISO.
C_W^B	Maximum wind power investment budget by the wind power investor.
c_{nm}^{line}	Cost of a line added to the $n-m$ right of way.
c_n^{wind}	Unit wind power investment cost at bus n.
c_n^W	Unit wind power production cost at bus n.
$c_n^{w,spi}$	Unit wind power spillage cost at bus n.
$k_n^W(\xi)$	Wind power availability in scenario ξ.
c_d^{shed}	Unit load shedding cost of the dth demand.
x_{nm}^0	Number of existing lines between n and m buses.
$\pi(\xi)$	Possibility of scenario ξ.
$Q(\xi)$	Operation cost of system in scenario ξ.
$\overline{P}_i^G$	Maximum Power scheduled to be produced by the ith generation unit.
$R_i^{UP,max}$	Maximum spinning reserve up scheduled for unit i.
$R_i^{DO,max}$	Maximum spinning reserve down scheduled for unit i.
$X_n^{W,max}$	Maximum wind power capacity that can be installed at bus n.
$\overline{x}_{nm}$	Maximum number of prospective lines between n and m bus.
$T_{nm}^{E,max}$	Existing transmission line capacity line $n-m$.
$T_{nm}^{N,max}$	Prospective transmission line capacity line $n-m$.
B_{nm}^N	Susceptance of prospective $n-m$ line.
B_{nm}^E	Susceptance of existing $n-m$ line.

Symbol	***Variables***:
x_{nm}	Number of prospective lines between the bus m and n.
X_n^W	Wind power capacity to be built at bus n.
R_i^{UP}	Spinning reserve up scheduled for unit i.
R_i^{DO}	Spinning reserve down scheduled for unit i.
$r_i^{UP}(\xi)$	Spinning reserved up deployed by unit i in scenario ξ.
$r_i^{DO}(\xi)$	Spinning reserved down deployed by unit i in scenario ξ.
$L_d^{shed}(\xi)$	Load shedding of demand d in scenario ξ.
$P_n^{W,s}$	Wind power scheduled to market at bus n.
$P_n^{W,spi}(\xi)$	Wind power spillage to market under the scenario ξ at bus n.
$\delta_n(\xi)$	Angle of the nth bus in the day-ahead market under the scenario ξ.
$P_i^{G,s}$	Power scheduled to be produced by unit i.
$\lambda_n(\xi)$	Day-ahead price of the nth bus under the scenario ξ.
$w_{nm}(\xi)$	Power flow of existing $n-m$ line under the ξ scenario.
$f_{nm}(\xi)$	Power flow of prospective $n-m$ line under the ξ scenario.

4.2.2 Bilevel problem incoporating two-stage stochastic programming

The Senate Bill 20 instructed the Public Utility Commission of Texas (PUCT) to establish Competitive Renewable Energy Zones (CREZ) throughout the State, and to designate new transmission projects to serve these zones. To fulfill the requirement of this Bill 20, ERCOT must design transmission expansion planning to connect these areas to loads [75]. Transmission system planning has mutual effect on the operations of systems and markets, and hence static planning is hard to satisfy the real requirements. A bilevel formulation can solve the interaction between system planning including transmission and wind power investment, and the operations of system including the dispatch of energy and reserve. A two-stage stochastic programming can simultaneously dispatch energy and reserve, which effectively reduces the total dispatch cost. Therefore, we propose a method of bilevel formulation with two stage stochastic programming to effectively solve the problems of modern transmission expansion planning facing the deregulated electric markets and the renewable energy integration. Specifically, in the upper level problem, ISOs make transmission expansion decisions considering wind power investment to minimize the social cost, and the objective function of the upper level problem includes the cost of wind power investment and transmission expansion planing, as well as the reliability cost of annual expected load shedding. The upper level problem is given by:

$$\min_{\Delta^{UL}} \sum_{n\in\Omega^N} \sum_{m\in\theta_n} c_{nm}^{line} x_{nm} + \sum_{n\in\Omega^N} c_n^{wind} X_n^W + \kappa \sum_{\xi\in\Omega^\xi} \pi(\xi) \sum_{d\in\Omega^D} c_d^{shed} L_d^{shed}(\xi) \tag{4.1a}$$

subject to

$$\sum_{n\in\Omega^N} \sum_{m\in\theta_n} c_{nm}^{line} x_{nm} \leq C_{max}^{line} \tag{4.1b}$$

$$0 \leq \sum_{n\in\Omega^N} c_n^{wind} X_n^W \leq C_{max}^{wind} \tag{4.1c}$$

$$0 \leq X_n^W \leq X_n^{W,max}, \forall n \tag{4.1d}$$

$$0 \leq x_{nm} + x_{nm}^0 \leq \overline{x}_{nm}, \forall n, \forall m \in n \tag{4.1e}$$

$$x_{nm} \in \{0,1\}, \forall n, \forall m \in n \tag{4.1f}$$

where $L_d^{shed}(\xi)$ is from the second stage of the following lower level problem and κ is time horizon ratio between load shedding and transmission expansion planning. In this model load shedding works in hours while transmission expansion planning consider the target year, so κ is fixed to be equal to 8760.

ISOs like ERCOT operate voluntary day-ahead energy and ancillary services market with bid-based security constraint unit commitment, and co-optimization of energy and reserves, based on bids and offers from loads and generators. Therefore, the lower level problem is a two-stage stochastic programming problem, where the first stage represents energy and reserve schedule in the electricity market, and the second stage shows the operation of power system operation and physical limitations.

$$\min_{\Delta^{LL,f}} \sum_{i\in\Omega^G} (\lambda_i^G P_i^{G,s} + \lambda_i^{UP} R_i^{UP} + \lambda_i^{DO} R_i^{DO}) + \sum_{n\in\Omega^N} c_n^W P_n^W + \sum_{\xi\in\Omega^\xi} \pi(\xi) Q(\xi) \tag{4.2a}$$

subject to

$$\sum_{n\in\Omega^n} \sum_{i\in\Psi_n^G} P_i^{G,s} + \sum_{n\in\Omega^n} P_n^{W,s} = \sum_{n\in\Omega^n} \sum_{d\in\Psi_n^D} P_d^D : \chi \tag{4.2b}$$

$$0 \le P_n^{W,s} \le X_n^W : \varrho_n^{min}, \varrho_n^{max}, \forall n \tag{4.2c}$$

$$0 \le P_i^{G,s} \le \overline{P}_i^G : \vartheta_i^{min}, \vartheta_i^{max}, \forall i \tag{4.2d}$$

$$0 \le R_i^{UP} \le R_i^{UP,max} : \zeta_i^{min}, \zeta_i^{max}, \forall i \tag{4.2e}$$

$$0 \le R_i^{DO} \le R_i^{DO,max} : \eta_i^{min}, \eta_i^{max}, \forall i \tag{4.2f}$$

where, $Q^(\xi)$ is equal to

$$\min_{\Delta^{LL,s}(\xi)} \sum_{i\in\Omega^G} \lambda_i^G \big(r_i^{UP}(\xi) - r_i^{DO}(\xi)\big) + \sum_{n\in\Omega_n} c_n^{w,spi} P_n^{W,spi}(\xi) + \sum_{d\in\Omega^D} c_d^{shed} L_d^{shed}(\xi) \tag{4.2g}$$

subject to

$$\sum_{i\in\Psi_n^G}\left\{P_i^{G,s}+r_i^{UP}(\xi)-r_{ib}^{DO}(\xi)\right\}+k_n^W(\xi)X_n^W-P_n^{W,spi}(\xi)$$

$$-\sum_{d\in\Psi_n^D}\left(P_d^D-L_d^{shed}(\xi)\right)=\sum_{m\in\theta_n}\left(f_{nm}(\xi)+w_{nm}(\xi)\right):\alpha_n(\xi),\forall n,\forall\xi \tag{4.2h}$$

$$w_{nm}(\xi)-B_{nm}^E x_{nm}^0\Big(\delta_n(\xi)-\delta_m(\xi)\Big)=0:\varphi_{nm}(\xi),\forall n,\forall m\in n,\xi \tag{4.2i}$$

$$f_{nm}(\xi)-B_{nm}^N x_{nm}\Big(\delta_n(\xi)-\delta_m(\xi)\Big)=0:\beta_{nm}(\xi),\forall n,\forall m\in n,\xi \tag{4.2j}$$

$$-T_{nm}^{E,max}\le w_{nm}(\xi)\le T_{nm}^{E,max}:\psi_{nm}^{min}(\xi),\psi_{nm}^{max}(\xi),\forall n,\forall m\in n,\xi \tag{4.2k}$$

$$-T_{nm}^{N,max}\le f_{nm}(\xi)\le T_{nm}^{N,max}:\rho_{nm}^{min}(\xi),\rho_{nm}^{max}(\xi),\forall n,\forall m\in n,\xi \tag{4.2l}$$

$$0\le P_i^{G,s}+r_i^{UP}(\xi)-r_i^{DO}(\xi)\le\overline{P}_i^G:\phi_i^{min}(\xi),\phi_i^{max}(\xi),\forall i,\forall\xi \tag{4.2m}$$

$$0\le L_d^{shed}(\xi)\le P_d^D:\nu_d^{min}(\xi),\nu_d^{max}(\xi),\forall d,\forall\xi \tag{4.2n}$$

$$0\le P_n^{W,spi}(\xi)\le k_n^W(\xi)X_n^W$$

$$:\varpi_n^{min}(\xi),\varpi_n^{max}(\xi),\forall n,\forall\xi \tag{4.2o}$$

$$0\le r_i^{UP}(\xi)\le R_i^{UP}:\nu_i^{min}(\xi),\nu_i^{max},\forall i,\forall\xi \tag{4.2p}$$

$$0\le r_i^{DO}(\xi)\le R_i^{DO}:\tau_i^{min}(\xi),\tau_i^{max}(\xi),\forall i,\forall\xi \tag{4.2q}$$

$$\delta_1(\xi)=0:\kappa_1(\xi),\forall\xi \tag{4.2r}$$

$\}$

where the optimization variables of the upper-level problem are $\Delta^{UL}=\{x_{nm},\forall n,\forall m\in n;X_n^W,\forall n;\}$, and the optimization variables of the lower-level problem are composed of the first stage variables: $\Delta^{LL,f}=\{P_i^{G,s},R_i^{UP},R_i^{DO},\forall i;P_n^{W,s},\forall n;\}$ and the second stage variable: $\Delta^{LL,s}(\xi)=\{r_i^{UP}(\xi),r_i^{DO}(\xi),\forall i,\xi;P_n^{W,spi}(\xi),\forall n,\xi;L_d^{shed}(\xi),\forall d;\delta_n(\xi),\forall n,\xi;f_{nm}(\xi),w_{nm}(\xi),$ $\forall n,\forall m\in n,\xi\}$.

The upper level problem is to determine the transmission expansion planning that includes the binary decisions $x_{nm}\in\{0,1\}$, subject to a collection of the investment constraints (4.1a)-(4.1f). The objective function in (4.1a) aims to minimize the transmission investment cost, wind power investment cost and load-shedding cost. Constraints (4.1b) and (4.1c) impose an upper bounds on the investment cost of transmission lines and wind power separately, and the constraints (4.1d) express the limits on the capacity installed at each bus. Constraints (4.1e) represent the limits of the number of lines that can be added to between buses n and m, and constraints (4.1f) translate decision-making in building transmission lines to binary variables.

The lower level problem will make the decisions on energy schedule and reserve dispatch for the wind power forecast under each scenario ξ. The lower level problem consists of a two stage stochastic programming problem, where the first stage is composed of (4.2a)- (4.2f) and the second stage includes (4.2g)-(4.2r). The objective function (4.2a) of the lower level problem is to minimize the generation scheduled cost, reserve up and reserve down scheduled cost, and expected dispatch cost of the second stage. (4.2b) represents the day ahead market equilibrium. Constraints (4.2c) represent the wind production level offered to the day ahead market must be nonnegative and equal to or lower than the wind power capacity installed at each bus. Constraints (4.2d) represent the limits of generation scheduled in the day ahead market. (4.2e) and (4.2f) set the limits of research-up and reserver down separately. The objective function (4.2g) is to minimize the social cost under the specific demand scenario. Constraints (4.2h) guarantee the power balance at each bus of the power system. Equality constraints (4.2i) and (4.2j) represent the power flow of existing lines and perspective lines respectively, while constraints (4.2k) and (4.2l) impose the limits for existing and planning lines separately. (4.2n) show the upper and lower boundary of load shedding. Wind power spillage limits are shown in the constraints (4.2o). (4.2p) and (4.2q) link the real time reserve up and reserve down with scheduled reserve-up and reserve-down. Constraints (4.2m) confine the generation production.

4.2.3 Stochastic MPEC for Bilevel Problem

The two-stage stochastic programming problem (4.2) is equivalent to the following deterministic formulation.

$$\min \sum_{i\in\Omega^G} \varpi_i^G P_i^{G,s} + \lambda_i^{UP} R_i^{UP} + \lambda_i^{DO} R_i^{DO} + \sum_{n\in\Omega^N} c_n^W P_n^W + \sum_{\xi\in\Omega^\xi} \pi(\xi) \Big\{ \sum_{i\in\Omega^G} \lambda_i^G \big(r_i^{UP}(\xi) - r_i^{DO}(\xi) \big) + \sum_{n\in\Omega_n} c_n^{w,spi} P_n^{W,spi}(\xi) + \sum_{d\in\Omega^D} c_d^{shed} L_d^{shed,(t)}(\xi) \Big\} \tag{4.3a}$$

subject to

$$Constraints: (4.2b) - (4.2f); \tag{4.3b}$$

$$Constraints: (4.2h) - (4.2r); \tag{4.3c}$$

As the lower-level problem is perfectly linear, the bi-level model including the lower-level problems (4.3) and the upper-level problems (4.1) can be recast as a single-level mathematical problem by representing the lower-level mathematical program with equilibrium constraints (MPEC) by its Karush-Kuhn-Tucker (KKT) optimality conditions. Therefore, the primal bi-level problem can be reformulated as follows.

$$\min \sum_{n\in\Omega^N}\sum_{m\in\theta_n} c_{nm}^{line} x_{nm} + \sum_{n\in\Omega^N} c_n^{wind} X_n^W + \sum_{\xi\in\Omega^\xi} \pi(\xi) \sum_{d\in\Omega^D} c_d^{shed} L_d^{shed}(\xi) \tag{4.4a}$$

subject to $\Big\{$

$$Constraints \quad (4.1b) - (4.1f) \tag{4.4b}$$

$$Constraints \quad (4.2b) - (4.2f) \tag{4.4c}$$

$$Constraints \quad (4.2h) - (4.2r) \tag{4.4d}$$

$$\lambda_i^G - \chi - \sum_{\xi\in\Omega^\xi} \pi(\xi)\alpha_{n(i)}(\xi) + \vartheta_i^{max} - \vartheta_{ib}^{min} + \sum_{\xi\in\Omega^\xi}(\phi_i^{max}(\xi) - \phi_{ib}^{min}(\xi)) = 0, \forall i \tag{4.4e}$$

$$\lambda_i^{UP} - \vartheta_i^{min} + \vartheta_i^{max} - \sum_{\xi\in\Omega^\xi} \pi(\xi)\varsigma_{ib}^{max}(\xi) = 0, \forall i \tag{4.4f}$$

$$\lambda_i^{DO} - \eta_i^{min} + \eta_i^{max} - \sum_{\xi\in\Omega^\xi} \pi(\xi)\tau_i^{max}(\xi) = 0, \forall i \tag{4.4g}$$

$$\pi(\xi)\varpi_i^G - \alpha_n(\xi) + \nu_i^{max}(\xi) - \nu_i^{min}(\xi) + \phi_i^{max}(\xi) - \phi_i^{min}(\xi) = 0, \forall i, \forall \xi \tag{4.4h}$$

$$-\pi(\xi)\varpi_i^G + \alpha_n(\xi) + \tau_i^{max}(\xi) - \tau_i^{min}(\xi) - \phi_i^{max}(\xi) + \phi_i^{min}(\xi) = 0, \forall i, \forall \xi \tag{4.4i}$$

$$c_n^W + \varrho_n^{max} - \varrho_n^{min} = 0, \forall n \tag{4.4j}$$

$$c_n^{w,spi} + \alpha_n(\xi) - \varpi_n^{min}(\xi) + \varpi_n^{max}(\xi) = 0, \forall n, \forall \xi \tag{4.4k}$$

$$c_d^{shed} - \alpha_{n(d)}(\xi) + \nu_d^{max}(\xi) - \nu_d^{min}(\xi) = 0, \forall d, \forall \xi \tag{4.5a}$$

$$\alpha_n(\xi) - \alpha_m(\xi) - \beta_{nm}(\xi) + \rho_{nm}^{max}(\xi) - \rho_{nm}^{min}(\xi) = 0, \forall n, \forall m \in \theta_n, \forall \xi \tag{4.5b}$$

$$\alpha_n(\xi) - \alpha_m(\xi) - \varphi_{nm}^{(t)}(\xi) + \psi_{nm}^{max}(\xi) - \psi_{nm}^{min}(\xi) = 0, \forall n, \forall m \in \theta_n, \forall \xi \tag{4.5c}$$

$$B_{nm}^E x_{nm}^0 \varphi_{nm}(\xi) + B_{nm}^N x_{nm} \varphi_{nm}(\xi) + \eta_n^{max}(\xi)$$

$$- \eta_n^{min}(\xi) - \kappa_1(\xi)_{n=1} = 0, \forall n, \forall m \in n \tag{4.5d}$$

$$0 \le P_n^{W,s} \perp \upsilon_n^{min} \ge 0, \forall n \tag{4.5e}$$

$$0 \le X_n^W - P_n^{W,s} \perp \upsilon_n^{max} \ge 0, \forall n \tag{4.5f}$$

$$0 \le P_i^{G,s} \perp \vartheta_i^{min} \ge 0, \forall i \tag{4.5g}$$

$$0 \le \overline{P}_i^G - P_i^{G,s} \perp \vartheta_i^{max} \ge 0, \forall i \tag{4.5h}$$

$$0 \le R_i^{UP} \perp \zeta_{ib}^{min} \ge 0, \forall i \tag{4.5i}$$

$$0 \le R_i^{UP,max} - R_i^{UP} \perp \zeta_i^{max} \ge 0, \forall i \tag{4.5j}$$

$$0 \le R_i^{DO} \perp \eta_{ib}^{min} \ge 0, \forall i \tag{4.5k}$$

$$0 \le R_i^{DO,max} - R_i^{DO} \perp \eta_{ib}^{max} \ge 0, \forall i \tag{4.5l}$$

$$0 \le T_{nm}^{E,max} + w_{nm}(\xi) \perp \psi_{nm}^{min}(\xi) \ge 0, \forall n, \forall m \in n \tag{4.5m}$$

$$0 \le T_{nm}^{E,max} - w_{nm}(\xi) \perp \psi_{nm}^{max}(\xi) \ge 0, \forall n, \forall m \in n \tag{4.5n}$$

$$0 \le T_{nm}^{N,max} + f_{nm}(\xi) \perp \rho_{nm}^{min}(\xi) \ge 0, \forall n, \forall m \in n \tag{4.5o}$$

$$0 \le T_{nm}^{N,max} - f_{nm}(\xi) \perp \rho_{nm}^{max}(\xi) \ge 0, \forall n, \forall m \in n \tag{4.5p}$$

$$0 \le P_i^G(\xi) \perp \phi_i^{min}(\xi) \ge 0, \forall i \tag{4.5q}$$

$$0 \le \overline{P}_{ib}^G - P_i^G(\xi) \perp \phi_i^{max}(\xi) \ge 0, \forall i \tag{4.5r}$$

$$0 \le L_d^{shed}(\xi) \perp \nu_d^{min}(\xi) \ge 0, \forall d \tag{4.5s}$$

$$0 \le P_d^D(\xi) - L_d^{shed}(\xi) \perp \nu_d^{max}(\xi) \ge 0, \forall d \tag{4.5t}$$

$$0 \le r_i^{UP}(\xi) \perp \varsigma_i^{min}(\xi) \ge 0, \forall i, \forall \xi \tag{4.5u}$$

$$0 \le R_i^{UP} - r_i^{UP}(\xi) \perp \varsigma_i^{max}(\xi) \ge 0, \forall i, \forall \xi \tag{4.5v}$$

$$\}$$

where, equality constraints (4.4e)-(4.5d) are KKT optimality constraints, and constraints (4.5e)-(4.5v) are complementarity constraints, which are nonliear.

4.2.4 MINLP Reformulations for Stochastic MPEC

These complementary constraints are nonlinear, which makes the problem more complex. To solve nonlinear MPEC, several algorithms for solving MPECs, such as smoothing, penalizing, relaxation, and suitable modifications of standard NLP solvers. Among these algorithms, the relaxation schemes are effective methods to solve MPEC problems. In this paper, we employ the first and most popular relaxation scheme, the global relaxation method by Scholtes [52, 53]. Complementary constraints (4.5e)-(4.5v) are reformulated as follows. Finally, the transmission expansion planning considering wind power investment problem can be transferred into mixed integer nonlinear programming (MINLP) problem.

$$\min \sum_{n\in\Omega^N}\sum_{m\in\theta_n} c_{nm}^{line}x_{nm} + \sum_{n\in\Omega^N} c_n^{wind}X_n^W + \sum_{\xi\in\Omega^\xi}\pi(\xi)\sum_{d\in\Omega^D} c_d^{shed}L_d^{shed}(\xi) \tag{4.6a}$$

subject to

$$Constraints : (4.4b) - (4.5d) \tag{4.6b}$$

$$0 \le P_n^{W,s}, \forall n \tag{4.6c}$$

$$0 \le \upsilon_n^{min}, \forall n \tag{4.6d}$$

$$P_n^{W,s}\upsilon_n^{min} \le Relax, \forall n \tag{4.6e}$$

$$0 \le X_n^W - P_n^{W,s}, \forall n \tag{4.6f}$$

$$0 \le \upsilon_n^{max}, \forall n \tag{4.6g}$$

$$(X_n^W - P_n^{W,s})\upsilon_n^{max} \le Relax, \forall n \tag{4.6h}$$

$$0 \le P_i^{G,s}, \forall i \tag{4.6i}$$

$$0 \le \vartheta_i^{min}, \forall i \tag{4.6j}$$

$$P_i^{G,s}\vartheta_i^{min} \le Relax, \forall i \tag{4.6k}$$

$$0 \le \overline{P}_i^G - P_i^{G,s}, \forall i \tag{4.6l}$$

$$0 \le \vartheta_i^{max}, \forall i \tag{4.6m}$$

$$(\overline{P}_i^G - P_i^{G,s})\vartheta_i^{max} \le Relax, \forall i \tag{4.6n}$$

$$0 \le R_i^{UP}, \forall i \tag{4.6o}$$

$$0 \le \zeta_i^{min}, \forall i \tag{4.6p}$$

$$R_{ib}^{UP}\zeta_i^{min} \leq Relax, \forall i \tag{4.7a}$$

$$0 \leq R_i^{UP,max} - R_i^{UP}, \forall i \tag{4.7b}$$

$$0 \leq \zeta_i^{max}, \forall i \tag{4.7c}$$

$$R_i^{UP,max} - R_i^{UP}\zeta_i^{max} \leq Relax, \forall i \tag{4.7d}$$

$$0 \leq T_{nm}^{E,max} + w_{nm}(\xi), \forall n, \forall m \in n \tag{4.7e}$$

$$0 \leq \psi_{nm}^{min}(\xi), \forall n, \forall m \in n \tag{4.7f}$$

$$(T_{nm}^{E,max} + w_{nm}(\xi))\psi_{nm}^{min}(\xi) \leq Relax, \forall n, \forall m \in n \tag{4.7g}$$

$$0 \leq T_{nm}^{E,max} - w_{nm}(\xi), \forall n, \forall m \in n \tag{4.7h}$$

$$0 \leq \psi_{nm}^{max}(\xi) \leq 0, \forall n, \forall m \in n \tag{4.7i}$$

$$(T_{nm}^{E,max} - w_{nm}(\xi))\psi_{nm}^{max}(\xi) \leq Relax, \forall n, \forall m \in n \tag{4.7j}$$

$$0 \leq R_i^{DO}, \forall i \tag{4.7k}$$

$$0 \leq \eta_i^{min}, \forall i \tag{4.7l}$$

$$R_i^{DO}\eta_i^{min} \leq Relax, \forall i \tag{4.7m}$$

$$0 \leq R_i^{DO,max} - R_i^{DO}, \forall i \tag{4.7n}$$

$$0 \leq \eta_i^{max}, \forall i \tag{4.7o}$$

$$(R_i^{DO,max} - R_i^{DO})\eta_i^{max} \leq Relax, \forall i \tag{4.7p}$$

$$0 \leq T_{nm}^{N,max} + f_{nm}^{(t)}(\xi), \forall n, \forall m \in n \tag{4.7q}$$

$$0 \leq \rho_{nm}^{min}(\xi), \forall n, \forall m \in n \tag{4.7r}$$

$$(T_{nm}^{N,max} + f_{nm}(\xi))\rho_{nm}^{min}(\xi) \leq Relax, \forall n, \forall m \in n \tag{4.7s}$$

$$0 \leq T_{nm}^{N,max} - f_{nm}(\xi), \forall n, \forall m \in n \tag{4.7t}$$

$$0 \leq \rho_{nm}^{max}(\xi), \forall n, \forall m \in n \tag{4.7u}$$

$$(T_{nm}^{N,max} - f_{nm}(\xi))\rho_{nm}^{max,(t)}(\xi) \leq Relax, \forall n, \forall m \in n \tag{4.7v}$$

$$0 \leq P_i^G(\xi), \forall i \tag{4.7w}$$

$$0 \leq \phi_i^{min}(\xi), \forall i \tag{4.7x}$$

$$P_i^G(\xi) \perp \phi_{ib}^{min}(\xi) \leq Relax, \forall i \tag{4.7y}$$

$$0 \leq \overline{P}_i^G - P_i^G(\xi), \forall i \tag{4.7z}$$

$$0 \leq \phi_i^{max,(t)}(\xi), \forall i \tag{4.8a}$$

$$(\overline{P}_i^G - P_{ib}^G(\xi))\phi_{ib}^{max,(t)}(\xi) \leq Relax, \forall i \tag{4.8b}$$

$$0 \leq L_d^{shed}(\xi), \forall d \tag{4.8c}$$

$$0 \leq \nu_d^{min}(\xi), \forall d \tag{4.8d}$$

$$L_d^{shed}(\xi)\nu_d^{min}(\xi) \leq Relax, \forall d \tag{4.8e}$$

$$0 \leq P_d^D(\xi) - L_d^{shed}(\xi), \forall d \tag{4.8f}$$

$$0 \leq \nu_d^{max}(\xi), \forall d \tag{4.8g}$$

$$(P_d^D(\xi) - L_d^{shed}(\xi))\nu_d^{max}(\xi) \leq Relax, \forall d \tag{4.8h}$$

$$0 \leq r_i^{UP}(\xi), \forall i, \forall \xi \tag{4.8i}$$

$$0 \leq \varsigma_i^{min}(\xi), \forall i, \forall \xi \tag{4.8j}$$

$$r_i^{UP}(\xi)\varsigma_i^{min}(\xi) \leq Relax, \forall i, \forall \xi \tag{4.8k}$$

$$0 \leq R_i^{UP} - r_i^{UP}(\xi), \forall i, \forall \xi \tag{4.8l}$$

$$0 \leq \varsigma_i^{max}(\xi), \forall i, \forall \xi \tag{4.8m}$$

$$(R_i^{UP} - r_i^{UP}(\xi))\varsigma_i^{max}(\xi) \leq Relax, \forall i, \forall \xi \tag{4.8n}$$

where *Relax* is the relaxation index for the complementarity constraints transferred into nonlinear inequality constraints. In the simulations we set *Relax* equal to a small enough value 1e-7. The constraints (4.6b) includes the transmission investment constraints, the wind power investment constraints, and KKT constraints. The complementarity constraints (4.5e)-(4.5v) from the Stochastic MPEC function can be transferred into new forms (4.6c)-(4.8n) by a relaxation approach [76].

Now the proposed model of transmission expansion planing and wind power investment with co-optimization of energy and reserve is transformed into into MINLP formulations. The class of MINLP problems are difficult to obtain optimal solutions. To solve the MINLP formulations, we use the solver Branch-And-Reduce Optimization Navigator (BARON), which is a GAMS solver for the nonlinear problems and MINLP. Another approach to deal with the complementarity constraints is to use a large constant as in [7], and the problem will be transformed into a mixed integer linear programming.

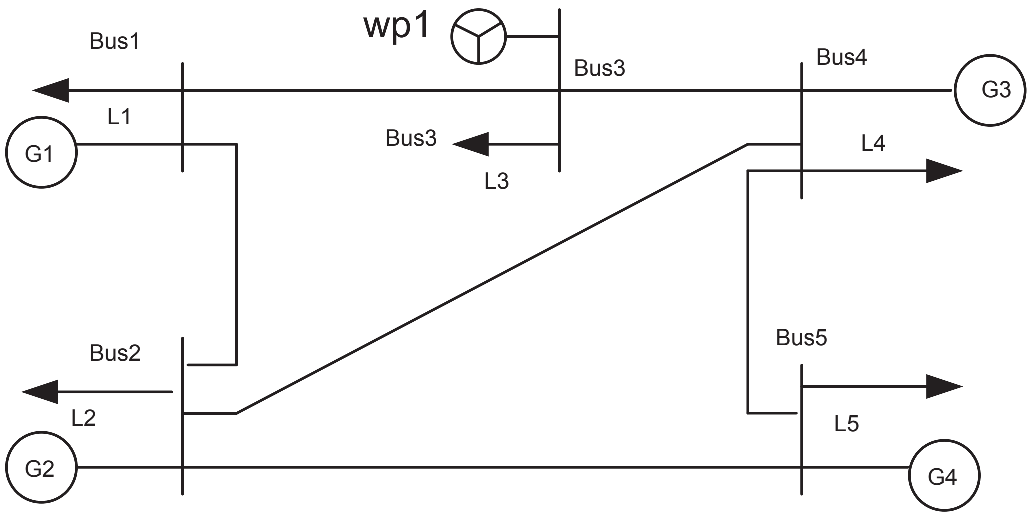

Figure 4.1: Five-bus system

Table 4.1: GENERATORS AND LOADS DEMAND DISTRIBUTION

	Generation Units		Loads Peak
Bus	Offer size (MW)	offer price ($/MWh)	(MW)
1	25	16	8
2	30	19	10
3	-	-	45
4	30	19	10
5	10	15	45

Table 4.2: THE DATA OF RESERVER-UP AND RESERVE-DOWN

Bus(from)	Bus(to)	$T_{nm}^{E,max}$ (MW)	Length (km)	Inv. Cost ($$10^5/km$)
$R_i^{UP,max}$[MW]	10	15	15	5
$R_i^{DO,max}$[MW]	10	15	15	5
λ_i^{UP}[$/MWh]	8	10	10	8
λ_i^{DO}[$/MWh]	8	10	10	8

4.3 Case Study

The proposed model is illustrated using the five-bus test system shown in Fig. 4.1. The system has five buses, six existing lines, four generating units (G1-G4) which are connected to Bus 1, Bus 2, Bus 4 and Bus 5 respectively, and five demands (L1-L5) are located to Bus 1, Bus 2, Bus 3, Bus 4 and Bus 5 successively. Table 4.1 shows the generators' offer size and prices, which are fixed through the whole planning horizon and the last column represents each bus peak demand. The data of reserve up and reserve down supplied by the generators is shown in Table 4.2. The detailed line data are given in Table 4.3. The capacity of wind power at Bus 3 is 110 MW. The unit wind power investment cost is $1M/MW. To deal with the uncertainty of wind power production, we assume nine scenarios to represent the wind power characteristic of the target year. The availability of wind power production to the installed rated wind power are 0.70, 0.66, 0.60, 0.57, 0.50, 0.45, 0.42, 0.30 and 0.2 with the corresponding probability of 0.0875, 0.1250, 0.1375, 0.1400, 0.200, 0.1225, 0.075, 0.060, and 0.0525. The unit wind power spillage cost is set as $10/MW, and the unit load shedding cost is $1000/MW. To simplify the calculation, we do not consider the uncertainties of loads demand, but it is easily extended to integrate the uncertainties of loads demand.

Table 4.3: EXISTING LINE DATA FOR FIVE-BUS TEST SYSTEM

Bus(from)	Bus(to)	Reactance (p.u.)	$T_{nm}^{E,max}$ (MW)
1	2	0.010	5
1	3	0.008	8
2	4	0.0067	5
2	5	0.010	5
3	4	0.008	8
4	5	0.0067	5

The distribution of the generators and loads in the five-bus system is shown in Fig. 4.1. Bus 3 is simulated as a wind farm site which will be invested by wind power investor. Table 4.4 shows the prospective lines for transmission investment, which includes line parameter and investment cost [77].

Table 4.4: PROSPECTIVE LINES INVESTMENT DATA FOR FIVE-BUS TEST SYSTEM

Bus(from)	Bus(to)	Reactance (p.u.)	$T_{nm}^{E,max}$ (MW)	Length (km)	Inv. Cost ($\$10^5/km$)
1	2	0.010	10	9	10
1	5	0.008	15	12	20
2	5	0.0067	15	12	10
3	5	0.008	10	6	20
4	5	0.0067	15	8	10

Based on the above data, we solve the proposed MINLP reformulations for transmission investment considering wind power investment with co-optimization of energy and reserve. From the simulation result, we can see that 2 prospective lines, this is, lines (3-5, 4-5) are going to be invested on the current network to support wind power investment which is connected to the bus 3. The investment cost of transmission lines is $20M. The wind power incitement installed on the bus 3 is invested by 80.63 MW, and the wind power investment cost is $80.63M, while in the day-ahead market the wind power scheduled by market operator is equal to 42.66 MW. Simulation results also show load shedding and wind power spillage in different scenarios, as pages are limited, we do not provide these results here. Therefore, the social cost reaches up to $134.21M. The generation and reserve scheduled are shown in Table 4.5. From this table, we can see the units supply both reserve down and reserve up regulations, that is because wind power produced in different scenarios fluctuate around the value of wind power scheduled.

Table 4.5: THE RESULT OF GENERATION AND RESERVER SCHEDULED

Unit (i)	1	2	3	4
G_i	14.50	20.84	30	10
R_i^{UP}	7.26	1.94	0	5
R_i^{DO}	7.79	2.77	0	0

Table 4.6 shows the simulation results change with increasing loads demand level. The first column represents the percent of demand increase for all loads. The planning lines to be built and wind power invested are shown in the second column and third column. The last column represents wind power scheduled in the day-ahead market. Power system expansion including transmission capacity and wind power investment is to satisfy the requirements of future loads demand. The upper level problem of the proposed model integrates wind power investment and the lower level problem includes the wind power scheduled in the first stage and wind power realization in the second stage. From Table 4.6, we can conclude that wind power installed and power offer will increase with the increment of loads demand. As the objective function has the minimum load shedding cost, we also supply the information of generation production and load shedding under the different scenarios. These results show that the proposed model can satisfy the renewable energy requirement economically, promote investment on renewable energy, facilitate the coordination of transmission planning and wind power investment in the electricity market.

Table 4.6: RESULT FOR DIFFERENT LOADS DEMAND

Loads Increase(%)	Lines Planned	X_n^W(MW)	$P_n^{W,s}$(MW)
0	3-5; 4-5	80.63	42.66
10	2-5; 3-5; 4-5	90	44.01
20	1-5; 3-5; 4-5	105	51.98
30	1-5; 3-5; 4-5	110	66.49

4.4 Conclusion

In this chapter we have proposed a new model for the coordination of transmission expansion planning and wind power investment within a modern electricity market environment. This model is formulated as a bilevel problem with two-stage stochastic programming, which is further reformulated as a stochastic mixed-integer nonlinear program. The model of transmission expansion planning takes account into account wind power investment, wind power scheduled and uncertain realization, and co-optimization of energy and reserve. We reach the following conclusions from this.

1)Wind power investment and transmission investment have interacting effect on each other. Transmission expansion is critical for effectively introducing wind power into market, and the decision making for transmission planning depends on wind power investment. The proposed model combines the electricity planning market and power system operation, and is the first to develop a transmission planning model considering wind power investment.

2) The proposed bilevel problem with two-stage stochastic programming model can be reformulated as a MINLP problem that has been solved optimally by the branch-and-bound solver GAMS/BRAON with a relaxation approach.

3) The planed wind power invested and power scheduled will increase with the higher level of loads demand.

4) The proposed model solves simultaneously the problem of transmission expansion planning, wind power investment, and the requirement of reserve for uncertain wind power. Therefore, this model provides a comprehensive solution that satisfies the requirement of modern electricity market, improving the integration of renewable energy.

Chapter 5

Maximum Loadability of Security Constrained Power Systems using Semidefinite Programming Method

Studies in Chapter 3 and 4 are based on a linear DC-OPF model, while actual power system problems are non-linear and non-convex. The importance of voltage stability has been regarded by system operators as major force driving the development of modern electricity markets. Power system maximum loadability is a crucial index to determine voltage stability, but this problem is an NP-hard problem. This chapter proposes a Lagrange semi-definite programming (SDP) method to solve the non-linear and non-convex optimization problem of maximum loadability of security constrained power systems. We derive the Lagrange function of the primal maximum loadability, further get the dual problem of the primal maximum loadability problem through equivalent transformations, which is a convex SDP optimization. Simulation results from the IEEE three-bus system and IEEE 24-bus RTS show that the proposed method in this chapter is effective to handle the complicated non-liner and non-convex maximum loadability problem.

5.1 Introduction

Renewable energy has been widely recognized as an effective way to address global warming [8, 9, 42]. Nevertheless, the inherent uncertainty and variability of renewable energy poses new challenges in maintaining the voltage stability of electric power systems [8–13]. Voltage instability has emerged as a large issue in modern electricity grid due to the continued growth in interconnections, new technologies, and the increased operation [78]. Power system maximum loadability has been attracting more attention as an effective method to determine voltage stability because of power industry restructuring [79].

Mathematically, maximum loadability problem is a non-convex and non-linear optimization problem. There are many methods developed for solving the problem of maximum loadability. [80] presents the method of continuation power flow (CPF), which determines the steady state voltage stability limit of the system through finding a continuum of power flow solutions starting at some base load. Although CPF method has been widely accepted to use, it fails to give the accurate result if the step length is not appropriate [81]. Moreover, this conventional power flow method suffers from providing proper maximum loadability under security constraints as Jacobian matrix becomes singular when system loading approaches its loadability limit [82]. Successive quadratic programming (SQP) adopts the second order derivatives to improve the convergence rate, but this method will become too slow with the incase of the number of control variables [83]. The method of interior point non-linear is supported to calculate the maximum loadability problem [84]. The interior point is computationally efficient, but the feasible solution depends on the appropriate step size in the original non-linear domain.

As the above traditional methods have limits to solve the problem of the maximum loadability, especially, the security constraints of phase angles, active power output, voltage magnitudes of load buses and reactive power of generator buses will bring more challenges for solving this complicated problem. Recently evolutionary techniques are becoming more popular to solve the non-linear and non-convex maximum loadabiliity problem. Genetic Algorithm (GA) is widely used to solve the maximum loadability [85,86]. [87] develops evolutionary particle swarm optimization (PSO) to find the margin from the current operating point to the maximum loadability point. The reference [88] utilizes the newly developed multiagent-based hybrid particle swarm optimization method to determine the maximum loadability limit. The particle swarm optimization method based on swarm intelligence is widely used to solve the complicated optimization problems. However, PSO methods easily suffer from the partial optimism, which is less accurate at the regulation of its speed and the direction, and also cannot work well for non-coordinate, such as the solution to the energy field and the moving rules of the particles in the energy field [89].

Existing methods are mainly based on exploring the Karush-Kuhn-Tucker (KKT) necessary conditions, which can only guarantee a locally optimal solution due to the non-convexity of the problem [90,91]. One popular solution technique for this kind of problem is sequential quadratic programming, which reduces the original problem into a sequence of quadratic programming subproblems and produces a locally optimal solution. Other numerical methods include, but are not limited to, the interior point algorithms adopted in [92], the novel linear sensitivity method in [93], and transfer-based security constrained optimal power flow method proposed in [94]. Albeit being computationally efficient, all the above methods yield suboptimal (conservative) evaluations. Recently semi-definite programming methods have widely attracted much research attention to solve the non-convex optimal power flow problem [91,95,96], as the application of SDP can effectively overcome the non-convex difficulties. Reference [95] reformulates the OPF problems into an SDP model and develops an algorithm of primal-dual interior point method (IPM) for SDP. SDP method is further developed in [91], which provides that the zero duality exists. [97] provides a sufficient condition for the global solution of OPF problem based on SDP methods.

Based on SDP methods' effectiveness to solve OPF problems, we apply the advanced tool of SDP to solve the problem of maximum loadaibility. Current approaches generally rely on suboptimal approaches and provide conservative estimates of the maximum loadaibility, the SDP approach adopted can guarantee the attainment of the optimal maximum loadaibility, as we prove the zero duality gap between primal problem and the dual model exists.

The rest of the chapter is organized as follows. Section 5.2 describes the problem description of the maximum loadability. Section 5.3 states the maximum loadability problem formulation including primal maximum loadaibility and SDP dual problem, and further proves zero duality gap between primal and dual form. Test results of the case study on our proposed algorithm are given in Section 5.4. Finally, conclusions are drawn in Section 5.5.

5.2 Problem Description

Maximum loadability can be represented as a static nonlinear optimization problem. The objective is to determine the maximum loadability within the limits of voltage stability and physical constraints of electric grid (either total system load, or the load of the specific load or the load of buses). The mathematical formulation can be expressed as follows [84].

$$\max \quad \alpha \tag{5.1a}$$

subject to

$$g(x, \alpha) = g(x) + \alpha D \tag{5.1b}$$

$$l \leq h(x) \leq u \tag{5.1c}$$

where $g(x, \alpha)$ represents power balance constrains with the scalar parameter α and $g(x)$ are standard balance constraints. $h(x)$ represent inequality constraints, including limits of voltage magnitudes, phase angles, real and reactive power outputs, as well as power flow of each branch.

On the other hand, reference [79] defines the total summation of loads in a big zone as maximum loadability, and assumes that active load and reactive load of each bus vary proportionally to the summation of total active loads. However, it is not appropriate for the situation of load shedding. In our proposed model we set the summation of active loads at the designed area as the objective function which is subject to security constrains, like limits of voltage, generation active power and reactive power, and transmission flow. In addition, active loads and reactive loads are treated as independent variables, which can effectively represent the varying loads in a real world. Meanwhile, active loads and reactive loads vary within the reasonable range.

5.3 Mathematical Formulation

The problem of maximum loadability considering security constraints is formulated as a highly nonconvex and nonlinear constraint problem. Optimal power flow technology is critical and effective for obtaining the optimal value of maximum loadability. In view of the fact that traditional methods cannot guarantee global optimal point, and non-zero duality gap exists, we propose to derive the equivalent dual form of primal maximum loadability. which can be efficiently computed as semi-definite programming (SDP), and prove zero duality gap between dual problem and primal maximum loadability.

5.3.1 Notation

Symbol	Indices and Sets :
$\mathcal{L}$	Lagrange function
n,m	Index for buses.
i	Index of candidate generating units.

$k \in \mathbf{S}$	Buses distributed in source areas.
$k \in \mathbf{G}$	Buses with traditional generators.
$k \in \mathbf{N}$	All buses on network.
$k \in \mathbf{D}$	Buses with loads.
$(l,m) \in \mathbf{L}$	The set of all branches $l-m$.
$\mathrm{Re}\{\}$	Real part of apparent power.
$\mathrm{Im}\{\}$	Imaginary part of apparent power.
$P_k^{g,max}$	Maximum active power output of the generator located at the kth bus.
$P_k^{g,min}$	Minimum active power output of the generator located at the kth bus.
$Q_k^{g,max}$	Maximum reactive power output of the generator located at the kth bus.
$Q_k^{g,min}$	Maximum reactive power output of the generator located at the kth bus.
$P_k^{d,max}$	Maximum active load located at the kth bus.
$P_k^{d,min}$	Minimum active load located at the kth bus.
$Q_k^{d,max}$	Maximum reactive load located at the kth bus.
$Q_k^{d,min}$	Minimum reactive load located at the kth bus.
V_k^{max}	Maximum voltage magnitude of the kth bus.
V_k^{min}	Minimum voltage magnitude of the kth bus.
S_{lm}^{max}	Maximum apparent power flow limit of the branch $l-m$.
y_{lm}	The mutual admittance between bus k and l.
$\overline{y}_{lm}$	The complex conjugate of y_{lm}.
Y	The admittance matrix of power systems.

Symbol	Primal and Dual Variables
P_k^g	The active power output of the generator located at the kth bus.
Q_k^g	The reactive power output of generator located at the kth bus.
P_k^d	The active load located at the kth bus.
Q_k^d	The reactive load located at the kth bus.
V_k	Voltage of the kth bus.
I_k	Current of the kth bus.
S_{lm}	Apparent power flow limit of the branch $l-m$.
$\nu_k^{d,max}$	Dual variable of maximum limit inequality constraint of reactive load located to the kth bus.
$\nu_k^{d,min}$	Dual variable of minimum limit inequality constraint of reactive load located to the kth bus.
$\varphi_k^{d,max}$	Dual variable of maximum limit inequality constraint of reactive load located to the kth bus.

$\varphi_k^{d,min}$ Dual variable of minimum limit inequality constraint of reactive load located to the kth bus.

μ_k^{max} Dual variable of maximum limit inequality constraint of voltage magnitude on the kth bus.

μ_k^{min} Dual variable of minimum limit inequality constraint of voltage magnitude on the kth bus.

τ_k^{max} Dual variable of maximum limit constraint of active power output of the generator on the kth bus.

τ_k^{min} Dual variable of minimum limit constraint of active power output of the generator on the kth bus.

λ_k^{max} Dual variable of maximum limit constraint of reactive power output of the generator on the kth bus.

λ_k^{min} Dual variable of minimum limit constraint of reactive power output of the generator on the kth bus.

5.3.2 Primal Maximum Loadability

In an open-access environment, maximum loadability can be solved as a constrained non-linear programming problem with an objective function to determine the maximum loads demand at the total area, the specific area, or the sets of buses, subject to the system equality and inequality constraints, such as active power and reactive power output limits, thermal limits and voltage limits. maximum loadability calculation can be formulated as follows.

$$\max_{\mathbf{V},\mathbf{P_g},\mathbf{Q_g},\mathbf{Q_d},\mathbf{P_d}} \quad \sum_{k\in\mathbf{D}} P_k^d \tag{5.2a}$$

subject to

$$V_k I_k^* = (P_k^g - P_k^d) + j(Q_k^g - Q_k^d)), \forall k \in \mathbf{N} \tag{5.2b}$$

$$Q_k^{g,min} \leq Q_k^g \leq Q_k^{g,max}, \forall k \in \mathbf{G} \tag{5.2c}$$

$$P_k^{g,min} \leq P_k^g \leq P_k^{g,max}, \forall k \in \mathbf{G} \tag{5.2d}$$

$$V_k^{min} \leq\mid V_k \mid\leq V_k^{max}, \forall k \in \mathbf{N} \tag{5.2e}$$

$$P_k^{d,min} \leq P_k^d \leq P_k^{d,max}, \forall k \in \mathbf{D} \tag{5.2f}$$

$$Q_k^{d,min} \leq Q_k^d \leq Q_k^{d,max}, \forall k \in \mathbf{D} \tag{5.2g}$$

$$\mid S_{lm} \mid\leq\mid S_{lm}^{max}, \forall (l,m) \in \mathbf{L} \tag{5.2h}$$

where $\mathbf{V}$, $\mathbf{P_g}$, $\mathbf{Q_g}$, $\mathbf{Q_d}$, $\mathbf{P_d}$ denote unknown variable vectors $\{V_k\}_{k\in\mathbf{N}}$, $\{P_k^g\}_{k\in\mathbf{G}}$, $\{Q_k^g\}_{k\in\mathbf{G}}$, $\{Q_k^d\}_{k\in\mathbf{D}}$, $\{P_k^d\}_{k\in\mathbf{D}}$ respectively. The equality constraints (5.2b) are the active power and reactive power balance constraints of each bus. The inequality constraints (5.2c), (5.2d) represent the limits of the generators' output reactive power, active power respectively. (5.2e) enhance the limits of buses voltage, and the constraints of loads at $\mathbf{D}$ as variables are shown by (5.2f) and (5.2g). Last inequality constraints (5.3g) are power flow limits of transmission lines. Reference [92] makes the simplest assumption all loads vary proportionally, but this assumption deviates from the reality. Therefore, in the proposed model all loads of the designated area are independent variables, and reactive power of the loads are also variables within the limits.

OPF methods have been proved effective to get maximum loadability. Previously when OPF methods are applied to solve maximum loadability functions, steep-descent method or SQP algorithm are used together with increasing the loads step by step until the security limits are reached, where loads are treated as fixed and given at each iteration. In this chapter, in the primal program we set loads as controllable variables like the output power of generators, voltage. Meanwhile, we can add loads limits to inequality constraints, so that we can directly solve the maximum value of maximum loadability, instead of trying to improve loads gradually as in the existing work. Since the primal problem is nonconvex, it is very hard to get the optimal value directly, and we propose to solve the equivalent dual form of primal problem which can be in convex form. To get the dual problem of primal maximum loadability, this chapter tries to formulate OPF model in different forms. From the optimization theory, firstly, use a scalar to replace the objective function, and then add corresponding inequality matrix constraints. Furthermore, based on mathematical transformations, we derive the dual problem of maximum loadability in an SDP model by using the linear matrix inequalities (LMIs) where the goal is to minimize a linear function subject to LMIs. Meanwhile, SDP is a convex model, which can be efficiently solved.

5.3.3 Maximum Loadability Reforemulation

To derive the dual problem of primal maximum loadability, we need equivalent transformation of (5.2). Firstly define some matrix and vectors as follows. Let us e_1,e_2,$\cdots$ e_n denote the standard basis vectors in R^n, and define $\mathbf{M}_k \in R^{2n\times 2n}$ as a diagonal matrix whose entries are all equal to zero, but (k, k) and $(n+k, n+k)$ entries equal to 1. For every k,$l \in 1, 2, \cdots, n$, define

$$
\begin{aligned}
&Y_k := e_k e_k^T Y \\
&Y_{lm} := (\overline{y}_{lm} + y_{lm}) e_l e_l^T - (y_{lm}) e_l e_m^T \\
&\mathbf{Y}_k := \frac{1}{2} \begin{bmatrix} \mathrm{Re}\{Y_k + Y_k^T\} & \mathrm{Im}\{Y_k^T - Y_k\} \\ \mathrm{Im}\{Y_k - Y_k^T\} & \mathrm{Re}\{Y_k + Y_k^T\} \end{bmatrix} \\
&\overline{\mathbf{Y}}_k = -\frac{1}{2} \begin{bmatrix} \mathrm{Im}\{Y_k + Y_k^T\} & \mathrm{Re}\{Y_k - Y_k^T\} \\ \mathrm{Re}\{Y_k^T - Y_k\} & \mathrm{Im}\{Y_k + Y_k^T\} \end{bmatrix} \\
&\overline{\mathbf{Y}}_{lm} = -\frac{1}{2} \begin{bmatrix} \mathrm{Re}\{Y_{lm} + Y_{lm}^T\} & \mathrm{Im}\{Y_{lm}^T - Y_{lm}\} \\ \mathrm{Im}\{Y_{lm} - Y_{lm}^T\} & \mathrm{Re}\{Y_{lm} + Y_{lm}^T\} \end{bmatrix} \\
&\mathbf{X} := [\mathrm{Re}\{\mathbf{V}\}^T \quad \mathrm{Im}\{\mathbf{V}\}^T]^T
\end{aligned}
$$

The balance constraints (5.2b) are equal to the following equations

$$
\begin{aligned}
\mathrm{Re}\{V_k I_k^*\} &= P_k^g - P_k^d \\
\mathrm{Im}\{V_k I_k^*\} &= Q_k^g - Q_k^d.
\end{aligned}
$$

Note that if some buses do not have the generators, or the loads demand, we fix P_k^g, P_k^d equal to zero respectively. Therefore, the optimization function (5.2) can be rewritten as

$$
\max_{\mathbf{V},\mathbf{P_g},\mathbf{Q_g},\mathbf{Q_d},\mathbf{P_d}} \quad \sum_{k \in \mathbf{D}} P_k^d \tag{5.3a}
$$

subject to

$$
\begin{aligned}
&Q_k^{g,min} \leq \mathrm{Im}\{V_k I_k^*\} + Q_k^d \leq Q_k^{g,max}, \forall k \in \mathbf{G} && (5.3b) \\
&P_k^{g,min} \leq \mathrm{Re}\{V_k I_k^*\} + P_k^d \leq P_k^{g,max}, \forall k \in \mathbf{G} && (5.3c) \\
&V_k^{min} \leq \mid V_k \mid \leq V_k^{max}, \forall k \in \mathbf{N} && (5.3d) \\
&P_k^{d,min} \leq P_k^d \leq P_k^{d,max}, \forall k \in \mathbf{D} && (5.3e) \\
&Q_k^{d,min} \leq Q_k^d \leq Q_k^{d,max}, \forall k \in \mathbf{D} && (5.3f) \\
&\mid S_{lm} \mid \leq \mid S_{lm}^{max}, \forall (l,m) \in \mathbf{L} && (5.3g)
\end{aligned}
$$

From reference [98], we get the following relationship as follows

$$\mathrm{Re}\{V_k I_k^*\} = \mathrm{Tr}\{\mathbf{Y}_k \mathbf{X}\mathbf{X}^T\} \tag{5.4a}$$

$$\mathrm{Im}\{V_k I_k^*\} = \mathrm{Tr}\{\overline{\mathbf{Y}}_k \mathbf{X}\mathbf{X}^T\} \tag{5.4b}$$

$$\mid S_{lm} \mid^2 = (\mathrm{Tr}\{\mathbf{Y}_{lm} \mathbf{X}\mathbf{X}^T\})^2 + (\mathrm{Tr}\{\overline{\mathbf{Y}}_{lm} \mathbf{X}\mathbf{X}^T\})^2 \tag{5.4c}$$

$$\mid V_k \mid^2 = \mathrm{Tr}\{\mathbf{M_k} \mathbf{X}\mathbf{X}^T\} \tag{5.4d}$$

According to the Schur's complement formula, combing with the inequality constraint (5.4c), (5.3g) can be equivalent to

$$\begin{bmatrix} \mid S_{lm}^{max} \mid^2 & \mathrm{Tr}\{\mathbf{Y}_{lm}\mathbf{X}\mathbf{X}^T\} & \mathrm{Tr}\{\overline{\mathbf{Y}}_{lm}\mathbf{X}\mathbf{X}^T\} \\ \mathrm{Tr}\{\mathbf{Y}_{lm}\mathbf{X}\mathbf{X}^T\} & -1 & 0 \\ \mathrm{Tr}\{\overline{\mathbf{Y}}_{lm}\mathbf{X}\mathbf{X}^T\} & 0 & -1 \end{bmatrix} \preceq 0 \tag{5.5}$$

Base on the above formulation transformation, the primal optimization problem can be reformulated as

$$\max_{\mathbf{V},\mathbf{P_g},\mathbf{Q_g},\mathbf{Q_d},\mathbf{P_d}} \quad \sum_{k\in\mathbf{D}} P_k^d \tag{5.6a}$$

subject to

$$Q_k^{g,min} \leq Q_k^d + \mathrm{Tr}\{\overline{\mathbf{Y}}_k \mathbf{X}\mathbf{X}^T\} \leq Q_k^{g,max} : \tau_k^{min}, \tau_k^{max}, \forall k \in \mathbf{G} \tag{5.6b}$$

$$P_k^{g,min} \leq P_k^d + \mathrm{Tr}\{\mathbf{Y}_k \mathbf{X}\mathbf{X}^T\} \leq P_k^{g,max} : \lambda_k^{min}, \lambda_k^{max}, \forall k \in \mathbf{G} \tag{5.6c}$$

$$\begin{bmatrix} \mid S_{lm}^{max} \mid^2 & \mathrm{Tr}\{\mathbf{Y}_{lm}\mathbf{X}\mathbf{X}^T\} & \mathrm{Tr}\{\overline{\mathbf{Y}}_{lm}\mathbf{X}\mathbf{X}^T\} \\ \mathrm{Tr}\{\mathbf{Y}_{lm}\mathbf{X}\mathbf{X}^T\} & -1 & 0 \\ \mathrm{Tr}\{\overline{\mathbf{Y}}_{lm}\mathbf{X}\mathbf{X}^T\} & 0 & -1 \end{bmatrix} \preceq 0$$
$$: \begin{bmatrix} \gamma_{lm}^1 & \gamma_{lm}^2 & \gamma_{lm}^3 \\ \gamma_{lm}^2 & \gamma_{lm}^4 & \gamma_{lm}^5 \\ \gamma_{lm}^3 & \gamma_{lm}^5 & \gamma_{lm}^6 \end{bmatrix}, \forall (l,m) \in \mathbf{L} \tag{5.6d}$$

$$(V_k^{min})^2 \leq \mathrm{Tr}\{\mathbf{M_k}\mathbf{X}\mathbf{X}^T\} \leq (V_k^{max})^2 : \mu_k^{min}, \mu_k^{max}, \forall k \in \mathbf{N} \tag{5.6e}$$

$$P_r^{d,min} \leq P_r^d \leq P_r^{d,max} : \nu_k^{d,min}, \nu_k^{d,max}, \forall k \in \mathbf{D} \tag{5.6f}$$

$$Q_k^{d,min} \leq Q_k^d \leq Q_k^{d,max} : \varphi_k^{d,min}, \varphi_k^{d,max}, \forall k \in \mathbf{D} \tag{5.6g}$$

(5.6h)

where τ_k^{min}, τ_k^{max} are the dual variables of the inequality constraints for the generators's output reactive power; λ_k^{min}, λ_k^{max} are the dual variables of the generators's output active power inequality constraints ; μ_k^{min}, μ_k^{max} are the dual variables of the buses voltage inequality constraints; $\nu_k^{d,min}$, $\nu_k^{d,max}$ are the dual variables of the loads of the designed area inequality constraints. $\varphi_k^{d,min}$, $\varphi_k^{d,max}$ are the dual variables of the reactive power loads of the designed area inequality constraints. All the above variables should be nonnegative. The matrix $\begin{bmatrix} \gamma_{lm}^1 & \gamma_{lm}^2 & \gamma_{lm}^3 \\ \gamma_{lm}^2 & \gamma_{lm}^4 & \gamma_{lm}^5 \\ \gamma_{lm}^3 & \gamma_{lm}^5 & \gamma_{lm}^6 \end{bmatrix}$ is the dual matrix variables of transmission lines' power flow inequality constraints, which must be semi-positive definite.

5.3.4 Dual Problem

The objective function (5.6a) can be made equivalent to the following minimization formulation

$$\min_{\mathbf{V},\mathbf{P_g},\mathbf{Q_g},\mathbf{Q_d},\mathbf{P_d}} \quad -\sum_{k\in\mathbf{D}} P_k^d \tag{5.7}$$

To derive the dual problem of maximum loadability, firstly we can get the Lagrange function of the problem including the objective function (5.7), and constraints (5.6b)-(5.6d).

$$\begin{aligned}
\mathcal{L}(\chi,\xi) = &-\sum_{k\in\mathbf{D}} P_k^d + \sum_{k\in\mathbf{G}} \Big\{ \tau_k^{min}(Q_k^{g,min} - Q_k^d - \mathrm{Tr}\{\overline{\mathbf{Y}}_k \mathbf{X}\mathbf{X}^T\}) + \tau_k^{max}(Q_k^d + \mathrm{Tr}\{\overline{\mathbf{Y}}_k \mathbf{X}\mathbf{X}^T\} \\
&- Q_k^{g,max}) - \lambda_k^{min}(P_k^{g,min} - P_k^d - \mathrm{Tr}\{\mathbf{Y}_k \mathbf{X}\mathbf{X}^T\}) + \lambda_k^{max}(P_k^d + \mathrm{Tr}\{\mathbf{Y}_k \mathbf{X}\mathbf{X}^T\} - P_k^{g,max}) \Big\} \\
&+ \sum_{k\in N} \Big\{ \mu_k^{min}((V_k^{min})^2 - \mathrm{Tr}\{\mathbf{M_k}\mathbf{X}\mathbf{X}^T\}) + \mu_k^{max}(\mathrm{Tr}\{\mathbf{M_k}\mathbf{X}\mathbf{X}^T\} - (V_k^{max})^2) \Big\} \\
&+ \sum_{k\in D} \Big\{ \nu_k^{d,min}(P_k^{d,min} - P_k^d) + \nu_k^{d,max}(P_k^d - P_k^{d,max}) \Big\} + \sum_{k\in D} \Big\{ \varphi_k^{d,min}(Q_k^{d,min} - Q_k^d) \\
&+ \varphi_k^{d,max}(Q_k^d - Q_k^{d,max}) \Big\} + \sum_{(l,m)\in\mathbf{L}} \Big\{ \gamma_{lm}^1 (S_{lm}^{max})^2 - \gamma_{lm}^4 - \gamma_{lm}^6 + 2\gamma_{lm}^2 \mathrm{Tr}\{\mathbf{Y}_{lm}\mathbf{X}\mathbf{X}^T\} \\
&+ 2\gamma_{lm}^3 \mathrm{Tr}\{\overline{\mathbf{Y}}_{lm}\mathbf{X}\mathbf{X}^T\} \Big\}
\end{aligned}$$

where χ is the summary set of primal variables $\Big\{\{V_k\}_{k\in\mathbf{N}},\ \{P_k^g\}_{k\in\mathbf{G}},\ \{Q_k^g\}_{k\in\mathbf{G}},\ \{Q_k^d\}_{k\in\mathbf{D}},$ $\{P_k^d\}_{k\in\mathbf{D}}\Big\}$ and ξ is the set of dual variables $\Big\{\{\tau_k^{min},\tau_k^{max}\}_{k\in\mathbf{G}},\ \{\lambda_k^{min},\lambda_k^{max}\}_{k\in\mathbf{G}},$ $\{\gamma_{lm}^1,\gamma_{lm}^2,\gamma_{lm}^3,\gamma_{lm}^4,\gamma_{lm}^5,\gamma_{lm}^6\}_{(l.m)\in\mathbf{L}},\ \{\mu_k^{min},\mu_k^{max}\}_{k\in\mathbf{N}},\ \{\nu_k^{d,min},\nu_k^{d,max}\}_{k\in\mathbf{D}},\ \{\varphi_k^{d,min},\varphi_k^{d,min}\}_{k\in\mathbf{D}}$ $\Big\}$.

The above Lagrange function can be transformed into the following formulation

$$\mathcal{L}(\chi,\xi) = g(\xi) + \mathrm{Tr}\{A^{opt}\{\mathbf{X}\mathbf{X}^T\} + \sum_{k\in\mathbf{G}} P_k^d\big(-\lambda_k^{min}+\lambda_k^{max}\big) + \sum_{k\in\mathbf{D}} P_k^d\big(-\nu_k^{d,min} + \nu_k^{d,max} - 1\big) + \sum_{k\in\mathbf{G}} Q_k^d\big(-\tau_k^{d,min}+\tau_k^{d,max}\big) + \sum_{k\in\mathbf{D}} Q_k^d\big(-\varphi_k^{min}+\varphi_k^{max}\big)$$

where

$$A^{opt} = \sum_{k\in\mathbf{G}}\Big\{-\tau_k^{min}\{\overline{\mathbf{Y}}_k\} + \tau_k^{max}\{\overline{\mathbf{Y}}_k\} - \lambda_k^{min}\{\mathbf{Y}_k\} + \lambda_k^{max}\{\mathbf{Y}_k\}\Big\} + \sum_{k\in N}\Big\{-\mu_k^{min}\{\mathbf{M_k}\} + \mu_k^{max}\{\mathbf{M_k}\}\Big\} + \sum_{(l,m)\in\mathbf{L}}\Big\{2\gamma_{lm}^2\{\mathbf{Y}_{lm}\} + 2\gamma_{lm}^3\{\overline{\mathbf{Y}}_{lm}\}\Big\}$$

and

$$g(\xi) = \sum_{k\in\mathbf{G}}\Big\{\tau_k^{min}Q_k^{g,min} - \tau_k^{max}Q_k^{g,max} + \lambda_k^{min}P_k^{g,min} - \lambda_k^{max}P_k^{g,max}\Big\} + \sum_{(l,m)\in\mathbf{L}}\big(-\gamma_{lm}^4 + \gamma_{lm}^1(S_{lm}^{max})^2 - \gamma_{lm}^6\big) + \sum_{k\in D}\big(\nu_k^{d,min}P_k^{d,min} - \nu_k^{d,max}P_k^{d,max} + \varphi_k^{d,min}Q_k^{d,min} - \varphi_k^{d,max}Q_k^{d,max}\big)$$

The Lagrange dual function is $\min_{\chi} \quad \mathcal{L}(\chi,\xi) = g(\xi)$, with conditions explained as follows. Since $\{\mathbf{X}\mathbf{X}^T\}$ is a positive definite matrix, the coefficient matrix A^{opt} should be nonnegative matrix in order for the minimum value of the $\mathrm{Tr}\{A^{opt}\{\mathbf{X}\mathbf{X}^T\}$ term to be zero. Otherwise the minimum value will be negative unbounded. Similarly, because as primal variables P_k^d and Q_k^d are nonnegative, the coefficient of P_k^d and Q_k^d should be non-negative so that the product terms have minimum zero value.. Hence, the dual problem of maximum loadability is obtained as follows

$$\max \quad g(\xi) \tag{5.8a}$$

subject to

$$A^{opt} \succeq 0 \tag{5.8b}$$

$$-\nu_k^{d,min} + \nu_k^{d,max} - 1 \geq 0, \forall k \in \mathbf{D} \tag{5.8c}$$

$$-\varphi_k^{d,min} + \varphi_k^{d,max} \geq 0, \forall k \in \mathbf{D} \tag{5.8d}$$

$$-\lambda_k^{min} + \lambda_k^{max} \geq 0, \forall k \in \mathbf{G} \tag{5.8e}$$

$$-\tau_k^{min} + \tau_k^{max} \geq 0, \forall k \in \mathbf{G} \tag{5.8f}$$

$$\begin{bmatrix} \gamma_{lm}^1 & \gamma_{lm}^2 & \gamma_{lm}^3 \\ \gamma_{lm}^2 & \gamma_{lm}^4 & \gamma_{lm}^5 \\ \gamma_{lm}^3 & \gamma_{lm}^5 & \gamma_{lm}^6 \end{bmatrix} \succeq 0, \forall (l,m) \in \mathbf{L} \tag{5.8g}$$

where all the dual variables are nonnegative.

5.3.5 Optimization of Maximum Loadability

The optimal power flow method deals with finding an optimal operating point of a power system that maximizes an appropriate maximum loadability, which means maximum loadability subject to certain constraints on power and voltage. Yet, the maximum loadability problem is nonlinear and nonconvex problem, and the global optimal point cannot be guaranteed if directly solving the primal problem. Instead of solving the primal maximum loadability problem directly, we firstly transfer the maximum loadability model into a semi-definite programming which is convex, and then solve its Lagrangian dual problem. This method can recover a primal solution from the dual optimal problem. Comparing with the primal optimal objective value, the value of the dual problem is only a lower bound on the optimal value of the primal problem, and the lower bound may not be tight (nonzero duality gap). Following the same argument in [99], the sufficient condition for zero duality gap is that there exists a dual optimal solution ξ such that $2n \times 2n$ positive semi-definite matrix A^{opt} has a zero eigenvalue of multiplicity equal to or less than 2. Under this condition, strong

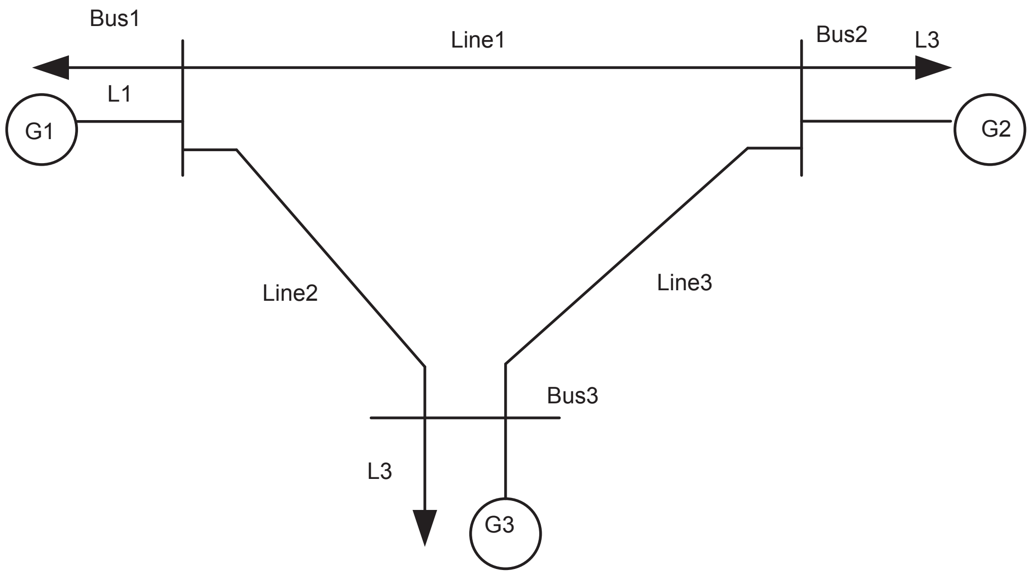

Figure 5.1: IEEE three-bus system

duality holds and the dual solution is indeed optimal for the original maximum loadability problem, allowing us to obtain the globally optimal solution.

5.4 Case Study

IEEE three-bus system

The proposed model is illustrated using the three-bus test system shown in Fig. 5.1. This work uses the SDP solver Sedumi in YALMIP toolbox of MATLAB platform to solve the dual problem of maximum loadability. The three-bus system contains one conventional generation unit per bus (G1 through G3). The value of base apparent power is 100 MVA. Detailed data for the conventional generators on the three-bus system is shown in Table 5.1.

Table 5.1: DATA FOR THE GENERATING UNITS OF THE THREE-BUS SYSTEM

Generator(i)	G1	G2	G3
$P_k^{g,max}$[MW]	400	400	200
$Q_k^{g,max}$[MW]	500	500	500
$P_k^{g,min}$[MW]	0	0	0
$Q_k^{g,min}$[MW]	-100	-100	-100

Table 5.2: THE DATA OF LOADS DEMAND OF THE IEEE THREE-BUS SYSTEM

Loads Demand (k)	L1	L2	L3
$P_k^{d,max}$[MW]	650	500	450
$Q_k^{d,max}$[MVar]	300	300	200
$P_k^{d,min}$[MW]	110	110	95
$Q_k^{d,min}$[MVar]	40	40	50

There are also three loads demand in this system (L1-L3). Table 5.2 shows the varying range of active loads and reactive loads, where $P_k^{d,min}$ and $Q_k^{d,min}$ are the minimum values of active loads and reactive loads respectively, and also the given initial values of loads demand used for solving the OPF or PF problem. The data of transmission lines are shown in Table 5.3. We also V_k^{max} =1.1 pu, and V_k^{min} =0.9 pu, and set all the transmission line capacity limits sufficiently large in order to eliminate congestions. Based on the above data, we solve the SDP dual problem of maximum loadability (5.8), and obtain the maximum loadability equal to 638.5 MW. The voltages of buses are approaching their limits, reaching 11.0000V, 10.9981-0.1458*i and 10.9798+0.6516*i successively from Bus 1 to Bus 2, and Bus 3. Simulation results show that the matrix-valued A^{opt} has a zero eigenvalue of multiplicity 2, which satisfies the sufficient condition of an optimal solution of the OPF problem [99]. Therefore, the calculated maximum loadability value 638.5 MW is the global optimization value. Fig. 5.2 shows the iteration process of the dual SDP problem being solved by the SDP solver SEDUMI. From this figure, the problem reachs the solution with a tolerance with 6.01E-17 after the total 49 iterations and the duality gap almost reaches to zero after the 5th iteration.

Table 5.3: THE DATA OF TRANSMISSION LINES OF THE IEEE THREE-BUS SYSTEM

Lines $((l,m))$	Line 1	Line 2	Line 3
Resistance (p.u.)	0.42	0.55	0.25
Reactance (p.u.)	0.90	0.90	0.75
Susceptance (p.u.)	0.30	0.45	0.70

From the reference [99], the sufficient condition that guarantees that the algorithm finds an optimal solution of OPF is there exists a dual optimal solution (x_{opt}, r_{opt}) such that $2n \times 2n$ positive semi-definite matrix A^{opt} has a zero eigenvalue of multiplicity 2. If the condition sufficient condition holds, there is no duality gap between the original maximum loadability and the dual problem. Apparently, the proposed three-bus system can satisfy

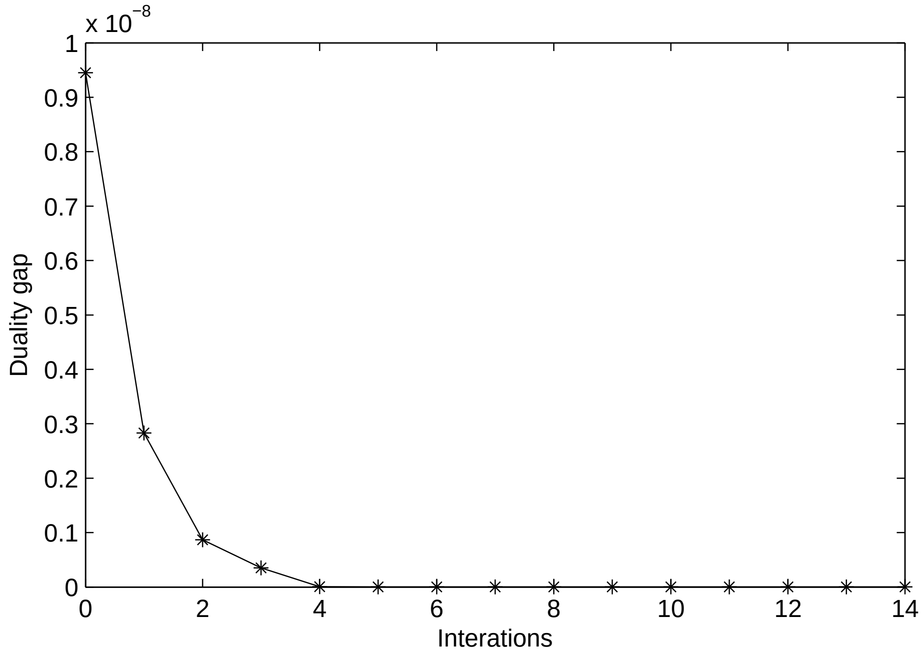

Figure 5.2: Duality gap Interations

strongly connected condition. Hence, the resistive part of the power system is strongly connected, the sufficient condition holds and the duality gap of the OPF is zero according to [98]. In [98], the author proved that all the five IEEE benchmark systems can satisfy the sufficient condition of zero duality gap after a small resistance (10^{-5}) has been added to each transformer that originally has zero resistance.

IEEE 24-bus RTS

The IEEE three-bus system case is used to calculate the maximum loadability of the whole area. In the practical industry, the maximum loadability of a sub-area is often needed to be provided. IEEE 24-bus Reliability Test System is adopted [100] to study the maximum loadability of sub areas, shown in Fig. 5.3. This system contains 24 nodes and 34 lines connecting them, 11 generating units and 17 loads are also included. IEEE 24-bus RTS is divided into two areas, one is 230 KV area and another is 138 KV area, shown in Fig. 5.3.

To get the maximum loadability of the low voltage area (138 KV), in the proposed model we set the loads of buses (Bus1-Bus10) as variables. We solve the dual maximum loadability model, then get the four smallest eigenvalues of the matrix A^{opt} as -124.5429, -124.5429, -28.6438, -28.6438. As the number of zero eigenvalues is 0, it means satisfying the zero duality gap sufficient condition. Therefore, we can get the optimal objective value maximum

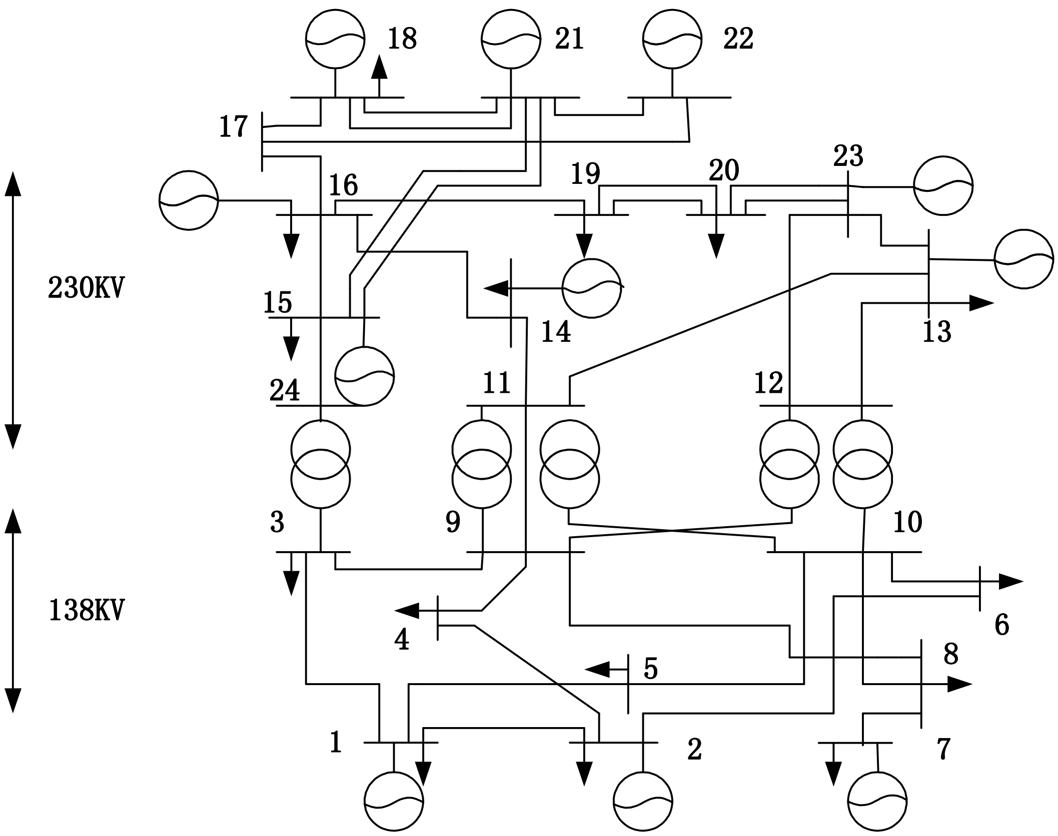

Figure 5.3: Single line diagram of IEEE RTS 24-bus system

loadability 3017 MW. Further calculating the maximum total transfer capability (TTC) from the higher voltage area to the lower voltage area which equal to 1490 MW without considering contigency. Alternatively, the maximum TTC is equal to 1182 MW calculated by the sequential quadratic programming (SQP) method [101]. The proposed SDP method provides a larger value than the traditional SQP method. The SQP method is based on the KKT conditions, and the quadratic programming subproblem is solved by Quasi-Newtons method with the optimal search of the step length. Therefore, the accuracy of the calculated results provided by SQP depends on the step length.

5.5 Conclusion

The Lagrange SDP method has been applied to solve the non-linear and non-convex maximum loadability of security constrained power system. The proposed model integrates security constraints such as limits of generation active power and reactive power output, voltage magnitudes, and transmission power flow. In addition, active loads and reactive loads vary within the reasonable range as independent variables. The proposed SDP method has been prove effective and guarantees the global optimal solution of the maximum loadability, with zero duality gap. The effectiveness of the Lagrange SDP method has been demonstrated in the IEEE three-bus and IEEE 24-bus RTS.

Chapter 6

Conclusions and Further Research Issues

6.1 Conclusions

In this dissertation, we have studied various optimization problems of electric power markets under modern power grid, including electricity marginal prices with uncertain wind power and loads demand, wind power producers' bidding in the stochastic market clearing, transmission expansion planning with wind power integration and co-optimization of energy and research, and SDP for the maximum loadability problem.

The study of the probabilistic spot pricing develops the optimal power flow method to calculate the local marginal prices considering load uncertainty and wind speed randomness. The extended objective function of the proposed optimization model has included emission cost to take into account environmental benefits and spinning reserve fee to address the reserve cost owning to the introduction of wind power. Simulation results show renewable wind energy is beneficial for cost reduction. However, once over penetration, intermittent wind power may bring serious reliability problem and cause cost climbing.

The proposed stochastic bilevel model for a strategic WPP as a price marker in the day-ahead market that employs stochastic market clearing and energy and reserver co-optimization. The proposed bidding model of the strategic WPP is able to obtain more steady expected profit in a reserved market than in a non-reserved market. In other words, considering the operation of the reserve market can reduce the risk of the day-ahead offer. And the strategic offering can increase the expected profit, reduce the conventional generators cost and decrease the social welfare, compared with the non-strategic WPP.

In the chapter of transmission planning, we develop an innovative model coordinating transmission expansion planning and wind power investment within a modern electricity market environment. This model comprehensively considers transmission expansion planning, wind power integration, as well as co-optimization of energy and reserve. According to our simulations, The planned wind power invested and power scheduled will increase with the higher level of loads demand. The proposed model effectively coordinates the contradiction between transmission expansion planning and wind power investment, and solves the interaction between systems planning and operations of power systems. In addition, this model can assess the requirement of reserve for the transmission planning.

We have also proposed the Lagrange SDP method to solve the non-linear and non-convex maximum loadability of security constrained power systems. The proposed SDP method has been proved to effectively solve the non-linear and non-convex complexity of the maximum loadability of systems, especially integrating security constraints. The proposed Lagrange SDP method guarantees the global optimal solution of the maximum loadability, and the zero duality gap is proved to exist. The simulation results on IEEE three-bus system and IEEE 24-bus RTS show the effectiveness and the accuracy of the Lagrange SDP method for the problem of the maximum loadability.

6.2 Further Research Issues

There are still some open research issues to study in the above mentioned topics in this dissertation.

The work of modeling bids of the strategic wind power producer does not consider non-convex constraints in the clearing algorithm, such as voltage constraints and reactive power output constraints. In future work, we will set AC-OPF as the lower level problem and consider solving the corresponding bilevel problem. Another, in this thesis only one strategic wind power producer makes bidding decisions without other wind power producers or traditional power producers, so we just use Stackelberg Equilibrium theory to model. While all the strategic power producers have rights to bid offers, for this situation, we could further consider to use Nash Equilibrium to solve.

For ISOs' transmission expansion planning, transmission planning of different regions must satisfy the requirements of different planning standards. To simplify the model, we did not integrate planning criteria in the mathematical model, like N-1,N-2, even N-1-1. Hence, we will further study the model of transmission expansion planning with various security criteria of systems planning and operations in different regions, such as WECC, AESO.

In the chapter of the SDP method for the maximum loadability, specifically we solved the problem of the maximum loadability based on the traditional static security constrained optimal power flow model. In the power industry, power systems suffer from many disturbances, and hence dynamic security constraints can be integrated into the traditional optimal power flow model. The extension of the SDP method to solve the maximum loadability will be considered into my future work to obtain the global optimization solution.

Bibliography

[1] H. Liu, L. Tesfatsion, and A. A. Chowdhury. Locational marginal pricing basics for restructured wholesale electricity markets. *in Proc. Power Energy Soc. Gen. Meet.*, 2009.

[2] Y. Jun. Locational marginal pricing in $ercot$ market. *Power Engineering Society General Meeting, 2006. IEEE*, 2006.

[3] Juan M Morales, Student Member, Antonio J Conejo, and Juan Pérez-ruiz. Economic valuation of reserves in power systems with high penetration of wind power. *IEEE Trans. Power Syst.*, 24(2):900–910, May 2009.

[4] Juan M.Morales, Antonio J Conejo, Kai Liu, and Jin Zhong. Pricing electricity in pools with wind producers. *IEEE Trans. Power Syst.*, 27(3):1366–1376, Aug. 2012.

[5] T. Zheng and E. Litvinov. Ex post pricing in the co-optimized energy and reserve market. *IEEE Trans. Power Syst.*, 21(4):1528–1538, Nov. 2006.

[6] A. L. Ott. Experience with PJM market operation, system design, and implementation. *IEEE Trans. Power Syst.*, 18(2):528–534, May 2003.

[7] L. Baringo and A. J. Conejo. Strategic offering for a wind power producer. *IEEE Trans. Power Syst.*, 28(4):4645–4654, Jul. 2013.

[8] J.J. Hargreaves and B. F. Hobbs. Commitment and dispatch with uncertain wind generation by dynamic programming. *IEEE Trans. Sustainable Energy*, 3(4):724–734, Oct. 2012.

[9] J. M. Morales, A. J. Conejo, and J. Pérez-ruiz. Short-term trading for a wind power producer. *IEEE Trans. Power Syst.*, 25(1):554–564, Jan. 2010.

[10] P. M. S. Carvalho, L. A. F. M. Ferreira, B. H. Krogh, N. Popli, and M.D. Ilic. Wind integration in power systems: operational challenges and possible solutions. *Proceedings of the IEEE*, 99(1):214–232, Oct. 2011.

[11] E. Kahn. Wind integration Studies: optimization vs. simulation. *The Electricity Journal*, 23(9):51–64, Nov. 2010.

[12] J. C. Smith, M. R. Milligan, E.A. Demeo, and B. Parsons. Utility wind integration and operating impact state of the art. *IEEE Trans. Power Syst.*, 22(3):900–908, Aug. 2007.

[13] Y.V. Makarov, C. Loutan, J. Ma, and P.D. Mello. Operational impacts of wind generation on california power systems. *IEEE Trans. Power Syst.*, 24(2):1039–1050, May 2009.

[14] M. H. Albadi and E. F. El-Saadany. Overview of wind power intermittency impacts on power systems. *Electric Power Systems Research*, 80(6):627–632, Jun. 2010.

[15] C. Abbey and D. G. Joós. A stochastic optimization approach to rating of energy storage systems in wind-diesel isolated grids. *IEEE Trans. Power Syst.*, 24(1):418–426, Dec. 2009.

[16] R. Bo and F. X. Li. Probabilistic LMP forecasting considering load uncertainty. *IEEE Trans. Power Syst.*, 24(3):1279–1289, Aug. 2009.

[17] S. Lotfifard, L. Xie, and M. Kezunovic. Quantifying the impact of unscheduled line outages on locational marginal prices. In *North American Power Symp. (NAPS)*, 2010.

[18] Bruno a. Gomes, Joao T Saraiva, and Luis M Neves. Impact of load and generation price uncertainties in spot prices. In *IEEE Bucharest PowerTech*, 2009.

[19] D. P. Chen and D. W. Bunn. Analysis of the nonlinear response of electricity prices to fundamental and strategic factors. *IEEE Trans. Power Syst.*, 25(2):595–606, May 2010.

[20] J. Huang, Y. S. Xue, and Z.Y. Dong. An adaptive importance sampling method for probabilistic optimal power flow. In *Power and Energy Society General Meeting*, 2011.

[21] K. Xie, Y.H. Song, and J. Stonham. Decomposition model and interior point methods for optimal spot pricing of electricity in deregulation environments. *IEEE Trans. Power Syst.*, 15(1):39–50, Feb. 2000.

[22] Y.Y. Dai, J. Huang, and K. Meng. LMP estimation considering the uncertainty of wind power. In *Universities Power Eng. Conf. (AUPEC)*, 2011.

[23] Juan M Morales, Student Member, Antonio J Conejo, and Juan Pérez-ruiz. Simulating the impact of wind production on locational marginal prices. *IEEE Trans. Power Syst.*, 26(2):820–828, May 2011.

[24] C. K. Woo, I. Horowitz, J. Moore, and A. Pacheco. The impact of wind generation on the electricity spot-market price level and variance: The texas experience. *Energy Policy*, pages 3939–3944, Jul. 2011.

[25] T. Jónsson, P. Pinson, H. A. Nielsen, H. Madsen, and T. S. Nielsen. Forcasting electricity spot prices accounting for wind power predictions. *IEEE Trans. Sustainable Energy*, 4(1):210–218, Jan. 2013.

[26] Hui Zhang. Chance constrained programming for optimal power flow under uncertainty. *IEEE Trans. Power Syst.*, 26(4):2417–2424, Jun. 2011.

[27] M. A. Abido. Environmental/economic power dispatch using multiobjective evolutionary algorithms. *IEEE Trans. Power Syst.*, 18(4):1529–1537, Nov. 2003.

[28] K. S. Verma and H. O. Gupta. Impact on real and reactive power pricing in open power market using unified power flow controller. *IEEE Trans. Power Syst.*, 21(1):365–371, Feb. 2006.

[29] L. Xie, P. M. S. Carvalho, L. A. F. M. Ferreira, J. Liu, B. H. Krogh, N. Popli, and M. D. Ilic. Wind integration in power systems: operational challenges and possible solutions. *Proc. of the EEE*, 99(1):214–232, Jan. 2011.

[30] X.. Y. Ma, Y. Z. Sun, and H. L. Fang. Scenario generation of wind Power based on statistical uncertainty and variability. *IEEE Trans. Power Syst.*, 4(4):894–904, Oct. 2013.

[31] V. Miranda A. Botterud, J.Wang and R. J. Bessa. Wind power forecasting in U.S. electricity markets. *Electr. J.*, 23(2):72–82, Apr. 2010.

[32] P. R. Bijwe S. S. Reddy and A. R. Abhyankar. Joint Energy and Spinning Reserve Market Clearing Incorporating Wind Power and Load Forecast Uncertainties. *IEEE Syst. J.*, 9(1):152–164, Jul. 2015.

[33] M. I. Blanco. The economics of wind energy. *Renewable and Sustainable Energy Reviews*, 13(6):1372–1382, Aug. 2009.

[34] Federal Energy Regulatory Commission (FERC). Integration of variable energy resources. *Final Rule-Docket No. RM10-11-000; Order No. 764*, June 22 2012.

[35] F. Bouffard and F. Galiana. Stochastic security for operations planning with significant wind power generation. *IEEE Trans. Power Syst.*, 23(2):306–316, May 2008.

[36] J. M. Morales A. J. Conejo and J. A. Martnez. Tools for the analysis and design of distributed resources Part III: Market studies. *IEEE Trans. Power Del.*, 26(3):1663–1670, Jul. 2011.

[37] J. Perez-Ruiz J. M. Morales, A. J. Conejo. Economic valuation of reserves in power systems with high penetration of wind power. *IEEE Trans.Power Syst.*, 24(2):900–910, May 2009.

[38] J. I. Munoz A. A. S. de la Nieta, J. Contreras and M. O'Malley. Modeling the impact of a wind power producer as a price-maker. *IEEE Trans. Power Syst.*, 29(6):2723–2732, Nov. 2014.

[39] J. Matevosyan and L. Söder. Minimization of imbalance cost trading wind power on the short-term power market. *IEEE Trans. Power Syst.*, 21(3):1396–1404, Aug. 2006.

[40] J. P. S. Catalao, H. M. I. Pousinho, and V. M. F. Mendes. Optimal offering strategies for wind power producers considering uncertainty and risk. *IEEE Syst. J*, 6(2):270–277, June 2012.

[41] P. Pinson, C. Chevallier, and G. N. Kariniotakis. Trading wind generation from short-term probabilistic forecasts of wind power. *IEEE Trans. Power Syst.*, 22(3):1148–1156, Aug. 2007.

[42] Eilyan Y. Bitar, Ram Rajagopal, Pramod P. Khargonekar, Kameshwar Poolla, and Pravin Varaiya. Bringing wind energy to market. *IEEE Trans.Power Syst.*, 27(3):1225–1235, Aug. 2012.

[43] S Jalal Kazempour and Hamidreza Zareipour. Equilibria in an oligopolistic market with wind power production. *IEEE Trans. Power Syst.*, 29(2):686–697, Mar. 2014.

[44] M. Zugno, J. M. Morales, P. Pinson, and H. Madsen. Pool strategy of a price-maker wind power producer. *IEEE Trans. Power Syst.*, 28(3):3440–3450, Aug. 2013.

[45] J. J. Ye, D. L. Zhu, and Q. J. Zhu. Exact penalization and necessary optimality conditions for generalized bilevel programming problems. *SIAM J.Optim.*, 7(2):481–507, May 1997.

[46] J. F. Amat and B. McCarl. A representation and economic interpretation of a two-level programming problem. *J. Oper. Res. Soc.*, 32:783–792, Sep. 1981.

[47] X. M. Hu and D. Ralph. Using EPECs to model bilevel games restructured electricity markets with locational prices. *Oper. Res.*, 55(5):809–827, 2007.

[48] H. Ahmadi, J. R. Marti, and A. Moshref. Piecewise linear approximation of generators cost functions using max-affine functions. *in Proc. IEEE PES Gen. Meeting,*, 2013.

[49] J. M. Arroyo F. D. Galiana, F. Bouffard and J. F. Restrepo. Scheduling and pricing of coupled energy and primary, secondary, and tertiary reserves. *Proc. IEEE*, 93(3):1970–1983, Nov. 2005.

[50] S. Gabriel. *Complementarity Modeling in Energy Markets*. Springer., 2012.

[51] R. T. Rockafellar. *Convex Analysis*. Princeton University Press, 1997.

[52] S. Scholtes. Convergence properties of a regularization scheme for mathematical programs with complementarity. *SLAM J. Optim*, 11(4):918–936, 2001.

[53] T. Hoheisel, C. Kanzow, and A. Schwartz. Theoretical and numerical comparison of relaxation methods for mathematical programs with complementarity constraints. *Math. Program.*, 137(1-2):257–288, Sep. 2011.

[54] R. E. Rosenthal. GAMS, A User' s Guide. *Washington, DC, USA: GAMS*, 2013.

[55] A. Sets. Coordinating large-scale wind integration and transmission planning. *IEEE Trans. Power Syst.*, 3(4):652–659, Oct. 2012.

[56] R. Piwko, D. Osborn, R. Gramlich, G. Jordan, D. Hawkins, and K. Porter. Wind energy delivery issues [transmission planning and competitive electricity market operation]. *IEEE Power and Energy Magazine*, 3(6):47–56, Dec. 2005.

[57] 10-year regional transmission plan: 2020 study report. *Council, Western Electricity Coordinating, Tech. Rep.*, 2011.

[58] Heejung Park, Student Member, and Ross Baldick. Transmission planning under uncertainties of wind and load : sequential approximation approach. *IEEE Trans. Power Syst.*, 28(3):2395–2402, Aug. 2013.

[59] F. D. Munoz, B. F. Hobbs, J. L. Ho, and S. Kasina. An engineering-economic approach to transmission planning under market and regulatory uncertainties: WECC case study. *IEEE Trans. Power Syst.*, 29(1):307–317, Jan. 2014.

[60] M. Madrigal and S. Stoft. Transmission Expansion for Renewable EnergyScale-up. *Washington, DC, USA: World Bank*, 2012.

[61] L. Baringo and A. J. Conejo. Transmission and wind power investment. *IEEE Trans. Power Syst.*, 27(2):885–893, May 2012.

[62] M. Milligan et al. Operating Reserves and Wind Power Integration: An International Comparison. *Proceedings of 9th International Workshop on Large-Scale Integration of Wind Power into Power Systems*, Oct 2010, Quebec.

[63] J. Dillon M. J. OMalley D. J. Burke, A. Tuohy. Should unit commitment be endogenously included in wind power transmission planning optimisation models? *IET Renew. Power Gener. J.*, 8(2):132–140, 2014.

[64] S. Jin, S.M. Ryan, and A. Sets. A tri-level model of centralized transmission and decentralized generation expansion planning for an electricity market Part I. *IEEE Trans. Power Syst.*, 29(1):132–141, Jan. 2014.

[65] Masoud Jenabi, Seyyed Mohammad Taghi Fatemi Ghomi, and Yves Smeers. Bi-level game approaches for coordination of generation and transmission expansion planning within a market environment. *IEEE Trans. Power Syst.*, 28(3):2639–2650, Aug. 2013.

[66] H. Yu, C. Y. Chung, K. P. Wong, and J. H. Zhang. A chance constrained transmission network expansion planning method with consideration of load and wind farm uncertainties. *IEEE Trans. Power Syst.*, 24(3):1568–1576, Aug. 2009.

[67] R. Baldick H. Park. Transmission planning under uncertainties of wind and load: Sequential approximation approach. *IEEE Trans. Power Syst.*, 28(3):2395–2402, Aug. 2013.

[68] A. H. van der Weijde and B. F. Hobbs. The economics of planning electricity transmission to accommodate renewables: using two-stage optimisation to evaluate flexibility and the cost of disregarding uncertainty. *Energy Economics*, 34(6):2089–2101, November 2012.

[69] G. A. Orfanos, P. S. Georgilakis, and N. D. Hatziargyriou. Transmission expansion planning of systems with increasing wind power integration. *IEEE Trans. Power Syst.*, 28(2):1355–1362, May 2013.

[70] J. C. Villumsen, G. Brø nmo, and A. B. Philpott. Line capacity expansion and transmission switching in power systems with large-scale wind power. *IEEE Trans. Power Syst.*, 28(2):731–739, May 2013.

[71] S. Jin and S. M. Ryan. Capacity expansion in the integrated supply network for an electricity market. *IEEE Trans. Power Syst.*, 26(4):2275–2284, Nov. 2011.

[72] M. R. Hesamzadeh and M. Yazdani. Transmission capacity expansion in imperfectly competitive power markets. *IEEE Trans. Power Syst.*, 29(1):62–71, Jan. 2014.

[73] D. Pozo, E. E. Sauma, and J. Contreras. A three-level static MILP model for generation and transmission expansion planning. *IEEE Trans. Power Syst.*, 28(1):202–210, Feb. 2013.

[74] A. Motamedi, H. Zareipour, M. O. Buygi, and W. D. Rosehart. A transmission planning framework considering future generation expansions in electricity markets. *IEEE Trans. Power Syst.*, 25(4):1987–1995, Nov. 2010.

[75] W. P. Lasher. The development of Competitive Renewable Energy Zones in Texas. *IEEE PES Transmission and Distribution Conference and Exposition*, 2008.

[76] S. Steffensen and M. Bittner. Relaxation approach for equilibrium problems with equilibrium constraints. *Computers & Operations Research*, 41:333–345, Jan. 2014.

[77] M. O. Buygi A. Motamedi, H. Zareipour and W. D. Rosehart. A transmission planning framework considering future generation expansions in electricity markets. *IEEE Trans. Power Syst.*, 25(4):1987–1995, Nov. 2010.

[78] P. Kundur and J. Paserba. Definition and classification of power system stability. *IEEE Trans. Power Syst.*, 19(2):1387–1401, May 2004.

[79] J. D. McCalley, Y. J. Dai, and V. Vittal. Simplification, expansion and enhancement of direct interior point algorithm for power system maximum loadability. *IEEE Trans. Power Syst.*, 15(3):1014–1021, Aug. 2000.

[80] V. Ajjarapu and C. Christy. The continuation power flow: a tool for steady state voltage stability analysis. *IEEE Trans. Power Syst.*, 7(1):416–423, Feb. 1992.

[81] K. Gnanambal and C.K. Babulal. Maximum loadability limit of power system using hybrid differential evolution with particle swarm optimization. *Int J Electr Power Energy Syst*, 76:150–155, 2012.

[82] P. Acharjee. Identification of maximum loadability limit and weak buses using security constraint genetic algorithm. *Int J Electr Power Energy Syst*, 36(1):40–50, 2012.

[83] A. Shunmugalatha and S.M.R. Slochanal. Optimum cost of generation for maximum loadability limit of power system using hybrid particle swarm optimization. *Int J Electr Power Energy Syst*, 30:486–490, 2008.

[84] G. D. Irisarri, X. Wang, J. Tong, and S. Mokhtari. Maximum loadability of power systems using interior point nonlinear optimization method. *IEEE Trans. Power Syst.*, 12(1):162–172, Feb. 1997.

[85] T.M.Y.Law KPWong, A.Li. Advanced constrained genetic algorithm load flow method. *IEE Proc Gener Transm Distrib*, 140:609–616, 1999.

[86] T.O. Ting, K.P. Wong, and C.Y. Chung. Hybrid constrained genetic algorithm/particle swarm optimization load flow algorithm. *IET Gener Transm Distrib*, 2:800–812, 2008.

[87] A. A. EL-Dib, H. K. M. Youssef, M. M. EL-Metwally, and Z. Osman. Maximum loadability of power system using hybrid particle swarm optimization. *Elect. Power Syst. Res.*, 76:485–492, Feb. 2006.

[88] A. Shunmugalatha and S. Mary Raja Slochanal. Maximum loadability of a power system using multi agent-based hybrid particle swarm optimization. *Electric Power Compon. Syst.*, 36:575–586, 2008.

[89] Q. Bai. Analysis of particle swarm optimization algorithm. *Computer and Information Science*, 3(1):180–184, Feb. 2010.

[90] H. Wei, H. Sasaki, J. Kubokawa, and R. Yokoyama. An interior point nonlinear programming for optimal power flow problems with a novel data structure. *IEEE Trans. Power Syst*, 13(3):870–877, Aug. 1998.

[91] S. H. Lavaei, J.and Low. Zero Duality Gap in Optimal Power Flow Problem. *IEEE Trans. Power Syst.*, 27(1):92–107, Feb. 2012.

[92] Youjie Dai and Vijay Vittal J.D.McCalley. Simplification, expansion and enhancement of direct interior point algorithm for power system maximum loadability. *IEEE Trans. Power Syst.*, 15(3):1014–1021, Aug. 2000.

[93] M. H. Gravener and C. Nwankpa. Available transfer capability and first order sensitivity. *IEEE Trans.Power Syst.*, 14(2):512–518, May 1999.

[94] J Kubokawa, Y Yuan, and N Yorino. A solution of total transfer capability using transient stability constrained optimal power flow. In *IEEE Lausanne Powertech.*, 2007.

[95] X. Bai, H.Wei, K. Fujisawa, and Y.Wang. Semidefinite programming for optimal power flow problems. *Int. J. Elect. Power Energy Syst.*, 30(6-7):383–392, Aug. 2008.

[96] D. K. Molzahn, J. T. Holzer, B. C. Lesieutre, and C. L. DeMarco. Implementation of a large-scale optimal power flow solver based on semidefinite programming. *IEEE Trans. Power Syst.*, 28(4):3987–3998, Nov. 2013.

[97] D. Molzahn, B. Lesieutre, and C. DeMarco. A sufficient condition for global optimality of solutions to the optimal power flow problem. *IEEE Trans. Power Syst.*, 29(2):978–979, Mar. 2014.

[98] J. Lavaei and S. H. Low. Zero Duality Gap in Optimal Power Flow Problem. *IEEE Trans. Power Syst.*, 27(1):92–107, 2012.

[99] Javad Lavaei and Steven H. Low. Convexification of optimal power flow problem. *48th Annual Allerton Conference on Communication, Control, and Computing (Allerton)*, Sep. 2010.

[100] IEEE APM Subcommittee. IEEE reliability test system. *IEEE Trans. Power App. Syst.*, PAS-98(6):2047–2054, Nov. 1979.

[101] W. Li, P. Wang, and Z. Guo. Determination of optimal total transfer capability using a probabilistic approach. *IEEE Trans. Power Syst.*, 21(2):862–868, May 2006.